

ABSTRACT

Nutrient Enrichment Modulates The Structure and Temporal Assembly of Riverine Benthic Algal and Macroinvertebrate Assemblages

Stephen C. Cook, Ph.D.

Mentor: Ryan S. King, Ph.D.

Nutrient enrichment has become one of the most widespread anthropogenic forces impacting freshwater biodiversity worldwide. Stream communities are frequently limited by nutrient availability, and enrichment over natural concentrations can impact both the distribution of species and the temporal assembly of natural communities. By studying benthic algal and macroinvertebrate assemblages from 35 streams over two years that spanned a wide gradient of nutrient enrichment, I found that the temporal assembly patterns of both assemblages were heavily influenced by novel nutrient concentrations. Eutrophication reduced seasonally driven variation in macroinvertebrate assemblages, which resulted in more temporally homogenous communities. Declines in seasonal macroinvertebrate variation suggests that enrichment decreases the competitive advantage that seasonal specialists gain by occupying particular temporal niches, which degrades an important facet of stream biodiversity. In assemblages of periphytic algae, temporal niche partitioning has evolved in response to seasonal oscillations in environmental conditions. Compensatory dynamics of algae under natural nutrient

regimes broke down at relatively low levels of total phosphorus (TP) enrichment ($\sim 25 \mu\text{g L}^{-1}$). More species were able to coexist at any given time, and the fitness of a subset of species was increased by enrichment which led to seasonal variation characterized by synchronous swings in species biovolumes. Also, assemblage biovolumes during the study were much more unstable with greater enrichment, which indicates that anthropogenic alteration of nutrient regimes can affect community stability by changing the dominant mode of seasonal succession. I examined how enrichment changed the distribution of species among study sites, and found algal assemblage structure displayed sharp, non-linear changes in response to TP enrichment. Many algal species (57) synchronously increased in frequency and biovolumes with modest increases in TP concentrations of $\sim 16 \mu\text{g L}^{-1}$, and 17 species declined at TP enrichment of $\sim 20 \mu\text{g L}^{-1}$. Macroinvertebrate assemblage responses to TP concentrations were generally weak when compared to the algal assemblages, but there was some evidence of synchronous changes of taxa in response to periphyton nutrient content. These findings provide insight into how nutrient enrichment alters natural communities and leads to serious structural alterations to natural patterns in community composition.

Nutrient Enrichment Modulates The Structure and Temporal Assembly of Riverine Benthic Algal
and Macroinvertebrate Assemblages

by

Stephen C. Cook, B.S.

A Dissertation

Approved by the Department of Biology

Dwayne D. Simmons, Ph.D., Chairperson

Submitted to the Graduate Faculty of
Baylor University in Partial Fulfillment of the
Requirements for the Degree
of
Doctor of Philosophy

Approved by the Dissertation Committee

Ryan S. King, Ph.D., Chairperson

Robert D. Doyle, Ph.D.

J. Thad Scott, Ph.D.

Sanghoon Kang, Ph.D.

David Kahle, Ph.D.

Accepted by the Graduate School

August 2019

J. Larry Lyon, Ph.D., Dean

Copyright © 2019 by Stephen C. Cook

All rights reserved

TABLE OF CONTENTS

LIST OF FIGURES	vii
LIST OF TABLES	xii
ACKNOWLEDGMENTS	xiii
DEDICATION	xv
ATTRIBUTIONS	xvi
CHAPTER ONE	1
Introduction.....	1
Rise of the Novel Environment.....	1
The Impacts of Nutrient Enrichment on Stream Communities	2
Spatial and Temporal Niche Partitioning.....	4
Problem Statement	5
Study Objectives	6
Study Area	6
Summary of Chapter Contents.....	7
CHAPTER TWO	9
Freshwater Eutrophication Drives Sharp Reductions in Temporal Beta Diversity	9
Introduction.....	9
Methods.....	12
Study Area and Site Characterization	12
Periphyton Sampling.....	14
Macroinvertebrate Sampling.....	14
Measures of Temporal β Diversity	16
Modeling.....	17
Results.....	19
Discussion	23
CHAPTER THREE	29
Compensatory Dynamics of Stream Algae Nonlinearly Break Down with Increasing Nutrient Enrichment.....	29
Introduction.....	29
Methods.....	32

Study Area	32
Data Collection	32
Data Analysis	34
Results.....	36
Compensatory Dynamics in Freshwater Algae.....	37
Spatiotemporal Variation in Community Structure	39
Community Stability.....	40
Discussion.....	42
CHAPTER FOUR.....	46
Riverine Benthic Algae Exhibit Much Stronger and More Synchronous Responses to Nutrient Enrichment Than Do Macroinvertebrate Assemblages.....	46
Introduction.....	46
Methods.....	49
Study Area	49
Data Collection	50
Data Analysis	52
Results.....	55
Discussion.....	62
CHAPTER FIVE	69
Summary and Conclusions	69
Summary of Chapter Contents.....	69
Future Directions	70
APPENDIX A.....	74
Chapter Two Supplementary Material.....	75
Additional Supporting Information.....	79
Data Accessibility	79
APPENDIX B	80
Chapter Three Supplementary Material.....	81
APPENDIX C	84
Chapter Four Supplementary Materials	85
REFERENCES	94

LIST OF FIGURES

- Figure 1.1.** Locations of sampling sites ($n = 35$) in the Illinois River and several surrounding watersheds spanning the border of Oklahoma and Arkansas (USA, 1:250000 landsat shaded basemap, USGS). Watersheds of study sites are highlighted by a semi-transparent mask placed on the adjacent landscape. Lake Tenkiller is shown in the southwestern portion of the map, and is formed by the damming of the Illinois River. 7
- Figure 2.1.** Temporal β diversity (β_t) of macroinvertebrate assemblages declined in response to total phosphorus (TP, $\mu\text{g L}^{-1}$) and mean macroinvertebrate biomass (g m^{-2}), which indicates increased temporal homogenization of community composition with increasing nutrient enrichment. β_t was quantified as the multivariate dispersion (MVD) around site centroids in ordination space. (a) Raw data points are sized by mean macroinvertebrate biomass observed at each site over the 2 y study duration. The model describing the most variation in β_t (MVD, 71.74% deviance explained) included an interactive effect between TP and macroinvertebrate biomass. (b) The GLM response surface of β_t (MVD) to TP and macroinvertebrate biomass shows the modeled response of β_t (MVD) to TP at different levels of macroinvertebrate biomass (represented by lines ranging from 1-20 g m^{-2})..... 21
- Figure 2.2.** (a) Temporal β diversity (β_t) of macroinvertebrate assemblages declined in response to increasing chlorophyll-*a* (chl-*a*) and mean macroinvertebrate biomass (1-20 g m^{-2} , points scaled by size), and showed a positive relationship with increasing temperature variability ($^{\circ}\text{C}$, interquartile range [IQR], with variability decreasing from red to blue). β_t was quantified using the exponentiated Shannon diversity index (Shannon). (b) The GLM response surface of β_t (Shannon) in response to temperature variability and macroinvertebrate biomass shows the modeled response of β_t (Shannon) to temperature variability at different levels of eutrophication (67.45% deviance explained, chl-*a* represented by lines ranging from 25-525 g m^{-2}). Macroinvertebrate biomass was included in the model, and was held constant at the mean observed value across all study sites to calculate the temperature response surface. 22
- Figure 2.3.** (a) Spatial β diversity (β_{spat}) displayed seasonal oscillations over the 2 year study duration, and tracked with (b) site water temperatures ($^{\circ}\text{C}$), which suggests that the declines in temporal β diversity with increasing eutrophication stem from losses in seasonally driven biodiversity. β_{spat} was quantified as the multivariate dispersion (MVD) around sampling event centroids in ordination space, and represents the degree of assemblage differentiation between spatial localities during a given sampling event. β_{spat} was overlaid with a GAM smoother

(a, dotted line) to highlight the oscillations. (c) β_{spat} was generally higher in the cooler months than in the summer, and displayed a negative relationship with mean site water temperature (GLM regression, $p = 0.032$, 38.87% deviance explained)..... 24

Figure 3.1. Richness based measures of biodiversity at both local (α -diversity, a) and temporally integrated (temporal γ -diversity) scales across a phosphorus enrichment gradient (as total phosphorus, TP). α -diversity increased with TP enrichment ($p < 0.001$), while TP was not predictive of temporal γ -diversity. (c) Temporal β_{TOT} also displayed no relationship with TP enrichment. 37

Figure 3.2. Two different modes of temporal β -diversity displayed markedly different relationships with total phosphorus (TP) enrichment. (a, blue graphics) Temporal β_{BAL} declined sharply with increasing TP (segmented regression, $p < 0.001$), while (b, green graphics) temporal β_{GRA} increased with increasing TP (seg. regression, $p < 0.001$). Histograms shown are the distribution of computed changepoints in the relationships between temporal β_{BAL} and β_{GRA} with TP, and vertical red lines are the means of those distributions. 38

Figure 3.3. Spatiotemporal dissimilarity in community structure across 35 streams and 2 years constructed from pair-wise dissimilarity measures of β_{TOT} (total β -diversity, left column, stress = 0.13), β_{BAL} (measuring compensatory dynamics, center column, stress = 0.18), and β_{GRA} (measuring abundance-gradients, right column, stress = 0.22). Points are colored by low total phosphorus (TP, green triangles) and high TP (orange circles) sites as determined by changepoint analysis. Top panel arrows display significant ($p < 0.001$) environmental vectors predictive of spatiotemporal structure in community composition. Bottom panel displays the 2D spatial mean of each sampling event split by high and low TP sites, and are connected by successional vectors. Numbers are sampling events (1 – Jun '14, 2 – Aug '14, 3 – Oct '14, 4 – Dec '14, 5 – Feb '15, 6 - April '15, 7 – Jun '15, 8 – Aug '15, 9 – Oct '15, 11 – Feb '16, 12 – April '16). 39

Figure 3.4. Community stability (CS) as measured by the ratio of mean biovolume to the biovolume standard deviation for algae from each site against two modes of temporal β -diversity, (a, top) β_{BAL} and (b, bottom) β_{GRA} . CS increased with increasing levels of temporal β_{BAL} ($p < 0.001$, deviance explained = 37.1 %) and declined with increasing levels of temporal β_{GRA} ($p < 0.001$, dev. explained = 62.8 %). 41

Figure 4.1. Periphyton tissue C:P, C:N, and N:P all declined in response to total phosphorus (TP, log-scale) concentrations. GAM smoothers (all $p < 0.001$) indicated that TP explained more variation in C:P (deviance explained = 88.2%) and N:P (dev. exp. = 84.1%) than C:N (dev. exp. = 69.9%). 56

Figure 4.2. Nonmetric multidimensional scaling (NMDS) ordination of algal (left pane, green, 2D stress = 0.07) and macroinvertebrate (right pane, orange,

2D stress = 0.16) assemblages based on 2-year mean biovolumes ($\text{mm}^3 \text{m}^{-2}$) and abundances (m^{-2}), respectively. Point size indicates the degree of nutrient enrichment as measured by TP and periphyton tissue C:P. Arrow indicate correlations of environmental gradients associated with assemblage structure among sites. The direction of the arrow signifies the direction of correlation, and the length of the arrow the magnitude of correlation (all shown vectors $p < 0.001$)...... 57

Figure 4.3. Changes in algal (a, top pane) and macroinvertebrate (b, bottom pane) assemblages across a total phosphorus (TP, $\mu\text{g L}^{-1}$) gradient as identified by Threshold Indicator Taxa ANalysis (TITAN). Responses are split between taxa increasing (red, open point) and decreasing (blue, closed points) to TP enrichment. The bottom-most plot (continued) in each panel shows the filtered sum-z scores of significant indicator taxa, while the middle panes show the distribution of sum-z maxima as identified from 999 bootstrap replicates. Peaks in each distribution may be interpreted as evidence for a synchronous shift in assemblage composition. Candidate changepoint locations are displayed in the top panel, along with 95% confidence intervals around the changepoints. 59

Figure 4.4. Changes in algal (a, top pane) and macroinvertebrate (b, bottom pane) assemblages across a periphyton tissue C:P gradient as identified by Threshold Indicator Taxa ANalysis (TITAN). Responses are split between taxa increasing (red, open point) and decreasing (blue, closed points) to periphyton resource quality. The bottom-most plot (continued) in each panel shows the filtered sum-z scores of significant indicator taxa, while the middle panes show the distribution of sum-z maxima as identified from 999 bootstrap replicates. Peaks in each distribution may be interpreted as evidence for a synchronous shift in assemblage composition. Candidate changepoint locations are displayed in the top panel, along with 95% confidence intervals around the changepoints. 61

Figure 4.5. Significant indicator taxa as identified by Threshold Indicator Taxa ANalysis (TITAN) on 2-year mean algal biovolumes across a gradient of total phosphorus (TP, $\mu\text{g L}^{-1}$) enrichment. The distributions of individual taxa decreasing (a, blue) and increasing (b, red) with increasing TP represent the location and certainty of taxon changepoints generated from 1000 bootstrap replicates. Vertical black lines within the distribution represent the bootstrap median, with tighter density curves illustrating more certainty about taxon threshold responses to TP. The color gradients illustrate the magnitude of the response (z-score). Genus names are displayed, with species and variety names abbreviated for clarity (taxon codes and full species names in Appendix C)...... 65

Figure 4.6. Significant indicator taxa as identified by Threshold Indicator Taxa ANalysis (TITAN) on 2-year mean macroinvertebrate densities in response to periphyton nutrient content (tissue C:P). Note that the x-axis has been inverted so that enrichment is still represented by a left to right gradient. The distributions of individual taxa decreasing (a, blue) and increasing (b, red) with increasing

nutrient content represent the location and certainty of taxon changepoints generated from 1000 bootstrap replicates. Vertical black lines within the distribution represent the bootstrap median, with tighter density curves illustrating more certainty about taxon threshold responses to TP. The color gradients illustrate the magnitude of the response (z-score)..... 67

Figure A.1. Locations of sampling sites in the Illinois R. drainage basin and surrounding areas spanning the border of Oklahoma and Arkansas (USA, 1:750,000 Landsat shaded basemap, USGS), with points continuously scaled to 2 y mean total phosphorus concentration ($\mu\text{g L}^{-1}$). 75

Figure A.2. Site richness (left pane), cumulative site richness (middle pane), and β_t calculated as cumulative site richness/mean site richness (right pane) displayed across mean total phosphorus (TP) concentrations. Each black point (left pane) represents the number of taxa recorded at each site visit, whereas the red overlays denote the mean richness and TP for each site across all 12 sampling events. Dotted lines represent significant relationships from GLM regressions, with mean site richness displaying a weak but positive relationships with TP ($p = 0.03$), and $\beta_t(\text{Richness})$ declining as TP increases ($p = 0.003$). 75

Figure B.1. Total phosphorus (TP, $\mu\text{g L}^{-1}$) concentrations of study sites ranked by increasing mean TP over the 2 year study, which increased roughly log-linearly. Points denote site means, while the darker inner bars and lighter outer bars signify the 95% confidence interval and the range of TP concentrations observed during the study, respectively. 81

Figure B.2. Third NMDS axis displayed against NMDS axis 1 showing spatiotemporal dissimilarity in community structure across 35 streams and 2 years constructed from pair-wise dissimilarity measures of β_{TOT} (total β -diversity, left column, stress = 0.13), β_{BAL} (measuring compensatory dynamics, center column, stress = 0.18), and β_{GRA} (measuring abundance-gradients, right column, stress = 0.22). Points are colored by low total phosphorus (TP, green triangles) and high TP (orange circles) sites as determined by changepoint analysis. Top panel arrows display significant ($p < 0.001$) environmental vectors predictive of spatiotemporal structure in community composition..... 83

Figure C.1. Periphyton tissue C:P, C:N, and N:P all declined in response to total nitrogen (TN, log-scale) concentrations. GAM smoothers indicated that TN was predictive of C:P ($p < 0.001$, deviance explained = 73.4%) and N:P ($p < 0.001$, dev. exp. = 68.5%) content of periphyton, but explained less deviation in the response of periphyton C:N ($p < 0.001$, deviance explained = 48.0%). 85

Figure C.2. Significant indicator taxa as identified by Threshold Indicator Taxa ANalysis (TITAN) on 2-year mean algal biovolumes across a gradient periphyton nutrient content as measured by the ratio of tissue carbon to phosphorus (C:P) The distributions of individual taxa decreasing (a, blue) and increasing (b, red)

with increasing enrichment represent the location and certainty of taxon changepoints generated from 1000 bootstrap replicates. Vertical black lines within the distribution represent the bootstrap median, with tighter density curves illustrating more certainty about taxon threshold responses to C:P. The color gradients illustrate the magnitude of the response (z-score). Taxon codes are displayed (taxon codes and full species names in Appendix C, Table C.2). 88

Figure C.3. Significant indicator taxa as identified by Threshold Indicator Taxa ANalysis (TITAN) on 2-year mean macroinvertebrate abundances across a gradient of total phosphorus (TP, $\mu\text{g L}^{-1}$) enrichment. The distributions of individual taxa decreasing (a, blue) and increasing (b, red) with increasing TP represent the location and certainty of taxon changepoints generated from 1000 bootstrap replicates. Vertical black lines within the distribution represent the bootstrap median, with tighter density curves illustrating more certainty about taxon threshold responses to TP. The color gradients illustrate the magnitude of the response (z-score). 90

LIST OF TABLES

<p>Table A.1. Summary of results from generalized linear models (GLMs) relating both β_t (Shannon) and β_t (MVD) measures of temporal beta diversity (β_t) to two measures of eutrophication (Chlorophyll-a; Chl-a and total phosphorus; TP) with covariates. Models are grouped first between response variable (i.e. measure of β_t), then by measure of eutrophy (TP and Chl-a were correlated, and for this reason evaluated in separate models). Models were selected using AICc and deviance explained (%), and are ordered by increasing AICc values within groups, so that the model with the lowest AICc score is at the top of each grouping. Covariates that remained after model selection included temperature variability ($^{\circ}\text{C}$ IQR, interquartile range), mean total macroinvertebrate biomass (g m^{-2}), and mean snail biomass (g m^{-2}).</p>	76
<p>Table A.2. Summary environmental and biotic data collected at 34 study sites in the Illinois River drainage basin and surrounding area every-other-month from June 2014 to April 2016 (12 sampling events). One site was exposed to untreated wastewater during the study and was excluded from analysis. All means are presented with standard deviation in parentheses. Temporal habitat heterogeneity is a unitless measure. Scouring was the number of times we sampled within 10 d of a discharge event exceeding five times median base flow. Temperature variability (IQR) is the interquartile range of water temperature observed at each site over all sampling events. β_t (Richness) was calculated as mean site richness/cumulative site richness. β_t (Shannon) and β_t (MVD) incorporate abundance information, and are the exponentiated Shannon diversity index (Shannon), and multivariate dispersion (MVD) around group centroids, respectively.</p>	77
<p>Table B.1. Summary results from environmental vector fitting to NMDS ordinations (NMDS axis 1 and 2) of stream algae using three measures of spatiotemporal dissimilarity.....</p>	82
<p>Table C.1. Summary results from environmental vector fitting to NMDS ordinations of periphytic algae and benthic macroinvertebrates using Bray-Curtis dissimilarity as the distance measure.....</p>	86
<p>Table C.2. Summary of pure and reliable algal taxa as identified by Threshold Indicator Taxa ANalysis (TITAN) responding to total phosphorus enrichment, and comparison of these taxa to analysis by Potapova and Charles (2007).</p>	91

ACKNOWLEDGMENTS

I am indebted to Dr. Ryan King for both mentorship and financial support of my research. I also thank my committee: Robert Doyle, David Kahle, Sanghoon Kang, and Thad Scott. I am indebted to Jeff Back, whose hard-work and humor made the field and laboratory much more enjoyable. I would also like to acknowledge the Research Technicians working on the Oklahoma Scenic Rivers Joint Phosphorus Study: Morgan Bettcher, Stephen Elser, and Katherine Hooker. The data supporting this dissertation would not have been possible without them. I would also like to thank my lab-mates and fellow graduate students: Caleb Robbins, Lauren Housley, Brittany Perrotta, Moncie Wright, Dan Hiatt, Will Matthaesus, Elias Oziolor, Alyse Yeager, and Eric LeBrun for their friendship and collaboration.

My parents, Fred and Tammy, and my sister and her husband, Sarah and Steven, have provided immeasurable support and love, and I will never be able to properly thank them. My fiancé, Katherine, has been a source of unwavering support during my studies and has lent a critical eye to most parts of this document. I would also like to thank her father, David, and her grandmother, Bobbie, for making me feel a part of their family.

This dissertation was supported in part by the Arkansas-Oklahoma Joint Study Committee, and I thank Derek Smithee, Brian Haggard, Shanon Phillips, Marty Matlock, Shellie Chard, Ryan Benefield, and Thad Scott for their service on the Committee and for their input into the design of the Scenic Rivers Joint Phosphorus Study. I am grateful for the support of the Baylor University Department of Biology, and the Center for Reservoir

and Aquatic Systems Research (CRASR). I also thank Drs. Stephen Porter and Barbara Winsborough, who performed taxonomic identifications and biovolume estimates of soft algae and diatoms, respectively (Chapters Three and Four).

DEDICATION

To Katherine,
your love and support mean everything.

/ ^ ^ \
/ 0 0 \
v \ y /v
/ - \
| | (_v

ATTRIBUTIONS

Chapter Two of this document was previously published by Stephen C. Cook (SCC) with co-authors Lauren Housley, Jeffrey A. Back, and Ryan S. King (RSK). SCC conducted the analyses and wrote the manuscript. RSK designed the study, and all authors collected data and contributed to revisions.

CHAPTER ONE

Introduction

Rise of the Novel Environment

Natural ecosystems are increasingly moving towards novel states due to widespread human activity (Radeloff et al. 2015). Anthropogenic impact is so pervasive, and the effects so disrupting to natural communities that in recent years discussion has rapidly moved from the proposal that we are in a new geological epoch defined by human agency (Steffen et al. 2007, Zalasiewicz et al. 2011), to discussion about how best to delineate its beginning (Steffen et al. 2011, Lewis and Maslin 2015). Current abiotic conditions in altered ecosystems are highly dissimilar to conditions organisms experienced and adapted to throughout their evolution (Hobbs et al. 2009). These novel conditions can alter biotic interactions and species distributions and result in communities that bear little resemblance to their natural counterparts (Midgley et al. 2002, Bates et al. 2017).

Elevated nutrient concentrations, primarily nitrogen (N) and phosphorus (P), are the leading cause of novelty in freshwaters ecosystems worldwide (Carpenter et al. 1998, Smith et al. 2006, Paulsen et al. 2008, Dodds and Smith 2016). Most inorganic P enters aquatic environments naturally from the weathering of phosphate-rich rock (Turner and Condron 2013), while inert N₂ gas in the atmosphere is converted into bioavailable N by aquatic and terrestrial diazotrophs (Galloway et al. 2008). Potential growth of primary

producers far outpaces the natural rates of new N and P entering waterways, which results in nutrient limitation in many aquatic communities (Elser et al. 2007).

In streams and rivers, conditions are inexorably governed by features of the surrounding catchment (Hynes 1975, Allan 2004), and widespread changes in land use contribute large anthropogenic nutrient subsidies to waterways (Carpenter et al. 1998). Uptake of fertilizer N and P by crops is dwarfed by the nutrients that remain in the soil or are exported to waterways by surface and subsurface runoff (Sharpley et al. 2004). Changes in land-use, combined with point-source discharges of wastewater effluent high in N and P (Dorioz et al. 1998, Brooks et al. 2006) have significantly altered the concentrations of nutrients in lotic ecosystems. The impacts of anthropogenic nutrient enrichment on communities can persist long after the proximate causes are removed (Harding et al. 1998, Jarvie et al. 2012), therefore understanding how communities respond to nutrient enrichment is especially important.

The Impacts of Nutrient Enrichment on Stream Communities

Nutrient enrichment directly affects the fitness of algal species because algae are able to use the dissolved forms of N and P (Stewart 1987, Hillebrand and Sommer 1999). Because algae have adapted to conditions largely defined by limited nutrient availability (Elser et al. 2007), release from nutrient limitation upsets the competitive balance of resource exploitation that has evolved in algal assemblages (Snyder et al. 2002, Stevenson et al. 2008). Though extremely high nutrient concentrations may be toxic (Zhang et al. 2018), most of the effects of nutrient enrichment on higher trophic levels are mediated by the periphyton. Large standing stocks of benthic biomass associated with eutrophication may senesce and decompose, which leads to precipitous declines in

dissolved oxygen concentrations and mortality of benthic macroinvertebrates and fish (Carpenter et al. 1998). Even low levels of enrichment can alter consumer fitness by alleviating the stoichiometric mismatch between nutritionally poor periphyton and higher trophic levels with greater N and P demands (Singer and Battin 2007, Evans-White et al. 2009). These mechanisms can cause reorganization of species associations across multiple trophic levels (Hobbs et al. 2009, Taylor et al. 2014).

Nutrient enrichment frequently causes threshold changes in species distributions (i.e. a large shift in species presence or abundance in response to a disproportionately small change in environmental condition, *sensu* Groffman et al. 2006). Species' fitness across natural environmental gradients typically approximates a bell-curve in highly diverse communities (Gauch and Whittaker 1972), with optimal growth and reproductive success occupying a relatively narrow range of environmental conditions. Nutrient concentrations in excess of evolutionary norms causes strong, nonlinear changes in stream community structure (Wagenhoff et al. 2016). The direct effects of nutrient enrichment on primary producers acts through different mechanistic pathways than the indirect effects of enrichment on higher trophic levels, and for this reason the structure of different assemblages may respond uniquely to the effects of eutrophication (Taylor et al. 2014). Many species in a community changing synchronously to an environmental stressor may be indicative of a community-level threshold, which are often accompanied by changes in ecosystem function that are difficult to predict (Dodds et al. 2010).

Spatial and Temporal Niche Partitioning

A simple but powerful observation from studies of natural communities is that species are unevenly distributed over the Earth (Whittaker 1960). Different environments house different organisms, and species evolve to leverage the numerous dimensions of environmental variation to finely partition available space and resources (Whittaker 1972). In addition to the rich array of possible niches that species may occupy in a particular environment, ecologists have long recognized that community structure is continuously changing at multiple time-scales (Tansley 1935). Species associations reflect a shifting mosaic of biotic and abiotic conditions (Levin 1992), and much of this temporal variation is generated by seasonal changes (Korhonen et al. 2010, Tonkin et al. 2017). Stream ecosystems are especially variable and are characterized by predictable swings in hydrology (i.e. scouring and drying events, Resh et al. 1988, Stanford et al. 2005), irradiance and water temperature (Hillebrand 2009), and variation in resource supply (Rosemond et al. 2000).

Interested researchers and hobbyists alike have historically devoted much attention to the natural histories of stream-dwelling organisms, and these studies have revealed a rich variety of phenology that has evolved in response to seasonal variations in stream habitat (Wolda 1988, Merritt et al. 2008). Both benthic algae and macroinvertebrate growth is governed by thermal regimes (Lamberti and Resh 1985), and even closely related species can display different thermal optima (Vannote and Sweeney 1980). Macroinvertebrate life-stages are seasonally timed to coincide with temporal variation in food supply (Huryn and Wallace 2000) and hydrologic regime (Bonada and Resh 2013, Niu and Knouft 2017). Despite this body of work there remains a

conspicuous lack of analyses that attempt to describe how novel conditions influence seasonally driven changes in community composition.

Spatial and temporal heterogeneity in ecosystems provide opportunity for species to coexist by promoting finely partitioned niches and thereby offsetting competition (Questad and Foster 2008), and this results in higher spatial and temporal dissimilarity in community structure and function (Zuppinge-Dingley et al. 2014). Nutrient enrichment has been shown to decrease the spatial heterogeneity of aquatic communities (Donohue et al. 2009) and alter species distributions (Taylor et al. 2014). Because nutrient subsidies alter the way species partition environmental gradients, declines in temporal niche partitioning may be an important mechanism causing biodiversity declines in stream ecosystems.

Problem Statement

Given the high degree of temporal niche partitioning inherent in stream assemblages, and the lack of studies assessing intra-annual changes in assemblage composition, the impact of nutrient enrichment on seasonal patterns of succession may not be fully realized. If anthropogenic nutrient subsidies alter how species partition temporal niche space, it is possible that focus on spatial scales masks important declines in biodiversity. Further, despite marked differences between how primary producer and consumer assemblages respond to eutrophication, there are few studies assessing the impacts of nutrient enrichment on multiple assemblages at spatiotemporally relevant scales.

Study Objectives

My overarching objective was to assess how anthropogenic nutrient enrichment influenced the spatial distribution and temporal assembly of algal and benthic macroinvertebrate assemblages in stream ecosystems. Specifically, I aimed to (1) determine how nutrient enrichment changed temporal variation in benthic macroinvertebrate assemblages, a group of study organisms with rich life-history strategies able to exploit seasonal niches, (2) determine how nutrient enrichment alters temporal variation in benthic algal assemblages, and (3) quantify and compare both individual species and assemblage-level responses to nutrient enrichment between benthic algae and macroinvertebrates.

Study Area

I studied communities in wadeable streams that transected the border of Oklahoma and Arkansas, USA to address these objectives. The streams were located in the Illinois River drainage basin and several surrounding watersheds which originate in northwest Arkansas and flow southwest into Oklahoma (Fig 1.1) forming Lake Tenkiller and eventually joining the Arkansas River. Land use can vary widely between adjacent catchments, which can lead to different in-stream conditions among sites despite close proximity (Roy et al. 2003, Helms et al. 2009). Study sites were selected so that that stream nutrient concentrations spanned the wide gradient of nutrient enrichment present in the region. Nutrient enrichment among sites varied due to an uneven distribution of land-applied, P-rich poultry litter that serves as an inexpensive fertilizer for the region, and wastewater treatment plant discharges that serve a rapidly expanding human population in northwest Arkansas (Haggard 2010, Scott et al. 2011, Jarvie et al. 2012).

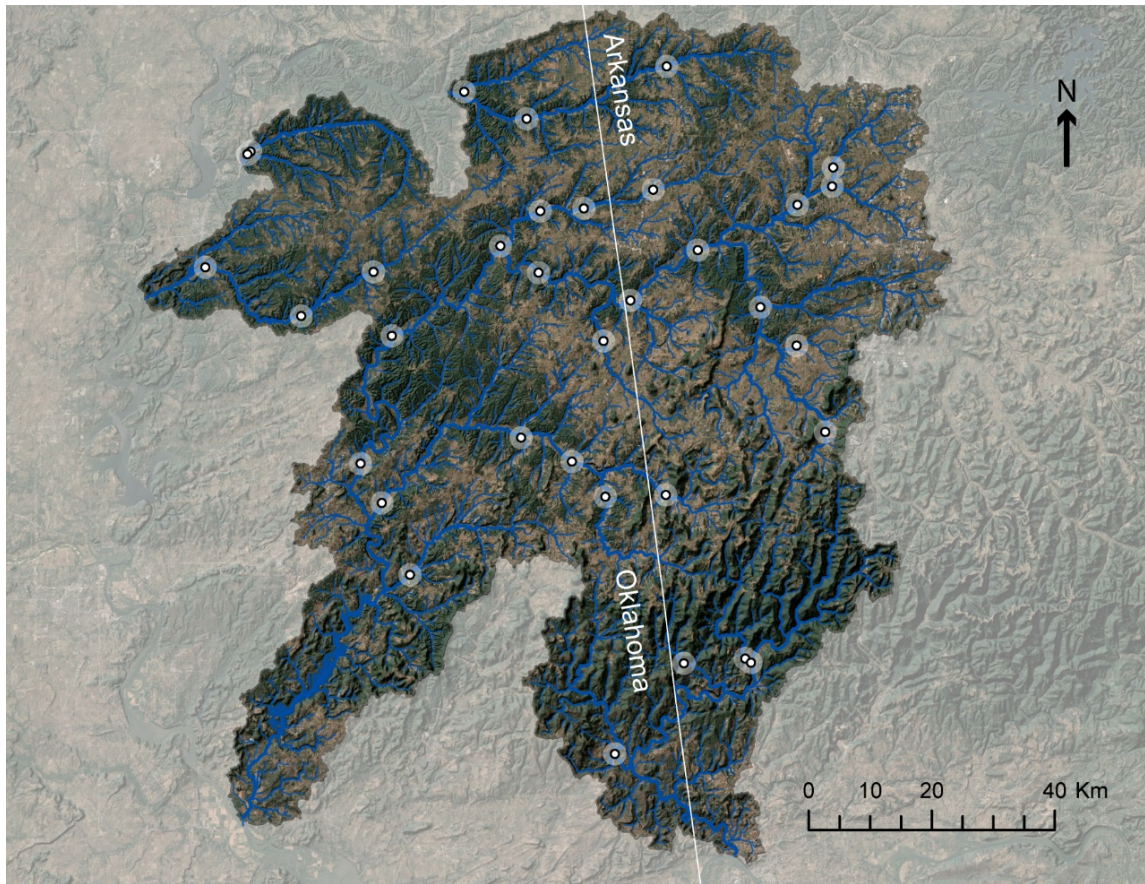


Figure 1.1. Locations of sampling sites ($n = 35$) in the Illinois River and several surrounding watersheds spanning the border of Oklahoma and Arkansas (USA, 1:250000 landsat shaded basemap, USGS). Watersheds of study sites are highlighted by a semi-transparent mask placed on the adjacent landscape. Lake Tenkiller is shown in the southwestern portion of the map, and is formed by the damming of the Illinois River.

Summary of Chapter Contents

This dissertation is divided into five chapters, beginning with the current chapter which includes introductory information and provides a general outline of proposed objectives. Chapter two details the effects of nutrient enrichment on temporal β -diversity in benthic macroinvertebrate assemblages across 35 wadeable streams representing a wide range of P enrichment. Chapter three describes changes in temporal β -diversity of benthic algal assemblages across the same P enrichment gradient, examines temporal

patterns of those assemblages within the framework of compensatory changes in seasonal composition, and explores how different modes of temporal β -diversity influence community stability. Chapter four details a comparative analysis between benthic macroinvertebrate and algal responses to nutrient enrichment, and compares how well direct (i.e. water column nutrient concentrations) and indirect (i.e. enrichment of periphyton nutrient content) measures of nutrient enrichment predict assemblage-level thresholds. Chapter Five synthesizes the findings of chapters two - four, and suggests future avenues of research that could build upon the work presented in this dissertation.

CHAPTER TWO

Freshwater Eutrophication Drives Sharp Reductions in Temporal Beta Diversity

This chapter published as: Cook, S. C., L. Housley, J. A. Back, and R. S. King. 2018. Freshwater eutrophication drives sharp reductions in temporal beta diversity. *Ecology* 99:47–56.

Introduction

Cultural eutrophication of lotic systems is leading to widespread declines in water quality, biodiversity, and valuable ecosystem services (Carpenter et al. 1998, Smith et al. 2006, Paulsen et al. 2008). Nutrient concentrations have increased over reference conditions in most ecoregions of North America (Dodds and Smith 2016), and have the capacity to increase algal biomass and primary production (Elser et al. 2007). Alteration of nutrient regimes in ecosystems limited by nitrogen (N) or phosphorus (P) dramatically shifts the competitive balance of organisms in basal compartments, which in turn elicits changes in higher trophic levels (Carpenter et al. 1998, Nelson et al. 2013). As the prevalence of cultural eutrophication continues to expand, so too does the potential for eutrophication to result in unforeseen, deleterious alterations to ecosystem structure and function (Dodds et al. 2010, Radeloff et al. 2015).

Freshwater assemblages respond strongly to increases in productivity associated with nutrient enrichment (Smith et al. 1999). Beta diversity (β), which is generally defined as the compositional dissimilarity in species assemblages across space or time (Whittaker 1972), reviewed by (Tuomisto 2010, Anderson et al. 2011), provides a conceptual and mathematical link between diversity at a particular locality (alpha

diversity, α) and the regional species pool (gamma diversity, γ). Declines in the compositional heterogeneity of aquatic communities (or spatial beta diversity; β_{spat}) exposed to nutrient enrichment indicate that eutrophication can act as a strong ecological filter, and increase the importance of species sorting mechanisms (Passy and Blanchet 2007, Donohue et al. 2009, McGoff et al. 2013, Goldenberg Vilar et al. 2014). The most striking direct effect of eutrophication on animal communities stems from large increases in benthic biomass, which in turn can lead to precipitous declines in dissolved oxygen concentrations following senescence and decomposition in the basal compartment (Carpenter et al. 1998). Even relatively low levels of nutrient enrichment can elicit shifts in producer community composition and alter the relative concentrations of nutrients in the basal compartments (Rosemond et al. 1993, Cross et al. 2006, Evans-White et al. 2009, Taylor et al. 2014), which can indirectly affect the ability of some consumers to effectively compete. While spatial beta diversity (β_{spat}) has been examined in response to eutrophication and a wide range of other ecological questions (Qian and Ricklefs 2007, Chase 2010, Bini et al. 2014, Heino et al. 2015a), comparatively little study has been devoted to the underlying factors that influence temporal patterns in community composition (but see Mykrä et al. 2011, Hatosy et al. 2013, Steiner 2014, Magurran et al. 2015, Heino et al. 2015b). Specifically, we do not have a clear understanding of how eutrophication impacts the temporal variability of community composition.

Seasonal oscillations in environmental conditions, and in turn the availability and quality of food resources, exert a controlling influence on communities (Tonkin et al. 2017). As a result, organisms have evolved unique life-history strategies to exploit seasonally generated niches (Bêche et al. 2006, Bonada and Resh 2013). Benthic

macroinvertebrates have evolved to time periods of peak growth and maturation at different times of the year to coincide with advantageous conditions (Wolda 1988), which can cause streams to harbor higher biodiversity than can be observed at a single point in time. Moreover, meta-analysis across a variety of aquatic ecosystems found that intra-annual variability was much higher than interannual variability (Korhonen et al. 2010), which suggests that seasonally driven variation in community composition could generate a large portion of biodiversity in aquatic systems.

Given the high degree of seasonal variation inherent in these assemblages, examining the effects of eutrophication at a single time-point across a spatial metacommunity (i.e. a watershed) may be insufficient to fully explain the impact of nutrient enrichment on aquatic communities (Heino et al. 2015b). If eutrophication negatively impacts the competitive ability of species that have evolved to utilize specific temporal niches, then this could cause significant declines in the temporal variation in community composition (or temporal beta diversity; β_t). Thus, spatiotemporally explicit studies are needed to examine the effects of nutrient enrichment on the temporal assembly process, as focusing on the spatial effects of eutrophication alone may mask important declines in biodiversity.

We examined benthic communities among stream reaches that spanned a wide range of P and benthic chlorophyll-a (chl-*a*) concentrations over two years with the goal of determining the relationship between eutrophication and β_t . We hypothesized that increasing nutrient inputs would decrease the degree to which macroinvertebrate assemblages partitioned temporal niche space, resulting in lower β_t with increasing eutrophication. We also considered other environmental variables that are known to

influence macroinvertebrate assemblage composition as potential additional drivers of β_t . As temporal trends can be driven by forces acting on either inter- or intra-annual time scales, we explored the possibility that the trends observed in β_t were the result of an aseasonal signal by also examining β_{spat} across the two-year study period.

Methods

Study Area and Site Characterization

We studied 35 mid-order (3rd-5th) stream reaches in the Ozark Highlands and Boston Mountains Level III ecoregions of Oklahoma and Arkansas, USA within the Illinois River drainage basin and surrounding area every-other-month for 2 years (Appendix A: Fig. A1, 12 sampling events from June 2014 to April 2016). Study sites were selected both to capture the steep P gradient present in the region, as well as to minimize among site habitat variability. We targeted reaches of streams and rivers with open canopies, riffle-run channel units, and cobble-dominated substrate. We collected a suite of in-stream and riparian habitat variables to characterize each site, and focused on total phosphorus (TP) and chlorophyll-a (chl-*a*) as measures of eutrophication. Increases in benthic biomass associated with nutrient enrichment in this region is dominated by filamentous green algae (Chlorophyta), cyanobacteria (Cyanophycota), and diatoms. Data gathered during a concurrent study indicated that periods of peak productivity were associated with rapid uptake of P with little change in ambient N concentrations, high N:P ratios (20 – 2000, typically >100) in the surface water indicative of P rather than N limitation (Dodds and Smith 2016), and proliferation of species known to be associated with P enrichment (*Cladophora glomerata*; Dodds and Gudder 1992).

We collected instantaneous water grab samples in triplicate upstream of macroinvertebrate and periphyton collection activity to quantify TP ($\mu\text{g L}^{-1}$) during each site visit. Water samples were analyzed pursuant to EPA QA/QC standards and APHA/CRASR protocols (APHA 2005, Center for Reservoir and Aquatic Systems Research). Water temperature ($^{\circ}\text{C}$) and turbidity (NTU) were measured using a YSI multiprobe (Yellow Springs International) at the grab sample location. We recorded wetted width (m) at each transect, as well as current velocity (m/s) and canopy cover (0-100%) at the midpoints of each transect. Current velocity was measured using a Marsh-McBirney flowmeter (Loveland, CO) following USGS protocols, and canopy cover was estimated using a densiometer. Substrate embeddedness (0-100%) was visually estimated at each Hess sample location (transect delineation described below). We calculated a measure of physical habitat disturbance (scouring) as the number of times we sampled within 10 d of a discharge event exceeding five times median base flow as determined from USGS gauges. For sites that were ungauged (15 of 35 sites), we associated flow data from neighboring sites that possessed similar hydrology and spatial proximity. While we were unable to directly measure bed stability (Schwendel et al. 2011), the proximity of sampling to high discharge events was included as a relative measure because physical disturbance could lead to higher variation in community composition (Tonkin and Death 2012). There were no impoundments above nor below any study site save for several low-water crossings that did not impede water flow. Elevation (m) and catchment area (km^2) were estimated using a 30-m digital elevation model (USGS National Elevation Dataset; <https://nationalmap.gov/elevation.html>) and a point shapefile of stream-reach locations as outlets. A flow accumulation raster was generated using the *flowacc* function

and, subsequently, catchment boundaries were delineated using the *watershed* function in ArcGIS 10.1 (ESRI, Inc., 2015). Catchment areas were estimated using the cumulative areas of the 30-m pixels within each catchment boundary

Periphyton Sampling

We collected composite periphyton samples at each site using three transects that spanned the width of the riffle-run habitat because within-reach sampling has shown that streams are heterogeneous in terms of biomass and community composition (Heino et al. 2012). Five equidistant points were selected along each transect, and a cobble nearest to each point 0.5 m upstream of the transect line was collected (totaling 15 cobbles site⁻¹ visit⁻¹). Benthic periphyton was removed from the cobbles by vigorous scrubbing and washing, and placed in dark bottles on ice for further processing. Cobble surface area was estimated using the aluminum foil mass-to-area conversion method (Lamberti et al. 1991). To ensure a representative sample all periphyton slurries were thoroughly homogenized with a hand-blender until no large particles or filaments remained, after which the slurry was suspended at a high rate of stirring. Volumetric pipette tips were widened to prevent clogging before 3 aliquots of 2-5 mL were filtered onto 0.8 µm glass fiber filters for chl-*a* (mg m⁻²) determination following Biggs and Kilroy (2000).

Macroinvertebrate Sampling

We estimated benthic macroinvertebrate assemblage structure by sampling the same three transects used for periphyton determination using 0.086 m² Hess samplers (Wildco, Yulee, FL). After periphyton sampling, taking care to choose undisturbed streambed 0.5 m upstream of the removed cobbles, we took 15 Hess samples per site visit

(totaling 1.29 m² of sampled benthos). Samples were aggregated and preserved in buffered formalin (5% v/v). In the lab, samples were rinsed through a large (4.75 mm) sieve and the retained organisms were identified in full. The sample was further rinsed through a medium (2 mm) sieve, and the retained organisms subsampled by homogenizing the organisms in a flooded, large diameter PVC pipe with a 363 µm screen at one end. As the water evacuated the pipe, organisms were evenly distributed on the screen, which allowed us to partition the subsample into quarters. Equal divisions of subsample were processed until both a fixed-area (at least 25% of the total sample) and a fixed-count minimum (at least 300 individuals) were reached for the 2 mm fraction. Using a coupled fixed-area/fixed-count approach has been shown to provide a representative sample of the entire assemblage (King and Richardson 2002). Concentrating on large-bodied taxa (> 2mm) potentially excluded some smaller size-classes and meiofauna, but allowed us to rigorously sample over a wide temporal and spatial extent while still capturing the majority of taxa contributing to local diversity (we detected 61 of 69 taxa at overlapping sites as compared to Petersen et al. 2014 - a regional survey, with 85 additional taxa observed in our study they did not detect). Macroinvertebrate specimens were counted and identified to the lowest operational taxonomic unit, typically genus (except for Chironomidae, Hydrachnidia, and Oligochaeta; Stewart and Stark 2002, Merritt et al. 2008). During identification 10 individuals of each taxa were randomly selected and measured using either an ocular micrometer or Vernier calipers for total length or head capsule width for biomass determination using length-mass regressions (Sample et al. 1993, Benke et al. 1999, Baumgärtner and Rothhaupt 2003, Edwards et al. 2009, Méthot et al. 2012). In instances

where taxa could not be reliably associated with published regressions, we either dried and weighed organisms to create our own, or directly weighed dried organisms (4 taxa – see Table A1 in Appendix A for complete listing). We averaged taxa-specific biomass by site and event, and multiplied this by their counts standardized to the area sampled (1.29 m²). All site-specific biomass was summed to calculate mean total biomass (cumulative site biomass / no. site visits).

Measures of Temporal β Diversity

Measures of β diversity can broadly be divided between values derived directly from classical metrics of α and γ , and multivariate measures which are calculated from pairwise dissimilarity values (*sensu* Anderson et al. 2011). We calculated the exponentiated Shannon index (also referred to as Hill numbers, Jost 2007) for both cumulative temporal diversity (γ_t) and mean time-point specific diversity ($\bar{\alpha}$) for each sampling site, which yields a metric of β_t diversity that incorporates relative abundance information (β_t [Shannon] = $\gamma_t/\bar{\alpha}$). We also calculated β_t (Richness) in a similar manner to the above, but used cumulative site richness and mean site richness (β_t [Richness] = cumulative richness/mean site richness). Though β_t (Richness) excludes abundance information, we included it both to determine if any trends observed in the study were driven by a richness gradient across the region, and for comparative purposes between our study and others.

We also calculated the multivariate dispersion (MVD) around site centroids in multivariate ordination space as a proxy of β_t using the *betadisper* function in R (Anderson et al. 2006). In the MVD method, community abundance data is compressed into a pair-wise dissimilarity measure of choice, after which group dispersion is

calculated in multivariate space from a principal coordinates ordination (PCO). We used a Bray-Curtis dissimilarity matrix due to its proven behavior along ecological gradients using abundance data. Also, we $\log(x+1)$ transformed macroinvertebrate counts to incorporate abundance information without manifold increases in abundant taxa clouding the contribution of rare taxa (McCune et al. 2002). As above, groups were considered as the aggregate of all sampling events of an individual site, with points in PCO space denoting the individual, locality-specific sampling events. The mean distances to group centroids were calculated, which we denote as β_t (MVD).

Modeling

We first determined if any richness trends were present along our main gradient of interest by directly regressing mean site richness, cumulative site richness, and β_t (Richness) on mean TP and chl-*a* using generalized linear models (GLMs). We then utilized GLMs within an iterative information-theoretic framework to examine the effect of eutrophication and other contributing or confounding variables on β_t (Shannon) and β_t (MVD) (Zuur 2009). We visually screened variables known to influence macroinvertebrate diversity through a series of bi-plots and multivariate bubble plots, which included the two measures of eutrophy with measures of habitat variability (discussed below), watershed area, frequency of scour, and mean total and snail macroinvertebrate biomass. This, coupled with correlation matrices, enabled us to select variables for model inclusion as well as assess collinearity and potential interactive effects. Although macroinvertebrate biomass was potentially non-independent, we viewed its use in the model as logical because the objective of this study was to characterize the effect of stream eutrophication on β_t , and a large amount of eutrophy-

driven biomass could be sequestered in the macroinvertebrate compartment. Also, the dominant grazers in the region were operculate snails (Pleuroceridae), and due to top-down suppression of benthic algal biomass, could potentially confound one measure of eutrophication (*chl-a*). For these reasons, mean total macroinvertebrate as well as mean snail biomass were each evaluated separately in modeling efforts. Because TP and *chl-a* are highly correlated, each was modeled and reported separately for β_t (Shannon) and β_t (MVD).

As a measure of physical habitat variability through time, we calculated the MVD of temporal centroids based on a Euclidean distance matrix constructed from 5 instream and riparian variables; canopy cover, wetted width, midpoint current velocity, substrate embeddedness, and turbidity (all variables standardized to mean = 0 and SD = 1, Astorga et al. 2014). Composite measures sometimes have failed to yield significant relationships with community variation, so we also considered individual predictors (interquartile range of the 5 environmental variables, IQR) as potential drivers of β_t (Heino et al. 2015a).

In summary, the GLMs modeled both β_t (Shannon) and β_t (MVD) in response to TP and *chl-a* with potential covariates. We specified a gamma distribution with a log-link function due to variance behavior, distributions of the residuals from each model, and positively-bound continuous response variables. Covariates were sequentially removed and AICc values examined in conjunction with deviance explained (%) to select the simplest models that explained the most variation in the response. We considered models with $\Delta AICc < 2$ to be comparable in explanatory power (Bolker 2008). In cases where the

most parsimonious model included covariates, we generated response surfaces examining the behavior of one predictor while holding the other predictors static.

As the analysis above is insensitive to the nature of the temporal trend (vectoral vs. cyclic *sensu* Korhonen et al. 2010), we needed to verify our hypothesis that any change to β_t in response to eutrophication was driven by the collapse of a seasonal signal rather than the presence of an interannual one. We revisited the MVD analysis framework, and specified sampling time-points as groups, with the distance to multivariate centroid interpretable as the degree of assemblage differentiation between spatial localities during a given sampling event; β_{spat} (MVD). If present, an interannual signal would manifest as the absence of any trend in β_{spat} plotted against the day of year. The *vegan* package was used to implement the *betadisper* function, and classical measure of β_t were calculated using functions written in the R language environment (S.C. Cook, unpublished scripts; version 3.3; R Project for Statistical Computing, Vienna, Austria). All calculations, modeling, and plotting was also conducted in R.

Results

Mean TP and chl-*a* ranged from 7.25 to 107.44 $\mu\text{g L}^{-1}$, and 43.53 to 638.91 mg m^{-2} , respectively (Appendix A: Table A2). One site was exposed to untreated wastewater discharge during the study, resulting in near complete macroinvertebrate mortality, and was excluded from analysis. We catalogued 212 unique taxa (Appendix A: Table A1), and mean and median richness per sample was 26.15 and 26, respectively. Cumulatively, we identified 331,728 individuals over the course of the study, and mean and median counts per sample were 829 and 545, respectively. Cumulative site richness ranged from 52 to 97, and displayed no trend with either measure of eutrophy, while mean site

richness and β_t (Richness) exhibited a weak but increasing ($p=0.03$, 1.2% deviance explained) and sharp decreasing trend ($p=0.003$, 25.1% dev. explained) with TP, respectively (Appendix A: Fig. A2). Both β_t (Shannon) and β_t (MVD) showed sharp decreases in response to increasing TP and chl-*a*, and displayed responses to secondary predictors including temperature variability (IQR), temporal habitat heterogeneity, disturbance frequency, and both total macroinvertebrate and snail biomass.

The model selection process resulted in 3 models of similar explanatory power using TP, and 4 models of similar explanatory power using chl-*a* as the measure of eutrophy. Below we report the most parsimonious models for both measures of β_t (see Appendix A: Table A1 for a complete listing). Secondary predictors that remained after model selection included temperature variability, and two measures of macroinvertebrate biomass (mean total and snail biomass). The most parsimonious GLM of all models considered included an interactive effect between mean total macroinvertebrate biomass and TP (Fig. 2.1, $p < 0.0001$, dev. explained = 71.74%), and showed β_t (MVD) declining in response to both TP and mean total macroinvertebrate biomass. Macroinvertebrate biomass played a particularly large explanatory role at low to moderate levels of P enrichment, and showed a wedge-shaped response with increasing P enrichment.

The most parsimonious model using chl-*a* as the measure of eutrophy included total macroinvertebrate biomass and temperature variability to predict β_t (Shannon) (Fig. 2.2, $p < 0.0001$, dev. explained = 67.45%). β_t (Shannon) declined in response to increased macroinvertebrate biomass, and increased in response to temperature variability.

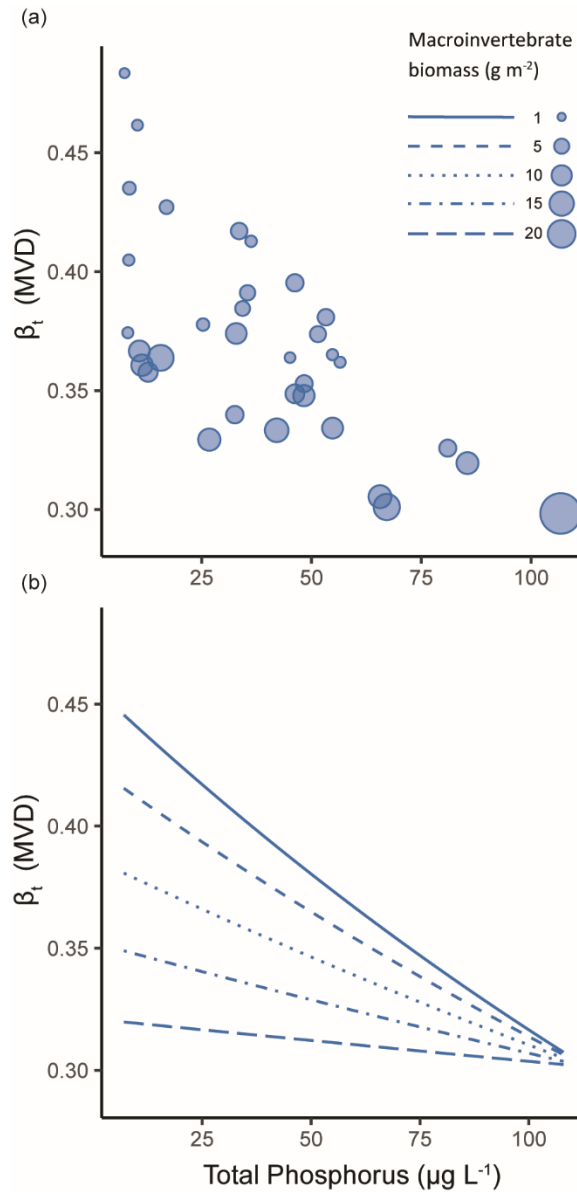


Figure 2.1. Temporal β diversity (β_t) of macroinvertebrate assemblages declined in response to total phosphorus (TP, $\mu\text{g L}^{-1}$) and mean macroinvertebrate biomass (g m^{-2}), which indicates increased temporal homogenization of community composition with increasing nutrient enrichment. β_t was quantified as the multivariate dispersion (MVD) around site centroids in ordination space. (a) Raw data points are sized by mean macroinvertebrate biomass observed at each site over the 2 y study duration. The model describing the most variation in β_t (MVD, 71.74% deviance explained) included an interactive effect between TP and macroinvertebrate biomass. (b) The GLM response surface of β_t (MVD) to TP and macroinvertebrate biomass shows the modeled response of β_t (MVD) to TP at different levels of macroinvertebrate biomass (represented by lines ranging from 1-20 g m^{-2}).

However, total macroinvertebrate biomass did not provide as large a boost in explanatory power over snail biomass when using chl-*a* as the measure of eutrophy. Instead, mean total macroinvertebrate and mean snail biomass provided comparable explanatory power for both β_t (Shannon) and β_t (MVD) when chl- *a* and temperature variability were included as covariates, with $\Delta AICc$ scores between models of 1.39 and 1.88, respectively. β_{spat} illustrates differences in the macroinvertebrate assemblages across the TP gradient during a particular sampling event, and tracked with seasonally-driven changes in water

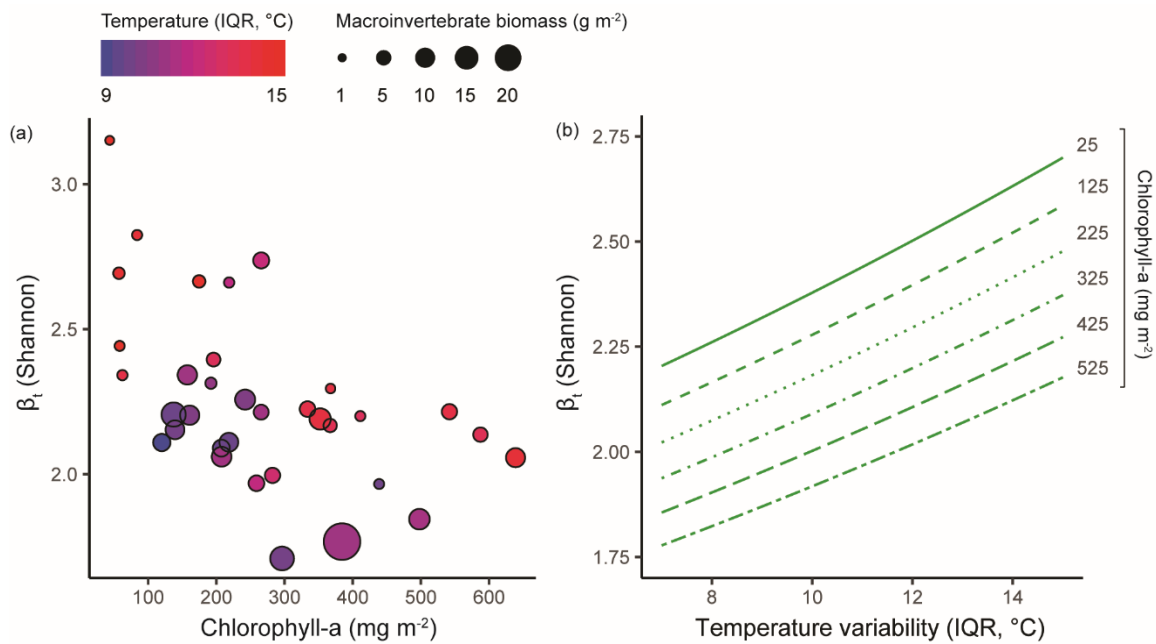


Figure 2.2. (a) Temporal β diversity (β_t) of macroinvertebrate assemblages declined in response to increasing chlorophyll-*a* (chl-*a*) and mean macroinvertebrate biomass (1-20 g m⁻², points scaled by size), and showed a positive relationship with increasing temperature variability (°C, interquartile range [IQR], with variability decreasing from red to blue). β_t was quantified using the exponentiated Shannon diversity index (Shannon). (b) The GLM response surface of β_t (Shannon) in response to temperature variability and macroinvertebrate biomass shows the modeled response of β_t (Shannon) to temperature variability at different levels of eutrophication (67.45% deviance explained, chl-*a* represented by lines ranging from 25-525 g m⁻²). Macroinvertebrate biomass was included in the model, and was held constant at the mean observed value across all study sites to calculate the temperature response surface.

temperature (Fig. 2.3a,b). The cyclic tracking of β_{spat} with water temperature, highlighted by the GAM smoother, indicates that declines in β_t stem from losses in seasonally generated biodiversity. When regressed against mean site water temperature, β_{spat} was generally higher in the cooler months, and lower in the summer (Fig. 2.3c, $p = 0.0318$, dev. explained = 38.87%).

Discussion

Our study shows that eutrophication stemming from anthropogenic nutrient inputs leads to more temporally homogenous communities. Species comprising benthic communities are intimately linked to seasonal cues that govern the timing of reproductive cycles and peak resource assimilation (Wolda 1988, Bêche et al. 2006, Johnson et al. 2012, Bonada and Resh 2013). The cyclic trend of β_{spat} (Fig. 2.3) strongly suggests that the decline in β_t with increasing eutrophication was generated by the collapse of naturally occurring seasonal oscillations in community composition.

High values of β_t at the low end of the eutrophication gradient argue for a larger role of temporal niche partitioning (Fig. 2.1), whereas the decreasing and narrowing range of β_t as eutrophication increases suggests an expansion of temporal niche space dominated by exploitative taxa. Finely partitioned temporal niches are occupied by taxa with life-history strategies that maximize resource utilization by temporally offsetting interspecific competition, or timing periods of peak cohort growth to co-occur with the availability of basal resources or ideal hydrology (Merritt et al. 2008). Freshwater systems are increasingly experiencing novel nutrient concentrations uncharacteristic of

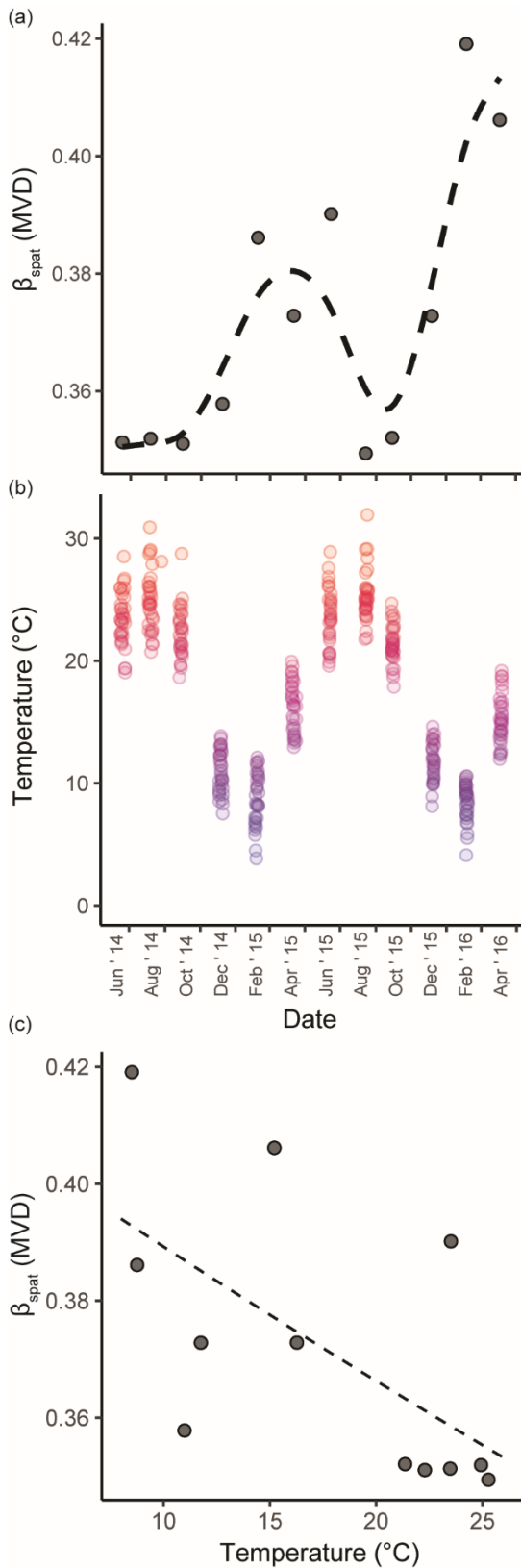


Figure 2.3. (a) Spatial β diversity (β_{spat}) displayed seasonal oscillations over the 2 year study duration, and tracked with (b) site water temperatures ($^{\circ}\text{C}$), which suggests that the declines in temporal β diversity with increasing eutrophication stem from losses in seasonally driven biodiversity. β_{spat} was quantified as the multivariate dispersion (MVD) around sampling event centroids in ordination space, and represents the degree of assemblage differentiation between spatial localities during a given sampling event. β_{spat} was overlaid with a GAM smoother (a, dotted line) to highlight the oscillations. (c) β_{spat} was generally higher in the cooler months than in the summer, and displayed a negative relationship with mean site water temperature (GLM regression, $p = 0.032$, 38.87% deviance explained).

their evolutionary past (King et al. 2011, Radeloff et al. 2015), which release communities from nutrient limitation (Carpenter et al. 1998). Novel increases in nutrient inputs alter the competitive balance of temporal resource exploitation, effectively reducing the benefit that specialist taxa gain by occupying a particular temporal niche. Both experimental evidence (Cross et al. 2006) and observational field studies (Singer and Battin 2007, Evans-White et al. 2009) show that taxa with faster growth rates and higher P demand respond strongly to nutrient enrichment. As nutrient inputs increase, taxa normally constrained by evolutionary P-limitation are released to rapidly complete their life-cycles (Elser et al. 2000, Brown et al. 2004), which would shift assemblage composition by altering the dominant form of voltinism present in the assemblage.

There were likely additional environmental filters concomitant with high levels of eutrophication that caused direct stress to sensitive taxa; such as diel fluctuations in dissolved oxygen (Carpenter et al. 1998), increased rates of sedimentation (Paulsen et al. 2008), and homogenization of the physical structure of the basal resource compartment (Dodds and Gudder 1992, Goldenberg Vilar et al. 2014). Declines in assemblage variation in response to anthropogenic stressors have primarily been attributed to large reductions in the number of taxa at impacted sites (Helms et al. 2009, Johnson et al. 2012). While we did not observe any reductions in cumulative site richness with increasing eutrophication, anthropogenic stressors have been shown to have a disproportionate effect on specialist taxa (Gutiérrez-Cánovas et al. 2013). Likely a combination of both direct taxa responses to the eutrophication gradient and indirect effects on interspecific interactions lead to declines in β_t .

Seasonal cues manifest primarily as changes in irradiance and precipitation (Newbold et al. 1994), which can vary widely by latitude and region. The magnitude of seasonality and the predictability of seasonal events govern the degree to which communities have evolved to utilize distinct temporal niches (Tonkin et al. 2017). Though we found a strong relationship between eutrophication and β_t , the degree to which β_t is reduced is likely dependent upon the degree of seasonality present in a given region (Bêche et al. 2006, Bonada and Resh 2013). The spatial extent of the study contains numerous ground-water seeps and several wastewater treatment plant discharges; both which buffer stream water temperature. Thermal regime is one of the primary controls of macroinvertebrate growth and life-history event synchronization, and even closely related taxa can display different optimal thermal conditions (Vannote and Sweeney 1980). Though we did not explicitly test the mechanism of action, it is likely that decreased variability in temperature selects against taxa that utilize fast-seasonal life cycle adaptations (Hawkins et al. 1997, Wood et al. 2005), thereby decreasing β_t .

Both the strength and weakness of community analysis lies in its ability to integrate abiotic conditions and biotic interactions across time, and difficulty arises when the antecedent conditions that led to the sampled community are no longer observable. These findings strongly suggest that treating temporally dynamic communities as relatively static assemblages is a simplification that may fail to detect temporally explicit assemblage-environment relationships (Heino et al. 2015c). Rather, sampling that occurs only annually may generally prove to be inadequate for the study of metacommunity structure at the regional level for a variety of aquatic assemblages with active dispersal capabilities (Johnson et al. 2012, Erős et al. 2012, Fernandes et al. 2014, Hewitt et al.

2016). Incorporating appropriate temporal extent into study design is vital to address ecological questions that may be influenced by temporal factors, and the majority of studies to date have either focused on a temporal scale too fine to detect seasonality (~ 1 mo. duration, Brown 2003), or on a temporal extent aimed at assessing long-term community stability (repeated sampling of the same time point over multiple years, Mykrä et al. 2011). The wide range of β_t observed in this study examined in light of the wide variation in temporal extents of other studies indicate that comparative examinations of β diversity between systems may be exceedingly difficult (see Heino et al. 2015b), and further study of the factors influencing seasonally driven community variation are needed. However, integrating biological data over sufficient time periods has been shown to reveal underlying environment-community relationships that are not readily apparent with single event sampling (e.g., King et al. 2016).

The increased explanatory power of snail biomass in models where chl-*a* was the measure of eutrophy highlights the importance of quantifying forces that remove benthic algae. Though chl-*a* provides a measure of algal productivity that directly influences macroinvertebrate taxa, it has the drawback of being influenced by both top-down suppression from grazing as well as by physical disturbance. Astorga and others (2014) reported a lack of significance between chl-*a* and β_{spat} when aggregating multiregional data, and attributed this to the confounding influence of physical disturbance (i.e. scouring events removing periphyton biomass). Our findings support their conclusion, as the temporal homogenization of communities may manifest spatially when comparing regions with different levels of productivity. TP, while being causally removed from direct effects on macroinvertebrate taxa, has the benefit of being robust to both physical

and biological disturbance (though rapid uptake by periphyton during bloom conditions may influence nutrient concentrations in the water column).

Measuring biodiversity loss and its impact on ecosystem structure and function is an imperative task that is complicated by the variety of spatial and temporal extents of observational data (Cardinale et al. 2012, Socolar et al. 2016). Our study demonstrates that eutrophication reduces seasonally driven variation in community composition, and adds to a growing body of literature exploring controls on intra-annual succession (Bêche et al. 2006, Bonada and Resh 2013, Steiner 2014, Tonkin et al. 2017). Benthic consumers occupy a key linkage in stream food-webs by remineralizing nutrients and aiding in the breakdown of allochthonous resources (Cross et al. 2005, 2006). Reduced temporal specialization of consumer assemblages could exert a top-down feedback that contributes to decreased ecosystem efficiency caused by increased dominance by generalist consumers. The current prevalence and projected increase in nutrient enrichment (Smith et al. 2006, Paulsen et al. 2008) may therefore have profound and unanticipated effects on the whole aquatic ecosystem that is significantly underestimated by examining the spatial component of biodiversity alone. More studies examining both the spatial and temporal dimensions of β diversity are needed for a robust understanding of community variation and its effects on aquatic ecosystems.

CHAPTER THREE

Compensatory Dynamics of Stream Algae Nonlinearly Break Down with Increasing Nutrient Enrichment

Introduction

Seasonal variation in environmental conditions is a key mechanism structuring biological diversity worldwide (Korhonen et al. 2010, Tonkin et al. 2017). Just as greater spatial heterogeneity provides opportunity for a larger number of species to coexist (Questad and Foster 2008), seasonal changes in abiotic conditions generate a variety of niches throughout the year, causing ecosystems to harbor greater biodiversity than can be observed at a single point in time (Korhonen et al. 2010, Cook et al. 2018). Lotic ecosystems are particularly variable and characterized by seasonally predictable and sometimes extreme swings in hydrology (i.e. scouring and drying events, Resh et al. 1988, Stanford et al. 2005), irradiance and water temperature (Hillebrand 2009), and variation in resource supply (Rosemond et al. 2000). These factors and others combine to form an abiotic template with extraordinarily high seasonal variability, which results in growth optima for different species throughout the year.

Niche partitioning, or evolved partitioning of resources in a heterogeneous environment, has been proposed as a way ecosystems maintain stability despite perturbations (Cardinale 2011, Loreau and de Mazancourt 2013). There is some evidence that the stabilizing effects of diversity on ecosystem properties should be strongest when communities consist of species that respond differently to environmental conditions (Descamps-Julien and Gonzalez 2005, Loreau and de Mazancourt 2013, Gross et al.

2014); that is, when one species declines in abundance another rises to take its place generating asynchrony in species fluctuations (i.e. compensatory dynamics, as reviewed by Gonzalez and Loreau 2009). While compensatory dynamics have been reported in a variety of ecosystems (Bai et al. 2004, Vasseur et al. 2005, Doležal et al. 2019), we do not yet have a clear understanding of how community stability is influenced by seasonal niche segregation.

Benthic algal species, typically the dominant component of stream periphyton biomass, are particularly sensitive to seasonal environmental variation (Fisher et al. 1982, Francoeur et al. 1999, Lange et al. 2011). Examinations of temporal phenomena in stream algae have largely been confined to emergent ecosystem properties such as changes in biomass or autotrophic activity (Dodds & Smith 2016), or to bloom-dynamics of nuisance algae that have negative ecosystem-wide impacts (but see Peterson and Grimm 1992, Rosemond 1994, and Beck et al. 2018). This focus is unsurprising; eutrophication is one of the most pervasive anthropogenic impacts to aquatic ecosystems worldwide (Carpenter et al. 1998, Smith et al. 2006), and can cause dramatic increases in autotrophic production that subsequently impacts higher trophic levels. Algae differentially respond to release from nutrient limitation, and even relatively low levels of enrichment can alter interspecific competition, influencing community composition at both spatial (Passy and Blanchet 2007, Donohue et al. 2009, Taylor et al. 2014) and temporal scales (Larson et al. 2016). Increased resource availability also has decreased the stabilizing effect of biodiversity in microcosms of algae exposed to thermal fluctuations (Zhang and Zhang 2006), which may indicate that nutrient subsidies alter seasonally driven fluctuations in

assemblage composition (i.e. temporal β -diversity) that normally stabilize community biomass.

Under oligotrophic conditions, resource availability places a ceiling on potential biomass (Korhonen et al. 2013, Larson et al. 2016), and temporal β -diversity may largely be driven by species turnover as local environmental conditions alter which species are able to effectively compete for limited resources (Tilman and Pacala 1993, Cardinale 2011). This type of compensatory stabilization, where decreases in some species are balanced by increases in others, while documented in terrestrial plant communities (Tilman 1996, Tilman et al. 1997, Gonzalez and Loreau 2009, Gross et al. 2014), is unexplored in stream ecosystems. Further, abrupt shifts in ecosystem response as are frequently observed under enriched conditions, such as dominance of nuisance algae at certain times of the year, may indicate a breakdown in seasonally driven compensatory dynamics (Jochimsen et al. 2013).

We conducted a natural experiment by selecting 35 large, wadeable streams that spanned a wide nutrient enrichment gradient but were otherwise environmentally similar. Among these streams, we estimated biovolumes of riffle-dwelling, benthic algae species over two years to test the hypotheses that (1) seasonal assembly of stream algae under oligotrophic conditions is characterized by compensatory dynamics, and (2) increased nutrient enrichment alter those dynamics by decreasing the importance of seasonal fluctuations in environmental condition. We also expected decreased stability in algal biovolumes as the mode of temporal dynamics changed with increased enrichment.

Methods

Study Area

We conducted our study in 35 mid-order streams (3rd to 5th) in the Illinois River drainage basin and several surrounding watersheds transecting the border of Oklahoma and Arkansas, USA (Fig. 1.1). The sites were selected to span a wide gradient of phosphorus (P) enrichment that stemmed both from an uneven distribution of land-applied P-rich poultry litter and wastewater treatment plant discharges (Haggard 2010, Scott et al. 2011, Jarvie et al. 2012). We targeted cobble-dominated riffle-run habitat with moderately fast, unobstructed flow (site means ranging from 0.31 – 0.77 m s⁻¹) and open canopies (typically <10% cover during peak growth in summer) to minimize among-site habitat variability so that the only substantive difference among study sites was the degree of nutrient enrichment. Total P (TP) concentrations among study streams ranged from a 2-year mean of ~ 7 to ~ 140 µg L⁻¹. To ensure we could observe seasonally driven variation in community composition, we began sampling in June 2014, and revisited sites every other month for 2 years ending in April 2016.

Data Collection

We sampled benthic algal species assemblages (including cyanobacteria) by collecting five cobbles (10-20 cm wide) at five equidistant points along each of three transects that were marked perpendicular to flow and did not exceed 0.5 m in depth. Benthic algae were removed from the upper surface of each cobble with a stainless-steel brush immediately after collection, and material from each cobble was rinsed into a collection basin. This process was repeated until all cobbles were processed, resulting in

a large composite sample representing the algal assemblage from all 15 cobbles. Total cobble surface area was estimated using the aluminum foil mass-to-area conversion method (Lamberti et al. 1991), which was later used to estimate algal species biovolume per unit area.

At the midpoint of each transect we estimated current velocity using a Marsh-McBirney flowmeter (Loveland, Colorado, USA), as well as canopy cover (0-100%) using a densiometer, and used the mean of these values for analysis. Upstream of sampling activity, we determined TP and total nitrogen (TN) concentrations from triplicate instantaneous water grab samples pursuant to EPA QA/QC standards and APHA protocols (APHA 2005). We also determined water temperature (°C) using a YSI multiprobe, and measured stream discharge ($\text{m}^3 \text{s}^{-1}$) using USGS protocols.

The composite periphyton sample was thoroughly homogenized using a hand-blender until no large aggregates remained, then placed on a stir plate to suspend the sample at a high rate of stirring to ensure the sample remained homogenized. We widened volumetric pipettes to prevent clogging in particularly dense samples, and pulled 10 mL aliquots from the suspended sample until a final volume of 100 mL was reached. We then preserved the sample in buffered formalin (4% v/v) for soft-algae taxonomy, and then repeated the process to obtain a separate sample for diatom taxonomy. Species identity and biovolume by species of non-diatom and diatom species were identified and estimated by expert taxonomists (see acknowledgements). Total biovolume ($\text{mm}^3 \text{m}^{-2}$) by species per sample was estimated based on the fraction of the total sample identified and the total area of the substrate sampled (Hillebrand et al. 1999). An additional 50 mL of

slurry was dried at 60°C and pulverized using a BioSpec bead beater to colorimetrically determine tissue P content using a Lachat Quik-Chem FIA (as g P m⁻²).

Data Analysis

We first assessed how species coexistence changed with increasing nutrient enrichment (as TP) at each site visit by determining species richness at each site visit (α -diversity) and for all species observed at a site (temporal γ -diversity) using generalized linear models (GLMs). We then quantified temporal variation in algae assemblage composition using the Baselga partitioning framework (Baselga 2017). This framework incorporates the relative abundance of species, and partitions total variation in community composition (temporal β_{TOT}) into two components that capture different temporal phenomena. Temporal β_{BAL} was used to quantify compensatory dynamics in the algal assemblage, and measures variation at a site that occurs when individuals of some species are replaced by the same number of individuals from another (i.e. balanced variation in abundances) Temporal β_{GRA} measures variation that occurs from abundance losses or gains without a corresponding balancing change (i.e. an abundance gradient where one community is a subset of another). We directly regressed temporal β_{TOT} on mean TP using a GLM.

Due to the strong non-linear response of both β_{BAL} and β_{GRA} to TP, we estimated the location where the relationship between temporal β -diversity and mean TP shifts using a bootstrapped deviance reduction technique (King and Richardson 2003). We iteratively partitioned the response variable of interest along the TP gradient, and identified the point that maximizes between-group variance relative to within-group variance. To quantify uncertainty around the locations of TP changepoints, we

bootstrapped (resampled with replacement) the original dataset and reran the deviance reduction 999 times. The results are presented as histograms which display the distribution of changepoint locations identified by the bootstrap simulations.

We also used segmented regression both to provide an additional estimate of changepoint locations, and to describe the response of temporal β_{BAL} and β_{GRA} to mean TP before and after the breakpoints. Both β_{BAL} and β_{GRA} are positively bound metrics, so we constructed generalized linear models (GLMs) using a gamma distribution and log-link function due to variance behavior and distributions of the residuals from each model, and the `segmented` package for segmented regression.

To visualize spatiotemporal dissimilarity in community structure, we used nonmetric multidimensional scaling (NMDS) ordinations. We ordinated three distance matrices of periphyton communities from each site visit using the pair-wise versions of β_{TOT} , β_{BAL} , and β_{GRA} and the `metaMDS` function in the *vegan* package. We excluded taxa observed at a single site and event (60 of 296 taxa) to reduce stress in the ordinations and specified 500 random starts to ensure global solutions (McCune and Grace 2002). A 3-dimensional solution was specified because higher dimensionality only marginally reduced stress in the final solutions. To explore environmental drivers of community structure, we fit vectors of linear correlations between periphyton structure and a suite of environmental variables known to influence algae using the `envfit` function. We assessed the significance of 6-month mean log TP and log TN ($\mu\text{g L}^{-1}$), log periphyton tissue P content (g m^{-2}), water temperature ($^{\circ}\text{C}$), discharge ($\text{m}^3 \text{s}^{-1}$), and canopy cover (%) with 999 random permutations, and retained significant variables for plotting.

We included periphyton tissue P because large amounts of anthropogenic P may be sequestered in periphyton. Because TP was our primary gradient of interest, we rotated the solutions so that the greatest variation in TP concentrations were aligned along the first NMDS axis. To aid in visualization, we found the spatial mean of each sampling event in ordination space for locations above and below the TP breakpoints identified above, and connected the spatial means with vectors to display successional trajectories through time.

To estimate how temporal assembly defined by different levels of β_{BAL} and β_{GRA} might influence algal community stability (CS), we calculated a common metric to assess stability of algal biovolumes; $\text{CS} = \mu_{\text{biovolume}} / \sigma_{\text{biovolume}}$ (Tilman et al. 2006), where μ and σ are the mean and standard deviation of summed biovolumes observed at a site over the study period, respectively. We then tested whether CS was influenced by temporal assembly patterns by regressing CS on temporal β_{BAL} and β_{GRA} using GLMs. We specified a Gamma distribution with a log-link after visual assessment of variance behavior and distribution of the residuals. All analyses and plotting were conducted in the R language environment (R Core Team, 2017).

Results

Over the 2-year study, we observed 296 total taxa from 382 unique site visits. Mean and median richness per sample was 36.35 and 36, and mean and median biovolumes per sample were 25071.6 and 9139.13 $\text{mm}^3 \text{m}^{-2}$, respectively. Mean TP ranged from 7.02 to 137.77 $\mu\text{g L}^{-1}$, and increased roughly log-linearly when sites were ranked by increasing P enrichment (Appendix B, Fig. B1). α -diversity increased positively with TP (Fig. 3.1a, $p < 0.001$), indicating that more species were able to

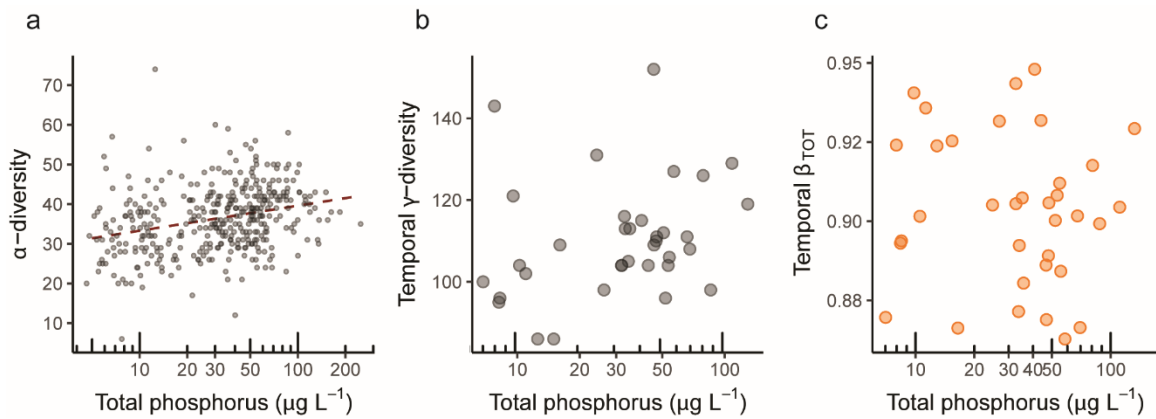


Figure 3.1. Richness based measures of biodiversity at both local (α -diversity, a) and temporally integrated (temporal γ -diversity) scales across a phosphorus enrichment gradient (as total phosphorus, TP). α -diversity increased with TP enrichment ($p < 0.001$), while TP was not predictive of temporal γ -diversity. (c) Temporal β_{TOT} also displayed no relationship with TP enrichment.

coexist at any given time with increased enrichment, but TP provided little explanatory power (7.89% deviance explained). Temporal γ -diversity ranged from 86 to 152, and displayed no relationship with TP (Figure 3.1b, $p = 0.143$). Likewise, temporal β_{TOT} showed no response to TP enrichment (Fig. 3.1c, $p = 0.813$), and ranged from 0.863 to 0.948.

Compensatory Dynamics in Freshwater Algae

Though unpartitioned temporal β_{TOT} showed no relationship with increasing nutrient enrichment, partitioning temporal β_{TOT} into β_{BAL} and β_{GRA} components uncovered markedly different temporal patterns in the periphyton as P enrichment increased (Fig. 3.2). β_{BAL} showed sharp, non-linear declines with increasing TP ($p < 0.001$, 49.5% deviance explained), while β_{GRA} displayed the opposite relationship ($p < 0.001$, 47.7% deviance explained). The segmented regressions placed the breakpoints at 24.6 ± 2.01 (SE) $\mu\text{g L}^{-1}$ TP and 24.7 ± 4.23 $\mu\text{g L}^{-1}$ TP for β_{BAL} and β_{GRA} , respectively. nCPA placed the breakpoints at slightly higher TP concentrations, and detected sharp

changes in the distributions of β_{BAL} at $37.0 \mu\text{g L}^{-1}$ TP (95% bootstrap quantiles 32.7 – 38.3), and β_{GRA} at $39.0 \mu\text{g L}^{-1}$ TP (95% bootstrap quantiles 33.9 – 47.4). Below these critical TP concentrations, temporal β -diversity in the periphyton was relatively stable among sites and characterized by compensatory fluctuations in species abundances ($\beta_{\text{BAL}} \sim 0.8$), with β_{GRA} contributing less to community variation (~ 0.1). Above the identified TP thresholds, the relative contribution of β_{BAL} and β_{GRA} to β_{TOT} began to switch, with β_{GRA} characterizing much more of temporal β -diversity at high levels of P enrichment (as much as 0.37).

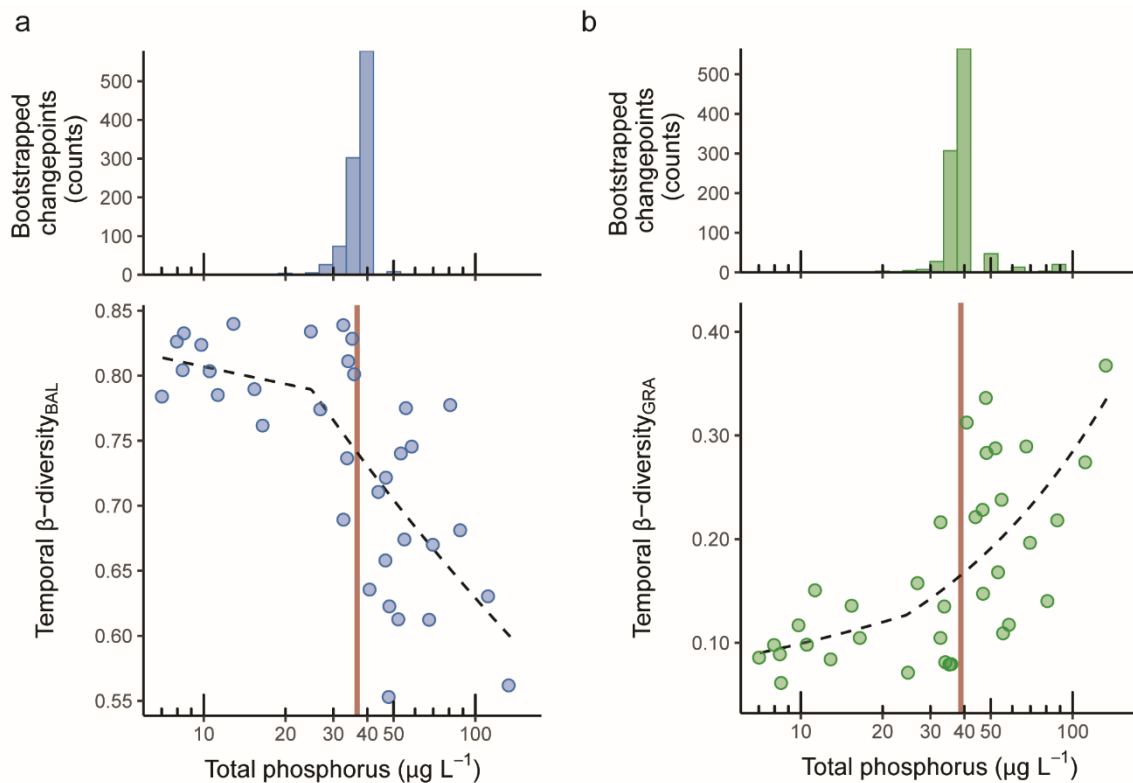


Figure 3.2. Two different modes of temporal β -diversity displayed markedly different relationships with total phosphorus (TP) enrichment. (a, blue graphics) Temporal β_{BAL} declined sharply with increasing TP (segmented regression, $p < 0.001$), while (b, green graphics) temporal β_{GRA} increased with increasing TP (seg. regression, $p < 0.001$). Histograms shown are the distribution of computed changepoints in the relationships between temporal β_{BAL} and β_{GRA} with TP, and vertical red lines are the means of those distributions.

Spatiotemporal Variation in Community Structure

NMDS ordinations of pair-wise temporal β_{TOT} (stress = 0.13) partitioned into β_{BAL} (stress = 0.18) and β_{GRA} (stress = 0.22) components identified several important environmental drivers of spatiotemporal community variation (Fig. 3.3, all presented

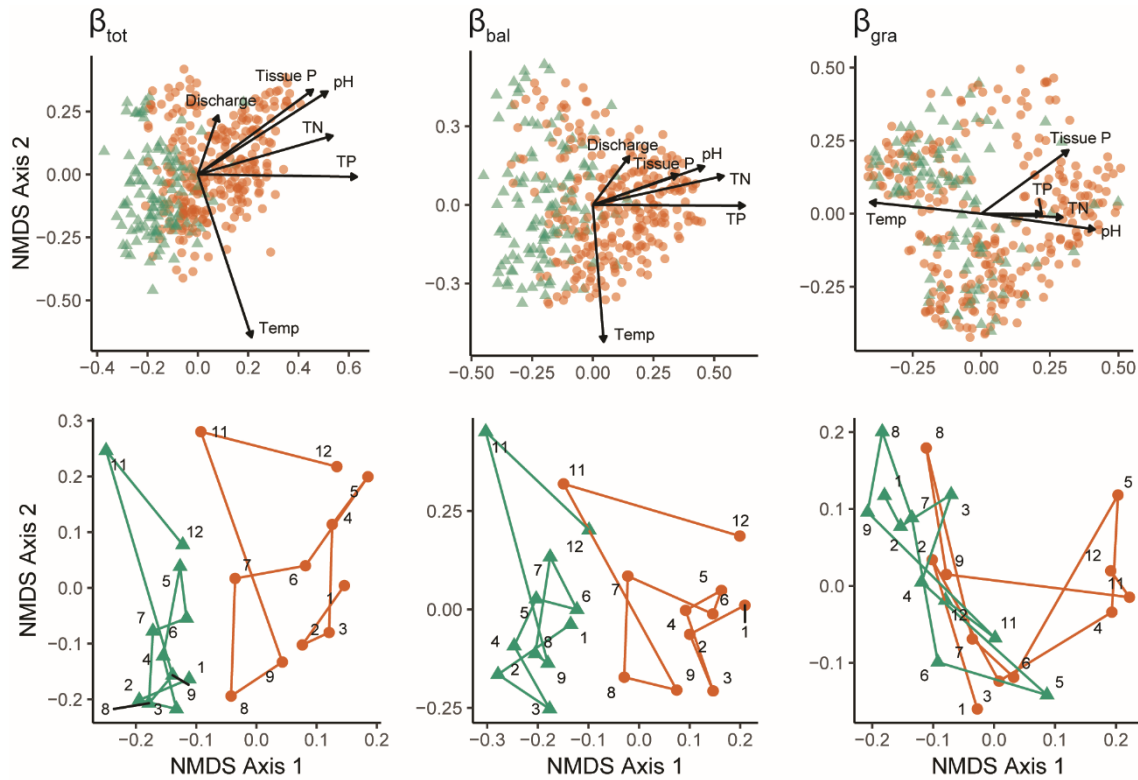


Figure 3.3. Spatiotemporal dissimilarity in community structure across 35 streams and 2 years constructed from pair-wise dissimilarity measures of β_{TOT} (total β -diversity, left column, stress = 0.13), β_{BAL} (measuring compensatory dynamics, center column, stress = 0.18), and β_{GRA} (measuring abundance-gradients, right column, stress = 0.22). Points are colored by low total phosphorus (TP, green triangles) and high TP (orange circles) sites as determined by changepoint analysis. Top panel arrows display significant ($p < 0.001$) environmental vectors predictive of spatiotemporal structure in community composition. Bottom panel displays the 2D spatial mean of each sampling event split by high and low TP sites, and are connected by successional vectors. Numbers are sampling events (1 – Jun '14, 2 – Aug '14, 3 – Oct '14, 4 – Dec '14, 5 – Feb '15, 6 – April '15, 7 – Jun '15, 8 – Aug '15, 9 – Oct '15, 11 – Feb '16, 12 – April '16).

environmental vectors $p < 0.001$). The first NMDS axis was strongly correlated with 6-month mean TP (log) for β_{TOT} and β_{BAL} ($r = 0.63$ and $r = 0.63$, respectively), while TP explained less community variation in β_{GRA} ($r = 0.22$). Overall, water temperature was

the second most important driver of periphyton structure, and aligned strongly with axis 2 in the β_{TOT} ($r = 0.68$) and β_{BAL} ($r = 0.52$) ordinations, and axis 1 in the β_{GRA} ordination ($r = 0.41$). For β_{BAL} (Fig. 3.3, upper middle plot), sampling units were widely dispersed at low levels of nutrient enrichment along a seasonally driven gradient of water temperature. As TP increased, separation along the temperature gradient decreased and created a wedge-shaped distribution. Variation in periphyton community structure also correlated with stream discharge, tissue P, TN, and pH for β_{TOT} and β_{BAL} , and for tissue P, TN, and pH for β_{GRA} (see Appendix B, Table B1 for full details). The first and second dimensions of the NMDS ordination captured most of the dissimilarity in community structure (see Appendix B, Fig. B2 for third NMDS axis).

Successional vectors (Fig. 3.3, lower panel) highlight broad differences in periphyton seasonal patterns above and below the identified TP breakpoint. The largest community differences as measured by β_{GRA} occurred at both low temperatures (sampling events 4, 5, 11, and 12 occurring in December 2014, February 2015, February 2016, and April 2016, respectively) and at high total- and tissue-P concentrations, which indicates the largest changes in species abundances occurred under these joint conditions. An outlier from the general trends mentioned above was the periphyton structure observed in February of the second year of sampling (sampling event 11) that followed several storms that caused historic flooding and subsequent streambed scouring.

Community Stability

Community stability displayed a positive relationship with temporal β_{BAL} (Fig. 3.4a, $p < 0.0001$, 37.1% dev. explained), which indicates increased stability with increased prevalence of compensatory dynamics. In turn, temporal β_{GRA} was associated

with increasing instability in community biovolumes, and displayed a negative relationship with community stability (Fig. 3.4b, $p < 0.0001$ 62.8% dev. explained).

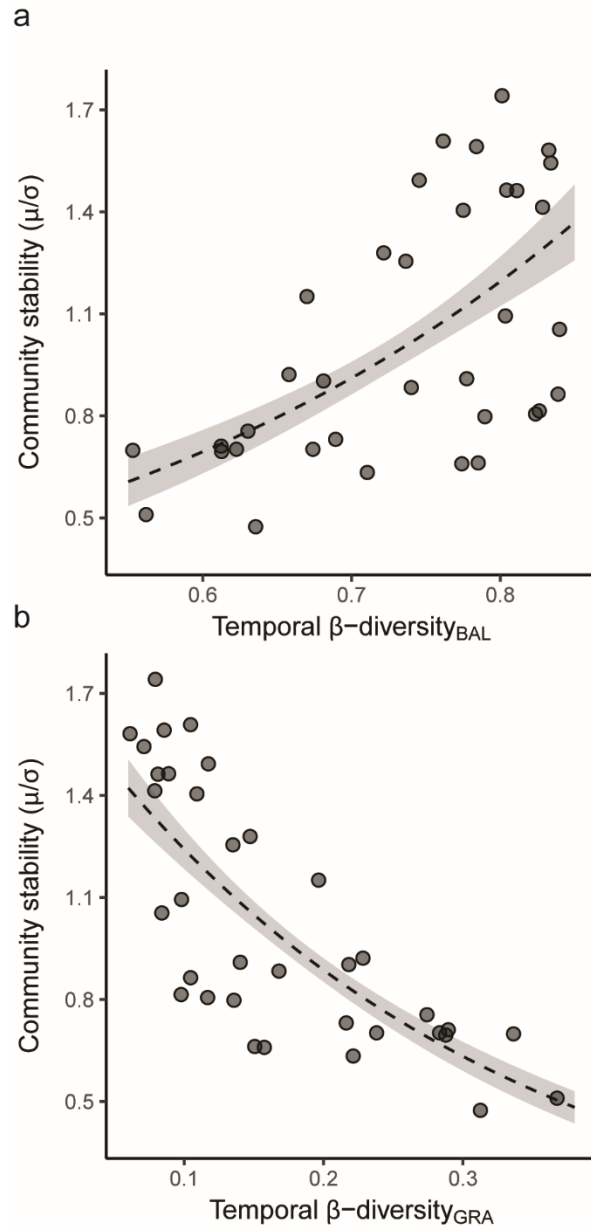


Figure 3.4. Community stability (CS) as measured by the ratio of mean biovolume to the biovolume standard deviation for algae from each site against two modes of temporal β -diversity, (a, top) β_{BAL} and (b, bottom) β_{GRA} . CS increased with increasing levels of temporal β_{BAL} ($p < 0.001$, deviance explained = 37.1 %) and declined with increasing levels of temporal β_{GRA} ($p < 0.001$, dev. explained = 62.8 %).

Discussion

Our study shows that algal assemblages under natural nutrient regimes display seasonally driven compensatory dynamics which nonlinearly break down with increasing eutrophication. Though we were unable to detect differences in community assembly with a composite measure of temporal β -diversity (β_{TOT}), partitioning temporal variation in community composition into components that measured compensatory dynamics (β_{BAL}) as well as variation due to gradients in abundance (β_{GRA}) revealed that community seasonality was governed by markedly different modes of assembly based on nutrient availability. Our results also support theoretical (Tilman 1985, Lehman et al. 2000) and empirical studies (Bai et al. 2004, Descamps-Julien and Gonzalez 2005) that indicate ecosystems with prevalent compensatory dynamics are more stable (Loreau and de Mazancourt 2013), as we observed increasingly stable algal biovolumes with increased β_{BAL} over the 2-year study.

The search for compensatory dynamics has yielded conflicting findings (as reviewed by Gonzalez & Loreau 2009), and there is some evidence that synchronous responses to environmental factors may dominate natural communities (Houlahan et al. 2007). However, under oligotrophic conditions we found algae community composition was driven primarily by seasonal factors extrinsic to the stream ecosystem, namely variation in water temperature and flow (Fig. 3.3, top panel). The ability to detect compensatory dynamics in natural communities may largely be a matter of scale, as examining community variation at interannual time scales overlooks assembly patterns that have evolved in response to seasonal variation in environmental conditions (Tonkin et al. 2017). Stream ecosystems are highly heterogeneous, and periphytic algae display a

rich variety of morphology, growth dynamics, and strategies for resource acquisition that enable them to avoid competitive exclusion by exploiting finely partitioned niches (Passy 2009, Cardinale 2011, Wehr et al. 2015). Our results indicate that seasonal drivers of biodiversity promote the coexistence of species by adding a temporal dimension to each spatial niche dimension that exists at any given time.

The rareness of readily observable compensatory dynamics in natural ecosystems may also be due in part to the increased prevalence of novel environments (Radeloff 2015), as we observed sharp declines in temporal β_{BAL} under relatively low levels of nutrient enrichment ($\sim 25 \mu\text{g L}^{-1}$ TP), a common anthropogenic stressor (Carpenter et al. 1998, Smith et al. 2006). Nonlinear responses of stream periphyton biomass and composition to anthropogenic changes are common (Taylor et al. 2014), and nutrient enrichment has spurred dramatic reorganization of interannual assembly patterns in lake phytoplankton following a regime shift (Jochimsen et al. 2013). Suppression of seasonal niche separation between organisms with increased fertilization also has been documented in a grassland community (Doležal et al. 2019), which indicates that nutrient enrichment is a threat common to the temporal maintenance of biodiversity in both terrestrial and aquatic ecosystems.

We observed increased community stability when temporal β -diversity was characterized by compensatory dynamics (temporal β_{BAL} , Fig. 3.4a), which adds to a growing body of literature noting strong relationships between biodiversity and ecosystem stability (Tilman et al. 2006, Ives and Carpenter 2007, Morin et al. 2014, Pennekamp et al. 2018). Increased stability, considering water temperature and flow were two primary drivers of community structure (Fig 3.3, lower panel), indicates that

asynchrony in species responses to abiotic conditions had a stabilizing effect on total biovolumes (i.e. increase in the portfolio effect, *sensu* Schindler et al. 2015). Further, had we only considered a composite measure of temporal β -diversity (β_{TOT}), or examined stability in response to either cumulative richness (temporal γ -diversity) or spot-measurements of biodiversity (α -diversity), we would have spuriously concluded either (1) no relationship between algal diversity and stability, or (2) decreased stability as richness increased. The seemingly disparate findings produced by studies of diversity-stability relationships (as reviewed by Ives and Carpenter 2007) therefore may not only be due to the multitude of definitions that attempt to quantify the concept of stability, but also because richness measures alone poorly account for community changes in seasonally dynamic ecosystems.

The increased instability we observed in enriched communities highlights the need to consider biotic interactions when examining temporal phenomena. The largest differences in β_{GRA} were jointly driven by increased TP and low temperatures (Fig. 3.3), which corresponded to times of the year when large blooms of nuisance algae carpeted eutrophic streams (dominated by the nuisance green alga *Cladophora glomerata*, Dodds 1991). Swings in algal biovolumes were likely due to seasonally variable top-down control by large numbers of stonerollers (*Campostoma anomalum*, the dominant vertebrate grazer) and pleurocerid snails (the dominant invertebrate grazer as documented in a concurrent study, Cook et al. 2018), as grazing rates are heavily dependent upon metabolic activity and thus thermally controlled (Hillebrand 2009). Numerous studies have noted the importance of top-down controls on producer biomass (Power et al. 1988, Hillebrand 2009, Beck et al. 2018), which can be sometimes be stronger than the bottom-

up effects of resource supply (Rosemond et al. 2000). It is likely that during the cooler months that the bottom-up effects of nutrient supply exceeded the ability of thermally suppressed grazers to control algal biomass.

Periphytic algae occupy a central role in stream ecosystem functioning (Battin et al. 2016), are the dominant contributors to autochthonous production (Vannote et al. 1980), mediate nutrient and organic matter cycling (Mulholland and Rosemond 1992), and provide food for many invertebrate and vertebrate grazers (Power and Matthews 1983). High degrees of seasonal variation in community composition could indicate a large amount of complementarity in stream algae, especially considering niche partitioning has been linked to increased uptake and storage of nutrients (Cardinale 2011). Diverse communities of producers use resources more efficiently than depauperate ones (Tilman 1996, Bracken and Stachowicz 2006, Zuppinger-Dingley et al. 2014), and the breakdown in seasonal patterns we observed may have especially important implications for the ability of periphyton to efficiently sequester anthropogenic nutrients and thereby inhibit a key ecosystem service of stream algae. Our results show nutrient enrichment strongly influences the structural aspect of seasonal biodiversity, which likely has widespread impact on the seasonally driven functioning of stream ecosystems.

CHAPTER FOUR

Riverine Benthic Algae Exhibit Much Stronger and More Synchronous Responses to Nutrient Enrichment Than Do Macroinvertebrate Assemblages

Introduction

Natural ecosystems are increasingly threatened by anthropogenic impacts that cause abiotic conditions to deviate from historical norms (Fox 2007, Radeloff et al. 2015). Novel environmental conditions can alter biotic interactions (Bates et al. 2017), cause physiological stress and the direct extirpation of some species (King et al. 2011), and convey an adaptive advantage to others (Anderson et al. 2002). Combined, individualistic responses to novel environments cause new species associations to form, which in turn leads to novel communities that may bear little resemblance to their natural counterparts (Hobbs et al. 2009). Coincident changes in ecosystem function frequently accompany structural reorganization and losses in biodiversity (Cardinale 2011, Cardinale et al. 2012, Nelson et al. 2013), therefore establishing how and at what degree of anthropogenic impact communities respond remains especially important.

Species frequently display threshold responses to novel gradients (King and Baker 2010). Here, thresholds are defined as disproportionately large changes in distribution or abundance of species in response to an incrementally small change in environmental condition (Groffman et al. 2006, see Dodds et al. 2010 for review). Phylogenetically related species in a community have coevolved to exploit ecologically similar but unique niches, and their fitness can be indiscriminately reduced by conditions that deviate strongly from their evolutionary past (King et al. 2011, Bernhardt et al. 2012). Tolerant

species can increase in abundance to fill niche-space left by declines in these sensitive taxa (Wallace and Biastoch 2016) or increase because they are better able to exploit a novel resource subsidy (Smucker et al. 2013). Many species changing synchronously under similar magnitudes of stressor may be indicative of a threshold response that impacts the entire community, though catastrophic shifts in ecosystem state may be foreshadowed by the loss of even a few species (Power et al. 1996, Pace et al. 1999). Therefore, characterizing species-specific responses to changing environments is necessary to assess anthropogenic impact and mitigate potential changes to ecosystems.

Elevated nitrogen (N) and phosphorus (P) concentrations are the leading cause of biological degradation in freshwaters worldwide (Carpenter et al. 1998, Smith et al. 2006, Paulsen et al. 2008, Dodds and Smith 2016). In lotic ecosystems, periphytic algae and benthic macroinvertebrates are the two assemblages most commonly used to quantify the degree of degradation (Bonada et al. 2006, Resh 2008), and despite their global distribution and near ubiquitous use as bioindicators, each assemblage is influenced by enrichment through markedly different pathways.

Algae can directly access the increased dissolved pools of inorganic and organic nutrients associated with eutrophication, which differentially affects the fitness of algal species (Tilman 1977, Hillebrand and Sommer 1999). While nutrient concentrations may be toxic to macroinvertebrates under highly eutrophic conditions (Zhang et al. 2018), most of the effects of enrichment on higher trophic levels are indirect and primarily mediated by the periphyton community. Oxygen concentrations decline to levels harmful to macroinvertebrates by the senescence and decomposition of large standing stocks of algae as a result of nutrient enrichment (Carpenter et al. 1998). Even low levels of

enrichment can alter the relative fitness of macroinvertebrate species by alleviating the mismatch between nutritionally poor basal food resources (high C:N and C:P) and macroinvertebrates with higher tissue N and P (Singer and Battin 2007), and there is evidence that changes to resource quality may drive threshold responses to eutrophication in macroinvertebrate assemblages (Evans-White et al. 2009).

Despite recommendations that biotic assessment consider multiple groups of organisms (Barbour et al. 1999), very few studies have comparatively assessed species and assemblage-level threshold responses to eutrophication in multiple assemblages (but see Taylor et al. 2014, Kovalenko et al. 2014, and Wagenhoff et al. 2016). Further, most assemblage-level comparisons available use univariate metrics or region-specific indices to compare biotic response to eutrophication (Mazor et al. 2006, Newall et al. 2006, Justus et al. 2010, Wagenhoff et al. 2017), which are often unable to detect the presence of ecological thresholds because they compress information about species-specific responses into a single value (Baker and King 2010). Both algal and macroinvertebrate assemblages are clearly altered by eutrophication, but because of the unique mechanisms that influence each assemblage there may be differences in the type and magnitude of response.

We examined algal and macroinvertebrate assemblages across 35 streams spanning a steep P gradient to (1) identify levels of nutrient enrichment that resulted in non-linear shifts in stream assemblage structure, and (2) assess whether algae and macroinvertebrates were impacted at similar levels of enrichment. We also contrasted assemblage responses to water column nutrient concentrations and periphyton nutrient content as measures of enrichment, since resource quality may be a better predictor of

changes in assemblage structure at higher trophic levels (Singer and Battin 2007, Evans-White et al. 2009). We hypothesized algal assemblage structure would display strong non-linear shifts in response to nutrient concentrations, but that macroinvertebrate assemblage response would be less synchronous because higher trophic levels are largely removed from the direct effects of nutrient enrichment. For the same reason, we also hypothesized periphyton nutrient content would better predict shifts in macroinvertebrate assemblage structure.

Methods

Study Area

The 35 study sites were mid-order streams (3rd to 5th order) located in the Ozark Highlands and Boston Mountains Level III ecoregions of Oklahoma and Arkansas, USA (Omernik and Griffith 2014). The streams were selected to span a wide gradient of nutrient enrichment due to an uneven distribution of land-applied P-rich poultry litter and wastewater treatment plant discharges (Haggard 2010, Scott et al. 2011, Jarvie et al. 2012). We targeted cobble-dominated riffle-run habitat with moderately fast, unobstructed flow (site means ranging from 0.31 – 0.77 m s⁻¹) and open canopies (typically <10% cover during peak growth in summer) to minimize among-site habitat variability so that the only substantive difference among study sites was the degree of nutrient enrichment. Sampling began in June 2014, and we revisited sites every other month for 2 years which resulted in 12 sampling events through April 2016.

Data Collection

We measured in-stream nutrient concentrations from collected instantaneous water grab samples in triplicate upstream of all other sampling activity. We also determined water temperature ($^{\circ}\text{C}$) at this location using a YSI EXO1 multiprobe (YSI, Inc., Yellow Springs, OH, USA), and stream discharge (c.f.s) using a Marsh-McBirney flowmeter (Loveland, Colorado, USA). Water samples were analyzed on a Lachat 8500 QuikChem Series 2 (Hach Corporation, Loveland Colorado, USA) for total P (TP) and total N (TN) pursuant to EPA QA/QC standards and APHA protocols (APHA 2005).

We estimated algal (including cyanobacteria) and macroinvertebrate assemblage structure by collecting a composite sample of each assemblage during every site visit. We ran three transects that spanned the width of the target habitat and placed 5 equidistant points along each transect. One cobble 0.5 m upstream of each point was collected (totaling 15 cobbles $\text{site}^{-1} \text{visit}^{-1}$), and we removed the periphyton by vigorously scrubbing the upper surface of the cobble with a stainless-steel brush immediately after collection. Material from all cobbles was washed from the surface to form a composite sample that was placed in a dark bottle on ice for further processing. Total cobble surface area was estimated using the aluminum foil mass-to-area conversion method (Lamberti et al. 1991), which allowed us to estimate algal species biovolumes per unit area. The benthic macroinvertebrate assemblage was sampled 0.5 m upstream of the collected cobbles in an undisturbed area using 0.086-m^2 Hess samplers, which resulted in 1.29 m^2 of sampled benthos from 15 Hess samples. We also recorded depth (m) at each point along the transects, and current velocity (m s^{-1}) and canopy cover (0-100%) at the

midpoint of each transect because these abiotic factors may influence algal (Jyrkänkallio-Mikkola et al. 2016) and macroinvertebrate community composition (Heino et al. 2012).

Benthic algae and macroinvertebrate assemblage composition was determined following EPA Rapid Bioassessment Protocols (1999). The composite periphyton sample was thoroughly homogenized using a hand-blender until no large aggregates remained, then placed on a stir plate to suspend the sample at a high rate of stirring to ensure the sample remained homogenized. We widened volumetric pipettes to prevent clogging in particularly dense samples, and pulled 10 mL aliquots from the suspended sample until a final volume of 50 mL was reached. We then preserved the sample in buffered formalin (4% v/v) for soft-algae taxonomy, and then repeated the process to obtain a separate sample for diatom taxonomy. Species identity and biovolume by species of non-diatom and diatom species were identified and estimated by expert taxonomists (see acknowledgements). Total biovolume ($\text{mm}^3 \text{m}^{-2}$) by species per sample was estimated based on the fraction of the total sample identified and the total area of the substrate sampled.

The composite macroinvertebrate sample was preserved in buffered formalin (5% v/v) for later identification and enumeration (sorting and identification procedures detailed in Cook et al. 2018). Macroinvertebrate specimens were typically identified to genus (except for Chironomidae, Hydrachnidia, and Oligochaeta), and taxa abundances standardized to the area sampled.

We also determined periphyton carbon (C), N, and P content of periphyton. At least 50 mL of periphyton slurry was evaporated and dried at 60 °C, and then homogenized using a bead-beater (Biospec Products, Virginia USA). Inorganic

carbonates were removed from the dried sample by acid fumigation (HCl), and then periphyton C and N were estimated using a ThermoQuest FlashTM elemental analyzer. Periphyton P was estimated using the alkaline persulfate digestion method and colorimetric analysis on a Lachat 8500 QuikChem Series 2.

Data Analysis

We used multiple distinct but complementary analyses to model algal and macroinvertebrate assemblage responses to measures of nutrient enrichment. We first examined the effect of water column nutrient enrichment on periphyton nutrient content to determine how enrichment was influencing the primary basal food resource among study streams. Then, to assess drivers of assemblage structure, we ordinated 2-year mean algal biovolumes and macroinvertebrate densities, and correlated assemblage dissimilarity to 2-year site means of predictor variables expected to be the most influential to stream algae and macroinvertebrates. Finally, we examined thresholds of both individual taxa, and assemblage-level thresholds in response to nutrient enrichment.

GAM modeling of periphyton nutritional quality. We used GAMs to model the strong non-linear response of periphyton nutrient content to nutrient enrichment. We modeled the ratios of mean periphyton C:P, C:N, and N:P to TP and TN enrichment, and specified a Gamma distribution and log-link due to variance behavior and visual distribution of the residuals (Zuur 2009). Response variables in each model were weighted by the inverse of their standard deviation to increase the influence of highly stable variables in the final models (Gurevitch and Hedges 1999). We used the mgcv

package in R, which uses cross-validation penalization to specify the optimal amount of smoothing to avoid overfitting (Wood 2017).

NMDS ordination of algal and macroinvertebrate assemblages. We visualized dissimilarities in assemblage structure among streams using two NMDS ordinations of 2-year mean algal biovolumes and macroinvertebrate densities. We used a Bray-Curtis dissimilarity metric and $\log(x+1)$ transformed taxa biovolumes and densities prior to analysis to down weight the contribution of taxa that frequently dominant eutrophic sites (McCune and Grace 2002). Singletons were excluded (60 of 296 algal taxa, and 52 of 213 macroinvertebrate taxa) to reduce stress in the final solutions. We used the vegan package in R to ordinate taxa data, specified 500 random starts to ensure a global solution, and specified a 2D solution after noting minimal reductions in stress upon adding additional dimensions.

We used environmental vector fitting in NMDS ordination space to identify significant correlations between potential environmental drivers (2-year means of TP, TN, water temperature, discharge, water depth, canopy cover, and periphyton nutrient content) and assemblage structure. Environmental drivers that showed strong non-linearity with assemblage structure were log-transformed prior to fitting (TP, TN, and periphyton C:P and N:P), and significance was assessed using 1000 random permutation. Significant ($p < 0.001$) variables were retained for plotting, and the final NMDS solutions were rotated so that the first axis aligned with log TP enrichment.

Threshold Indicator Taxa ANalysis (TITAN). The prior analyses informed which environmental gradients were used to analyze assemblage thresholds with Threshold

Indicator Taxa ANalysis (TITAN, Baker and King 2010, 2013). TP concentration provided more explanatory power than TN concentrations when modeling periphyton nutrient content, and periphyton C:P also was more highly correlated to macroinvertebrate assemblage structure than C:N in ordination space. These analyses, along with data gathered during a concurrent study that displayed rapid uptake of water column P with little change in N concentrations during periods of peak productivity, are more indicative of P than N limitation. Thus, we used water column TP and periphyton C:P to test our hypotheses concerning differences in threshold responses between assemblages.

TITAN iteratively partitions a gradient of interest into two groups and uses standardized IndVal scores (or IndVal z -scores, Dufrêne and Legendre 1997) to identify which side of the gradient a taxa is more associated with at each partition. The location along the gradient that maximizes a taxon association with one side of the gradient is identified as a candidate change point, and bootstrapping is used to identify pure (the change occurs in the same direction) and reliable (the change is distinguishable from a random distribution) taxa. Taxa both increasing (z^+) and decreasing (z^-) along an environmental gradient may be identified this way.

We used 2-year mean TP and periphyton C:P as gradients using TITAN to examine threshold responses of algal and macroinvertebrate assemblages. We specified the minimum number of observations needed on either side of a partition as ≥ 3 , and only retained taxa for analysis that occurred at more than 3 sites (192 of 296 algal taxa, and 124 of 213 macroinvertebrate taxa). We also left the biovolumes and abundances untransformed for this analysis (King and Baker 2014), and specified 1000 bootstrap

replicates. We considered the evidence of a taxon threshold to be strong if at least 95% ($p < 0.05$) of the bootstrap runs resulted in taxon change in the same direction, and at least 95% ($p < 0.05$) of the bootstrap runs were significantly different from a random distribution. We plotted the location of taxon-specific changepoints that met these criteria, and the distribution of changepoints generated from the bootstrapped replicates.

The sum of IndVal z -scores [$\text{sum}(z^+)$ for increasers and $\text{sum}(z^-)$ for decreasers] derived from individual taxa is used to identify regions of assemblage-level change, and was plotted against both TP and periphyton C:P. Peaks in the $\text{sum}(z)$ distribution indicate regions along an environmental gradient where many taxa are synchronously changing and may be used as evidence for an assemblage-level threshold. Wide plateaus in $\text{sum}(z)$ distributions result when taxa thresholds occur across a wider range of the environmental gradient, and provide less evidence for an assemblage-level threshold (Baker and King 2013). We also displayed probability densities of $\text{sum}(z)$ maxima generated during the bootstrapping procedure, because if maxima across many replicates form a narrow peak, this provides additional statistical evidence for an assemblage-level threshold.

Results

Mean TP ranged from 7.15 to 127.15 $\mu\text{g L}^{-1}$, mean TN ranged from 122.38 to 5136.58 $\mu\text{g L}^{-1}$. Periphyton nutrient content increased significantly at relatively low levels of TP enrichment (Fig. 4.1). Water column TP concentrations were strongly predictive periphyton C:P ($p < 0.001$, deviance explained = 88.2%), C:N ($p < 0.001$, dev. exp. = 69.9%), and N:P ($p < 0.001$, dev. exp. = 84.1%), while TN explained less variation in

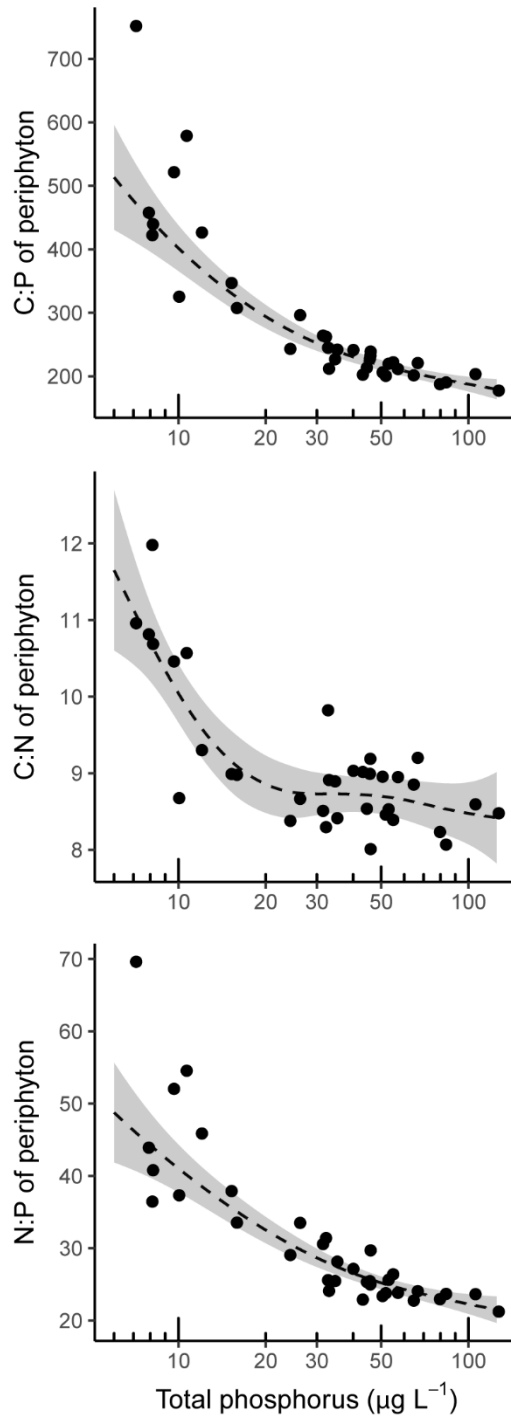


Figure 4.1. Periphyton tissue C:P, C:N, and N:P all declined in response to total phosphorus (TP, log-scale) concentrations. GAM smoothers (all $p < 0.001$) indicated that TP explained more variation in C:P (deviance explained = 88.2%) and N:P (dev. exp. = 84.1%) than C:N (dev. exp. = 69.9%).

periphyton C:P ($p < 0.001$, dev. exp. = 73.4%), C:N ($p < 0.001$, dev. exp. = 48%), and N:P ($p < 0.001$, dev. exp. = 68.5%, Appendix C, Fig. C.1). Periphyton C:P decreased rapidly from 700 to 300 where TP increased from < 10 to 20-30 $\mu\text{g L}^{-1}$ (Fig. 4.1, top pane).

NMDS ordination of both algal (2D stress = 0.07) and macroinvertebrate (2D stress = 0.16) assemblages were strongly structured by gradients that were correlated with nutrient enrichment (Fig. 4.2, all displayed environmental vectors $p < 0.001$). For algal assemblages, NMDS axis 1 aligned strongly with log TP ($r = 0.91$), log TN ($r = 0.88$), log C:P ($r = 0.90$), and log N:P ($r = 0.89$), while axis 2 was primarily ordered by stream

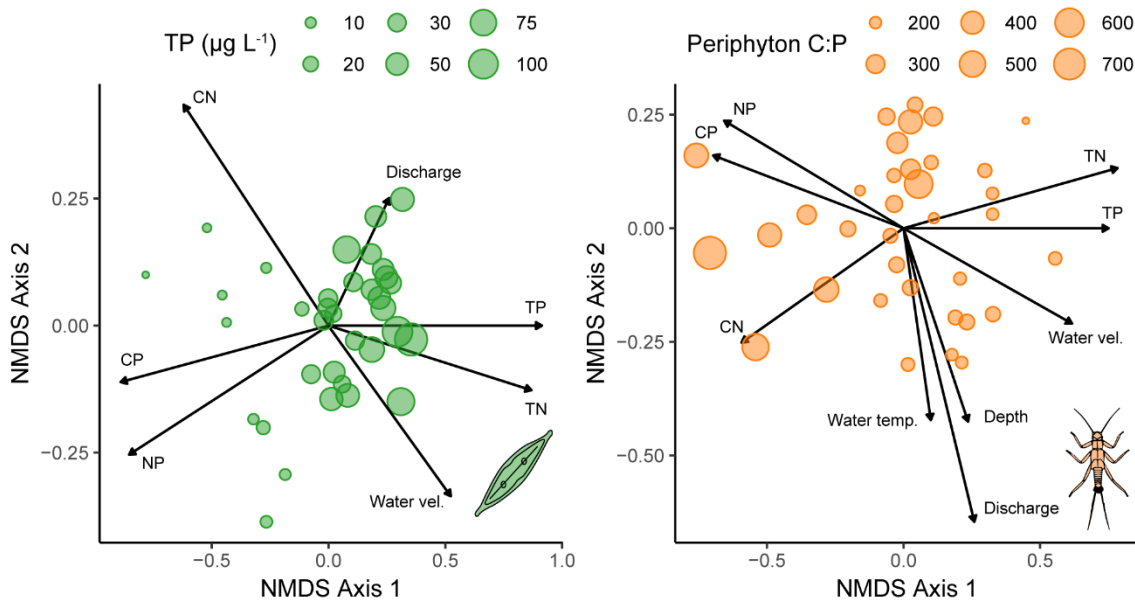


Figure 4.2. Nonmetric multidimensional scaling (NMDS) ordination of algal (left pane, green, 2D stress = 0.07) and macroinvertebrate (right pane, orange, 2D stress = 0.16) assemblages based on 2-year mean biovolumes ($\text{mm}^3 \text{m}^{-2}$) and abundances (m^{-2}), respectively. Point size indicates the degree of nutrient enrichment as measured by TP and periphyton tissue C:P. Arrow indicate correlations of environmental gradients associated with assemblage structure among sites. The direction of the arrow signifies the direction of correlation, and the length of the arrow the magnitude of correlation (all shown vectors $p < 0.001$).

discharge ($r = 0.43$), periphyton C:N ($r = 0.75$), and water velocity ($r = 0.62$). For macroinvertebrate assemblages, the first NMDS axis represented a strong gradient in log TP ($r = 0.75$) and log TN ($r = 0.79$) concentrations, as well as gradients in periphyton log C:P ($r = 0.72$), C:N ($r = 0.64$), and log N:P ($r = 0.70$). Less separation occurred along the second NMDS axis, which correlated with gradients in discharge ($r = 0.71$), stream depth ($r = 0.49$), and water temperature ($r = 0.43$). Full details of environmental vectors can be found in Appendix C, Table C.1.

Algae showed evidence of strong, synchronous changes at relatively low levels of TP enrichment (Fig. 4.3) for 57 increasing ($15.58 \mu\text{g L}^{-1}$, 95 % CI of 15.57-32.16) and 17 decreasing ($20.1 \mu\text{g L}^{-1}$, 95% CI of 11.05-24.09) taxa. Benthic macroinvertebrates showed a much wider distribution of observed changepoints for 20 increasing ($37.68 \mu\text{g L}^{-1}$, 95 % CI of 9.12 – 48.92) and 9 decreasing taxa ($37.68 \mu\text{g L}^{-1}$, 95 % CI of 9.86 – 48.92), which provided much less support for an assemblage-level threshold in response to TP enrichment. Rather, the bimodal distribution in sum-z maxima indicates that different subsets of the assemblage are altered at different levels of TP enrichment, with some macroinvertebrates changing in presence and abundance at TP concentrations as low as $\sim 10 \mu\text{g L}^{-1}$.

Though water column nutrient enrichment was not indicative of synchronous threshold responses in macroinvertebrate taxa, enrichment of periphyton nutrient content was predictive of synchronous change of multiple taxa (Fig 4.4b, note that the x-axes are inverted so that increasing nutrient enrichment, or lower C:P content, increases left to right). Eleven macroinvertebrate taxa declined with increasing resource quality around

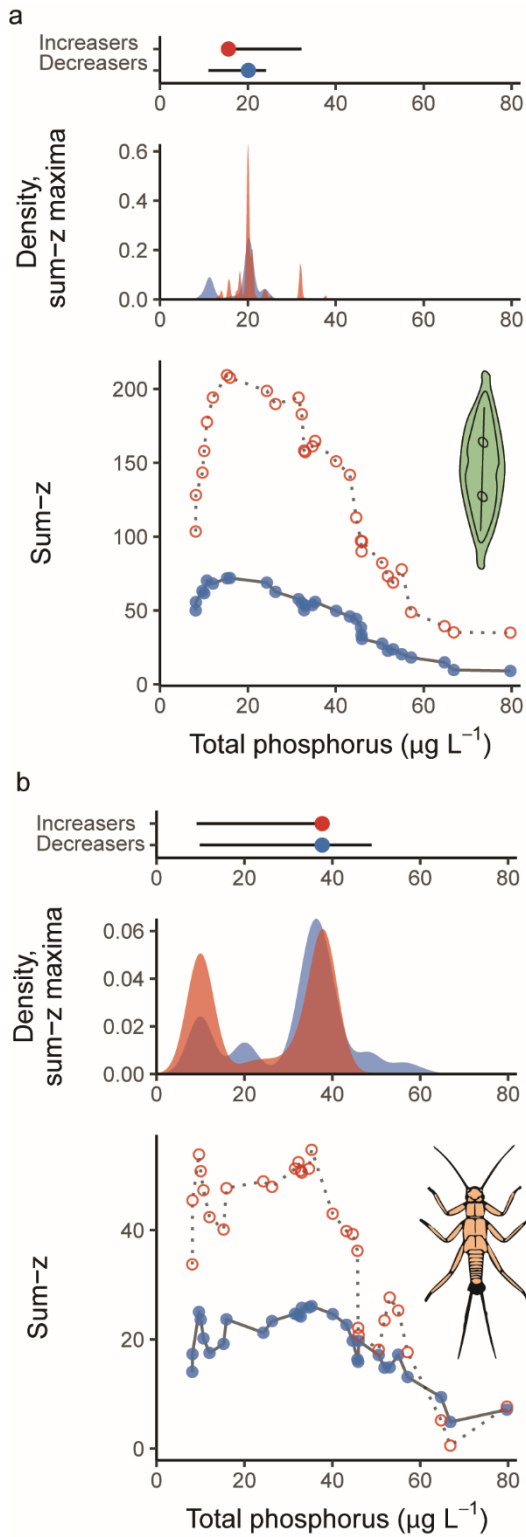


Figure 4.3. Changes in algal (a, top pane) and macroinvertebrate (b, bottom pane) assemblages across a total phosphorus (TP, $\mu\text{g L}^{-1}$) gradient as identified by Threshold Indicator Taxa ANalysis (TITAN). Responses are split between taxa increasing (red, open point) and decreasing (blue, closed points) to TP enrichment. The bottom-most plot (continued) in each panel shows the filtered sum-z scores of significant indicator taxa, while the middle panes show the distribution of sum-z maxima as identified from 999 bootstrap replicates. Peaks in each distribution may be interpreted as evidence for a synchronous shift in assemblage composition. Candidate changepoint locations are displayed in the top panel, along with 95% confidence intervals around the changepoints.

the same levels of C:P enrichment (235.65, 95% CI of 215 – 253), while 11 taxa increased at slightly lower levels of C:P enrichment (263.05, 95% CI of 237 – 321). Multiple macroinvertebrate taxa synchronously declining with increase periphyton C:P was consistent with an assemblage-level threshold, while taxa positively responding to increased nutrient availability did so at a broader range of periphyton C:P. For algae, periphyton C:P enrichment provided little additional explanatory power over TP enrichment (Fig. 4.4a), and TITAN identified wider thresholds in 16 declining taxa (301.8 C:P, 95% CI of 264 - 433) and 61 increasing taxa (301.82, 95% CI of 254 - 359).

Overall, algal assemblage-level responses were much stronger than responses of macroinvertebrate assemblages to measures of enrichment (Fig. 4.3, 4.4). The filtered sum-z maxima are indicative of the strength of predictors, which were much lower for macroinvertebrate assemblages using both TP (sum-z maxima = 26 for decreaseers, 55 for increaseers) and C:P (sum-z maxima = 33 for decreaseers, 36 for increaseers) when compared to algal assemblages using TP (sum-z maxima = 72 for decreaseers, 209 for increaseers) and C:P (sum-z maxima = 74 for decreaseers, 219 for increaseers).

We displayed individual taxa responses of algae to TP enrichment (Fig. 4.5a, 4.5b), and benthic macroinvertebrates to periphyton C:P (Fig. 4.5c, 4.5d) because taxa in the two assemblages displayed evidence of synchronous responses to different measures of enrichment (algae taxa responses to C:P shown in Appendix C Fig. C.2, and macroinvertebrate taxa responses to TP shown in Appendix C, Fig C.3).

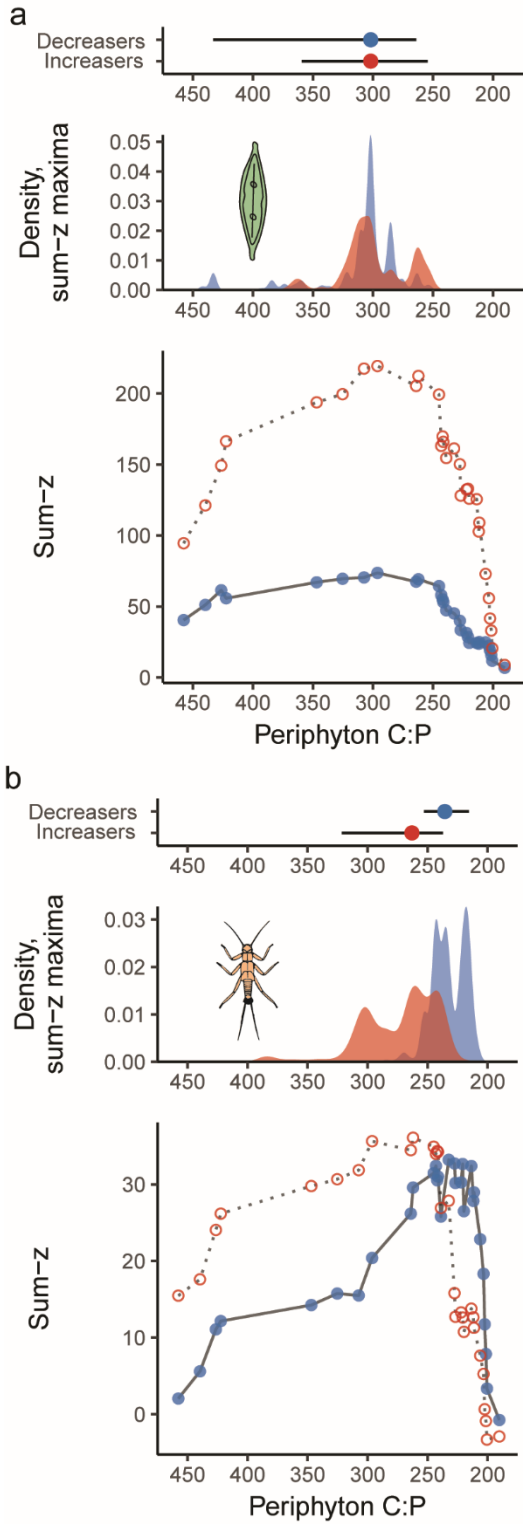


Figure 4.4. Changes in algal (a, top pane) and macroinvertebrate (b, bottom pane) assemblages across a periphyton tissue C:P gradient as identified by Threshold Indicator Taxa Analysis (TITAN). Responses are split between taxa increasing (red, open point) and decreasing (blue, closed points) to periphyton resource quality. The bottom-most plot (continued) in each panel shows the filtered sum-z scores of significant indicator taxa, while the middle panes show the distribution of sum-z maxima as identified from 999 bootstrap replicates. Peaks in each distribution may be interpreted as evidence for a synchronous shift in assemblage composition. Candidate changepoint locations are displayed in the top panel, along with 95% confidence intervals around the changepoints.

Discussion

We found large differences in the assemblage-level threshold responses of algae and macroinvertebrates to P enrichment that highlight the importance of quantifying the direct and indirect effects of enrichment. Algal taxa displayed synchronous changes to low increases in TP concentrations, while threshold changes of macroinvertebrate assemblages were best predicted by increased nutrient content of periphyton; the primary basal food resource in our study streams. The changes in periphyton nutrient content with enrichment was indicative of P rather than N limitation (Fig. 4.1, Fig C.1 Appendix C) even though N and P generally covaried across study sites. Though macroinvertebrate assemblage responses were generally weaker than shifts in algal assemblage structure, our results indicate macroinvertebrate responses corresponded to non-linear changes in periphyton nutrient content at low levels ($10\text{-}30\ \mu\text{g L}^{-1}$) of TP enrichment.

Algal assemblage-level thresholds occurred with modest increases over natural P concentrations ($\sim 10\ \mu\text{g L}^{-1}$ TP as estimated by Stevenson et al. 2008), and were driven both by taxa sensitive to P enrichment (shifts occurring *c.* $20\ \mu\text{g L}^{-1}$), and taxa able to exploit anthropogenic P subsidies (shifts occurring *c.* $16\ \mu\text{g L}^{-1}$). TITAN effectively parsed species-specific responses to enrichment and detected threshold responses of taxa that are prominently featured in regionally tested biotic metrics (Justus et al. 2010), such as 5 species of *Cymbella*, a diatom intolerant of low to moderate nutrient enrichment (Fig. 4.5a). Diatom taxa both increasing and decreasing in response to P enrichment generally aligned with analysis by Potapova and Charles 2007 of National Water-Quality Assessment data (Appendix C, Table C.2), but identified numerous taxa that they did not

because TITAN is robust to floristic differences between regions (12 taxa decreasing and 16 taxa increasing in response to P enrichment).

Our results also highlight the need to consider non-diatom taxa in water-quality assessments using algae (Stancheva and Sheath 2016), as *Cladophora glomerata* was identified as a pure and reliable indicator taxon (IndVal score of 93.8) and formed large blooms that carpeted the benthos in many P enriched streams (site mean biovolumes ranged from 0 – 53,881 mm³ m⁻²). *Cladophora* is a nuisance green-alga present in the majority of streams and rivers around the world (Dodds 1991, Dodds and Gudder 1992), and can act as an ecosystem engineer under enriched conditions by dramatically altering habitat complexity and increasing the amount and type of substrate available for other algae (Zulkifly et al. 2013). Many of the taxa TITAN identified as increasing with P enrichment were eutrathentic species and known *Cladophora* epiphytes such as *Cocconeis* (4 species), *Gomphonema* (4 species), *Rhoicosphenia* (1 species), and *Pseudulvella* (1 species). The wide range in observed changepoints for increasing taxa (Fig. 4.5) are likely due to a combination of some taxa being released from nutrient limitation at different levels of P enrichment, and tolerant epiphytes expanding into new niches that accompany *Cladophora* blooms physically restructuring available substrate in the benthos.

Though benthic macroinvertebrates provide a longer integrative proxy of in-stream conditions that can cover weeks to years (Merritt et al. 2008), our results show that at low to moderate levels of enrichment (site TP ranged from *c.* 7 - 130 µg L⁻¹), in-stream nutrient concentrations are poor at predicting assemblage-level shifts.

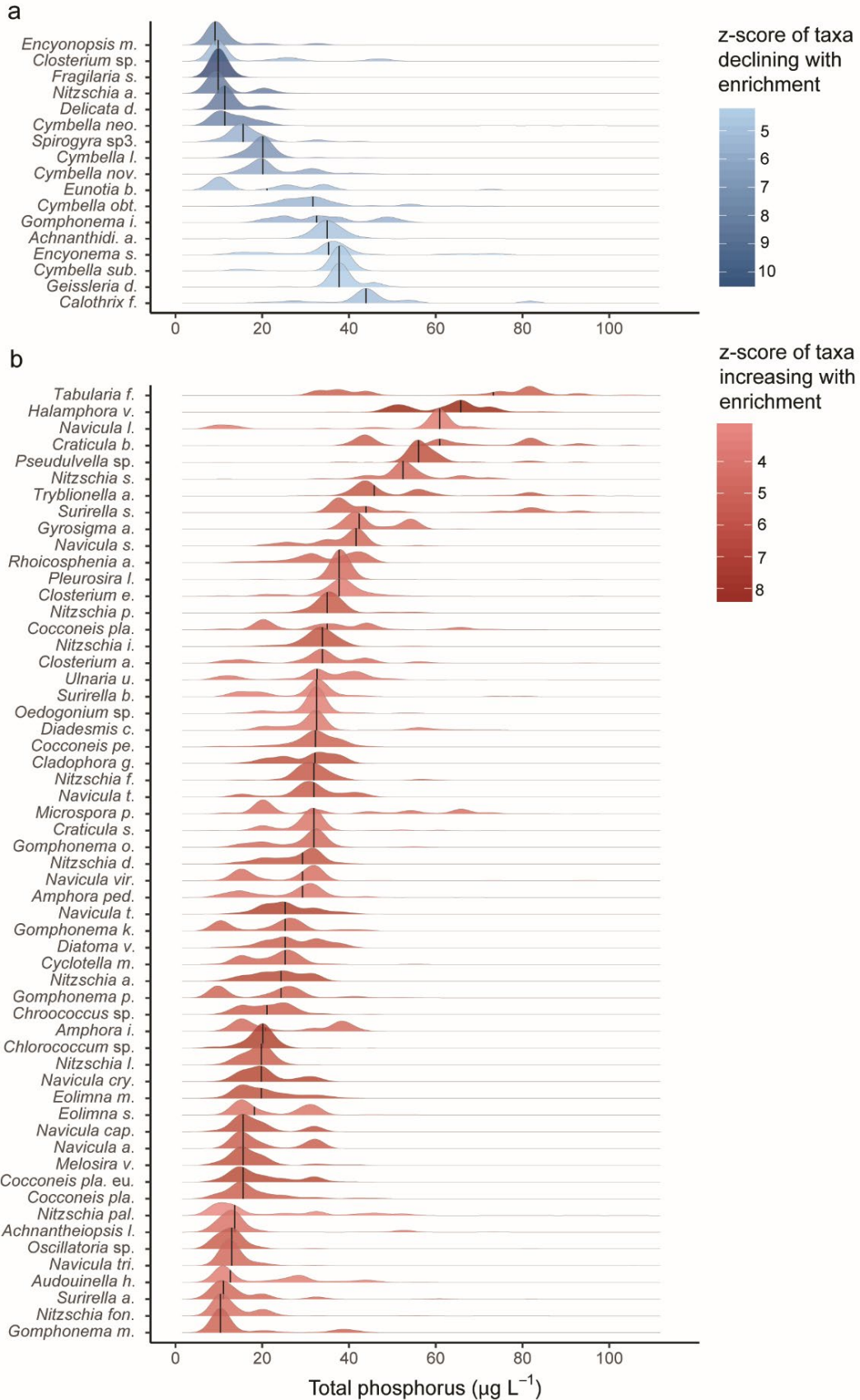


Figure 4.5. Significant indicator taxa as identified by Threshold Indicator Taxa ANalysis (TITAN) on 2-year mean algal biovolumes across a gradient of total phosphorus (TP, $\mu\text{g L}^{-1}$) enrichment. The distributions of individual taxa decreasing (a, blue) and increasing (b, red) with increasing TP represent the location and certainty of taxon changepoints generated from 1000 bootstrap replicates. Vertical black lines within the distribution represent the bootstrap median, with tighter density curves illustrating more certainty about taxon threshold responses to TP. The color gradients illustrate the magnitude of the response (z-score). Genus names are displayed, with species and variety names abbreviated for clarity (taxon codes and full species names in Appendix C).

There was some evidence of synchronous changes in macroinvertebrate response to periphyton nutrient content; most macroinvertebrates that became more effective competitors as a result of enriched periphyton C:P were primary consumers (> 90%, Fig. 4.5d), while declining taxa were spread among functional groups representing a wider range of trophic status (1 shredder, 4 scrapers, and 6 predators). Evans-White and others (2009) found that threshold declines in macroinvertebrate biodiversity were dependent on feeding mode, with the strongest impacts occurring in primary consumers. Benthic periphyton is the dominant basal food resource in many wadeable, open-canopied streams, and enrichment of periphyton nutritional quality can alleviate the stoichiometric mis-match between nutrient-poor producers and consumers with higher N and P demands (Frost et al. 2002, 2005, Singer and Battin 2007). P subsidies likely played a large role in altering competition to favor small-bodied, rapidly-growing taxa that are normally constrained by their relatively P poor food (Sterner and Elser 2002, Cross et al. 2005, Back and King 2013). Our results indicate that small shifts in food quality can correspond to large, non-linear shifts in macroinvertebrate assemblage structure.

Interestingly, we observed evidence that many macroinvertebrate taxa were released from P limitation at periphyton C:P that corresponded to TP concentrations of $\sim 25 \mu\text{g L}^{-1}$ (Fig. 4.1a, modeled relationship, Fig. 4.5d, taxa responses) even though macroinvertebrate response as predicted by TP alone occurred across a much wider range of enrichment. Therefore, multiple assemblages and mechanistic pathways should be assessed when developing nutrient criteria (Sundermann et al. 2015), as the bimodal response of the macroinvertebrate assemblages in response to TP would have spuriously suggested a P criterion at different concentrations than are supported by clear,

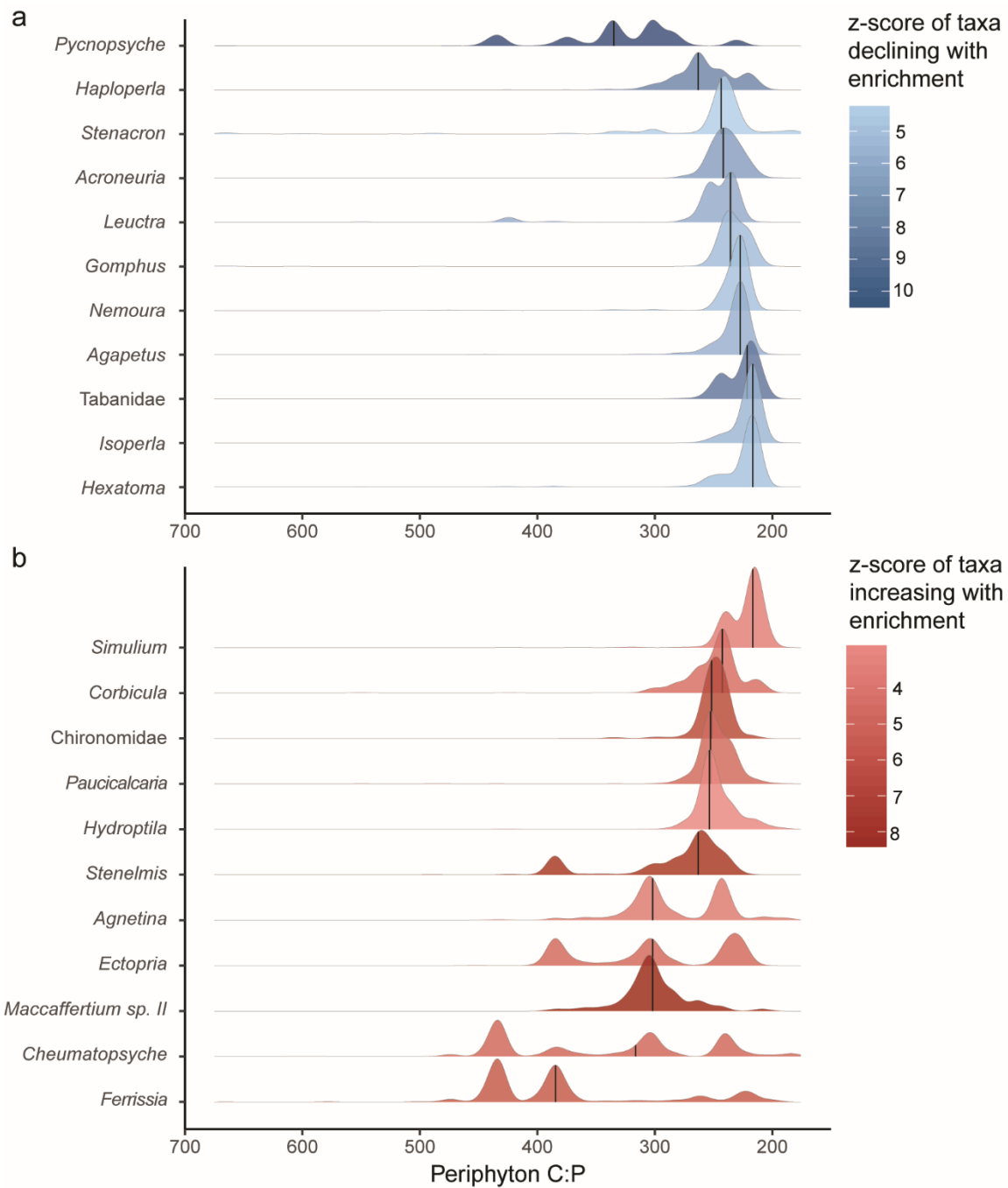


Figure 4.6. Significant indicator taxa as identified by Threshold Indicator Taxa ANalysis (TITAN) on 2-year mean macroinvertebrate densities in response to periphyton nutrient content (tissue C:P). Note that the x-axis has been inverted so that enrichment is still represented by a left to right gradient. The distributions of individual taxa decreasing (a, blue) and increasing (b, red) with increasing nutrient content represent the location and certainty of taxon changepoints generated from 1000 bootstrap replicates. Vertical black lines within the distribution represent the bootstrap median, with tighter density curves illustrating more certainty about taxon threshold responses to TP. The color gradients illustrate the magnitude of the response (z-score).

assemblage-level shifts in periphytic algae. Further, higher TP criterion sometimes suggested as protective of higher trophic levels (i.e. $> 30 \mu\text{g L}^{-1}$, Stevenson et al. 2008) may fail to prevent changes in assemblage structure that accompany changes in food nutrient content. The critical concentrations of P enrichment that corresponded to thresholds in algal assemblage structure support protective recommendations developed using similar methods in other regions (Smucker et al. 2013 in Connecticut streams, and Taylor et al. 2014 in Texas streams), which may indicate that maintaining P enrichment levels below *c.* $20 \mu\text{g L}^{-1}$ P may prevent precipitous changes in the structure of stream communities across ecosystems.

Establishing where ecological thresholds exist should be prioritized in a variety of ecosystems because it is difficult to predict the deleterious shifts in ecosystem function that oftentimes accompany structural changes to the community (Dodds et al. 2010, King and Richardson 2003). Novel communities may represent an alternative ecosystem state and resist restoration efforts (i.e. alternative stable-state *sensu* May 1977, Scheffer and Carpenter 2003), so identifying community stressors and protecting ecosystems before thresholds are crossed is equally important.

CHAPTER FIVE

Summary and Conclusions

Summary of Chapter Contents

Findings outlined in this dissertation demonstrate how eutrophication alters stream assemblages at both spatial and temporal scales. Benthic algal and macroinvertebrate seasonal patterns of succession were significantly altered by nutrient enrichment. Though species in both assemblages displayed threshold responses to enrichment, algae exhibited much stronger and more synchronous responses to enrichment at the assemblage-level than did macroinvertebrates.

The findings from Chapter Two indicate that nutrient enrichment leads to more temporally homogenous assemblages at intra-annual time scales. Seasonal macroinvertebrate species lose the competitive advantage they receive by occupying particular temporal niches, which results in assemblages dominated by generalist taxa that exhibit little seasonal turnover. These results indicate that eutrophication alters temporal assembly patterns in species with highly advanced phenology.

In Chapter Three I explored the mechanisms that govern the temporal maintenance of biodiversity in periphytic stream algae. Algal assemblages were characterized by seasonally-driven compensatory dynamics under natural nutrient regimes. Compensatory dynamics broke down at relatively low levels of total phosphorus enrichment ($\sim 25 \mu\text{g L}^{-1}$). More species were able to coexist at any given time, and the fitness of a subset of species was increased by enrichment which led to seasonal variation

characterized by synchronous swings in species biovolumes. I also observed much higher instability in assemblage biovolumes with declines in compensatory dynamics, which indicates that anthropogenic alteration of nutrient regimes can affect community stability by changing the dominant mode of seasonal succession. These findings provide insight about how nutrient enrichment impacts evolved drivers of species coexistence.

Nutrient enrichment impacts different aquatic assemblages through unique mechanistic pathways. Assemblage-level threshold responses to nutrient enrichment, described in Chapter Four, were best predicted by measures of eutrophication that captures how nutrient enrichment acts on different assemblages. Periphytic algae can directly access the dissolved inorganic and organic nutrient pools, and algae displayed threshold responses to water column P concentrations. There was no evidence of a macroinvertebrate assemblage-level threshold when TP was the measure of enrichment used, but periphyton C:P was predictive of abrupt, non-linear shifts in macroinvertebrate assemblage structure. Algae and macroinvertebrates are the two most commonly used groups of organisms to assess biotic integrity, and the results presented in this chapter underscore the need to use multiple assemblages to garner a full understanding of nutrient enrichment on stream communities.

Future Directions

Chapter Two and Chapter Three add to a growing body of literature that indicates seasonal changes in abiotic condition are an important mechanism that maintains biodiversity in a variety of ecosystems (Steiner 2014, Tonkin et al. 2017). Most studies to date, including the studies in this dissertation, are concerned with structural patterns in community composition. The hope of many scientists is that maintaining biodiversity will

buffer ecosystems against current and coming environmental change (Cardinale et al. 2012), and by extension preserve many of the valuable ecosystem services that humans hold dear. Spatial homogenization of biotic assemblages leads to declines in productivity and inefficient resource use (Loreau and Hector 2001, Zhang and Zhang 2006, Cardinale 2011), and it is reasonable to assume that temporal homogenization has similar impacts. Considering the results of this Dissertation, and the fact that most assessments of biodiversity downplay intra-annual fluctuations in community composition, it is highly unlikely that simply maintaining typical measures of biodiversity (i.e. snap-shot measures) will provide the hoped-for buffer against environmental change. Much more research is needed to assess the seasonally dependent alterations to ecosystem function that accompany structural changes noted in this Dissertation.

The assemblage-level thresholds covered in Chapter Four indicate that eutrophication has the potential to act uniquely on different assemblages based on trophic position and mechanism of action, and the second and third chapters indicate that nutrient enrichment disproportionately impacts seasonal specialists. A natural next step would be to examine how threshold responses in each assemblage change seasonally, as it is highly likely that there are important differences in the seasonality of tolerant and sensitive species to a variety of novel environmental gradients. For instance, if declining taxa are normally constrained to a narrow seasonal window, researchers are likely to underestimate the number of species sensitive to novel environments with typical sampling designs.

Since Hubbell's unified neutral theory of biodiversity (Hubbell 2001), there has been much discussion about the relative importance of niche and neutral mechanisms

governing the maintenance of biodiversity (Thompson and Townsend 2006, Adler et al. 2007, Chase 2007). This Dissertation focused on niche-based rationale to explain the structural changes of algal and macroinvertebrate assemblages, but it is likely that neutral mechanisms play a role in temporal assembly patterns in stream communities. For instance, Chapter Three presents evidence that the compensatory dynamics at low levels of P enrichment are driven by seasonal fluctuations in temperature (a niche-based process), but temporal change in the community could also be due to stochastic colonization following small disturbance events. The tools available to parse the relative contribution of these two mechanisms are in their infancy (Tucker et al. 2016), and more research on which mechanisms are governing temporal β diversity are needed.

APPENDICES

APPENDIX A

Chapter Two Supplementary Material

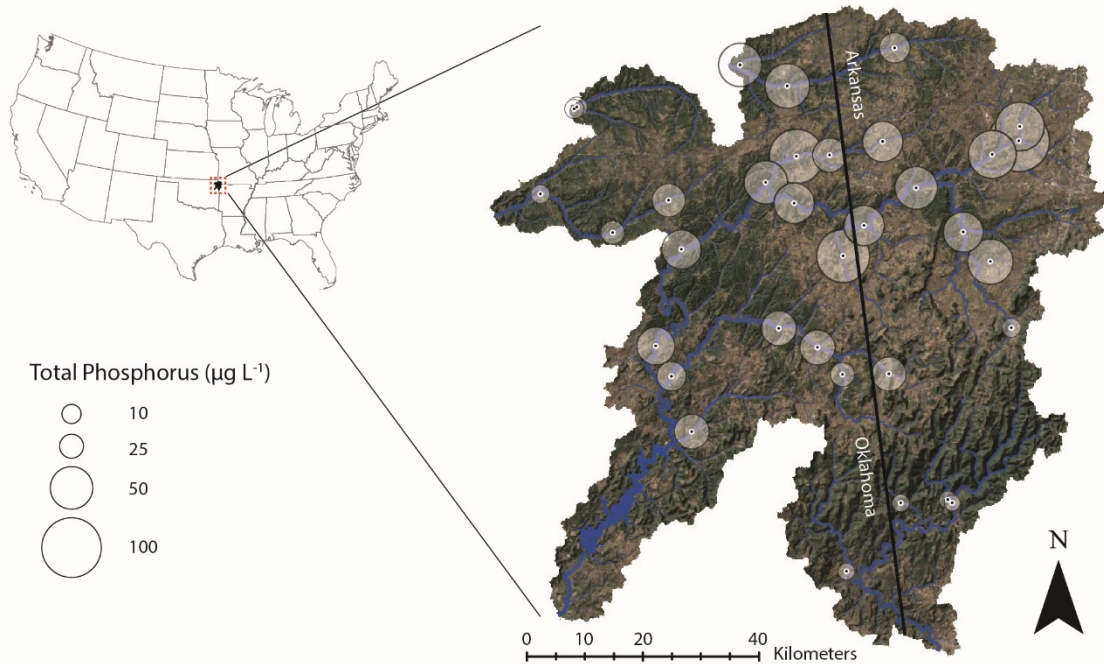


Figure A.1. Locations of sampling sites in the Illinois R. drainage basin and surrounding areas spanning the border of Oklahoma and Arkansas (USA, 1:750,000 Landsat shaded basemap, USGS), with points continuously scaled to 2 y mean total phosphorus concentration ($\mu\text{g L}^{-1}$).

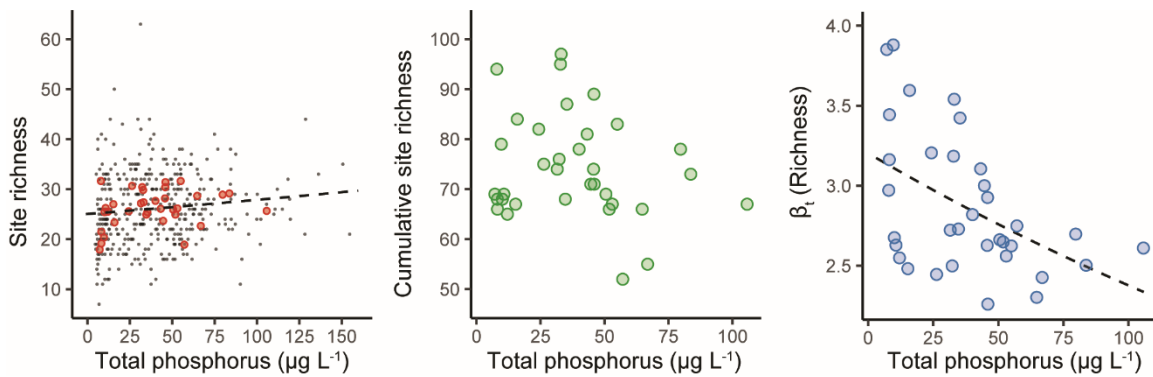


Figure A.2. Site richness (left pane), cumulative site richness (middle pane), and β_t calculated as cumulative site richness/mean site richness (right pane) displayed across mean total phosphorus (TP) concentrations. Each black point (left pane) represents the number of taxa recorded at each site visit, whereas the red overlays denote the mean richness and TP for each site across all 12 sampling events. Dotted lines represent significant relationships from GLM regressions, with mean site richness displaying a weak but positive relationships with TP ($p = 0.03$), and $\beta_t(\text{Richness})$ declining as TP increases ($p = 0.003$).

Table A.1. Summary of results from generalized linear models (GLMs) relating both β_t (Shannon) and β_t (MVD) measures of temporal beta diversity (β_t) to two measures of eutrophication (Chlorophyll-a; Chl-a and total phosphorus; TP) with covariates. Models are grouped first between response variable (i.e. measure of β_t), then by measure of eutrophy (TP and Chl-a were correlated, and for this reason evaluated in separate models). Models were selected using AICc and deviance explained (%), and are ordered by increasing AICc values within groups, so that the model with the lowest AICc score is at the top of each grouping. Covariates that remained after model selection included temperature variability ($^{\circ}\text{C}$ IQR, interquartile range), mean total macroinvertebrate biomass (g m^{-2}), and mean snail biomass (g m^{-2}).

Eutrophy measure	Variable	Coefficient	Std. Error	P-value	Significance	AICc	Deviance explained (%)		
β_t (Shannon)									
TP	Intercept	6.64e-01	8.44e-02	<0.0001	***	-11.40	62.02		
	Total phosphorus	-3.08e-03	5.98e-04	<0.0001	***				
	Temperature (IQR)	2.27e-02	6.40e-03	0.0013	**				
Chl-a	Intercept	6.64e-01	8.34e-02	<0.0001	***	-13.89	67.45		
	Chlorophyll-a	-4.30e-04	9.17e-05	<0.0001	***				
	Biomass (total)	-4.70e-06	1.90e-06	0.0196	*				
	Temperature (IQR)	2.53e-02	6.43e-03	0.0005	***				
	Intercept	6.20e-01	7.84e-02	<0.0001	***			-12.50	66.09
	Chlorophyll-a	-4.32e-04	9.39e-05	<0.0001	***				
	Biomass (snails)	-4.40e-06	2.00e-06	0.0385	*				
Temperature (IQR)	2.76e-02	6.31e-03	0.0001	***					
β_t (MVD)									
TP	Intercept	-7.70e-01	3.22e-02	<0.0001	***	-150.72	71.74		
	Total phosphorus	-3.76e-03	6.38e-04	<0.0001	***				
	Biomass (total)	-1.70e-05	3.50e-06	<0.0001	***				
	TP:Biomass(total)	1.00e-07	0.00e+00	0.0006	***				
	Intercept	-1.12e+00	7.02e-02	<0.0001	***			-145.76	64.54
	Total phosphorus	-2.76e-03	4.97e-04	<0.0001	***				
Temperature (IQR)	1.99e-02	5.33e-03	0.0008	***					
Chl-a	Intercept	-1.11e+00	7.32e-02	<0.0001	***	-144.68	66.25		
	Chlorophyll-a	-3.13e-04	8.05e-05	0.0005	***				
	Biomass (total)	-5.40e-06	1.70e-06	0.0031	**				
	Temperature (IQR)	2.04e-02	5.65e-03	0.0011	**				
	Intercept	-1.16e+00	6.93e-02	<0.0001	***			-142.80	64.33
	Chlorophyll-a	-3.14e-04	8.31e-05	0.0007	***				
	Biomass (snails)	-5.10e-06	1.80e-06	0.0074	**				
Temperature (IQR)	2.28e-02	5.58e-03	0.0003	***					

Note: ****' p < 0.001, ***' p < 0.01, **' p < 0.05

Table A.2. Summary environmental and biotic data collected at 34 study sites in the Illinois River drainage basin and surrounding area every-other-month from June 2014 to April 2016 (12 sampling events). One site was exposed to untreated wastewater during the study and was excluded from analysis. All means are presented with standard deviation in parentheses. Temporal habitat heterogeneity is a unitless measure.

Scouring was the number of times we sampled within 10 d of a discharge event exceeding five times median base flow. Temperature variability (IQR) is the interquartile range of water temperature observed at each site over all sampling events. β_t (Richness) was calculated as mean site richness/cumulative site richness. β_t (Shannon) and β_t (MVD) incorporate abundance information, and are the exponentiated Shannon diversity index (Shannon), and multivariate dispersion (MVD) around group centroids, respectively.

Site	Latitude	Longitude	Watershed area (km ²)	Elevation (m)	Temporal habitat heterogeneity	Turbidity (NTU)	Temperature variability (IQR)	Scouring	Canopy cover (%)	Wetted width (m)
BALL1	36.06137	-94.57315	90.15	300.6	1.397	1.85 (1.09)	12.210	5	5.71 (8.65)	10.17 (2.50)
BARR1	35.87954	-94.48221	105.64	300.8	1.225	1.09 (0.55)	13.270	5	10.5 (7.85)	12.29 (3.26)
BARR2	35.91906	-94.61932	409.53	258.1	1.406	0.70 (0.32)	12.978	5	0.08 (0.28)	19.64 (10.6)
BARR3	35.94727	-94.69353	542.89	243.6	1.199	0.63 (0.26)	11.366	4	3.24 (5.74)	19.54 (5.45)
BARR4	35.87013	-94.89697	879.86	200.4	1.582	1.34 (0.64)	9.980	4	0.21 (0.58)	33.00 (20.1)
BEAT1	36.35495	-94.77667	152.63	243.2	1.161	0.70 (0.50)	10.448	7	4.49 (8.26)	10.21 (3.25)
CANE1	35.78497	-94.85589	232.88	207.4	1.205	1.00 (0.64)	11.749	2	2.15 (2.13)	14.91 (4.17)
COVE1	35.68576	-94.36629	135.32	278.5	1.779	3.11 (2.50)	15.320	9	4.66 (8.31)	12.55 (5.69)
EVAN1	35.87742	-94.57058	164.18	278.5	1.105	0.96 (0.27)	14.950	5	9.52 (14.8)	13.73 (5.17)
FLIN1	36.23973	-94.50070	64.94	330.6	1.315	0.90 (0.44)	8.382	3	43.4 (14.7)	12.10 (3.49)
FLIN2	36.21771	-94.60190	145.91	291.9	1.557	1.04 (0.57)	11.438	4	33.0 (10.7)	9.363 (2.27)
FLIN3	36.21454	-94.66549	245.17	275.4	1.120	1.63 (0.75)	10.488	3	6.55 (7.36)	14.96 (2.60)
GOOS1	36.05603	-94.29123	35.46	336.2	1.213	0.75 (0.36)	8.710	4	51.5 (9.32)	10.67 (2.08)
ILLI1	35.95398	-94.24939	68.91	348.4	1.333	1.43 (0.65)	14.315	5	10.0 (11.6)	11.16 (5.18)
ILLI2	36.10135	-94.34410	420.43	291.7	2.010	4.40 (2.10)	13.678	5	20.0 (17.3)	18.83 (7.02)
ILLI3	36.16864	-94.43555	1239.80	291.7	1.469	3.05 (1.41)	13.225	2	0.65 (2.27)	29.55 (5.12)
ILLI4	36.10930	-94.53388	1473.71	276.8	1.253	3.01 (1.18)	13.788	3	0.25 (0.79)	40.90 (10.0)
ILLI5	36.14201	-94.66812	1716.95	259.5	2.174	4.59 (4.37)	14.338	3	1.63 (2.63)	41.06 (10.4)
ILLI6	36.17349	-94.72374	2092.83	253.8	1.536	2.47 (1.32)	12.938	4	3.82 (5.84)	34.15 (9.04)
ILLI7	36.06755	-94.88233	2294.62	235.3	1.439	2.60 (1.32)	13.943	4	1.07 (1.89)	42.15 (14.4)
ILLI8	35.91667	-94.92796	2465.63	203.0	2.022	3.08 (1.51)	14.035	5	0.61 (1.43)	50.79 (18.0)
LFE1	35.68091	-94.35779	252.17	214.2	2.470	4.30 (4.77)	15.148	9	0 (na)	25.45 (12.7)
LFE1	35.57263	-94.55667	264.07	154.3	1.647	3.41 (3.16)	13.768	8	2.21 (3.38)	22.30 (4.12)
LSAL1	36.28455	-95.08867	61.70	197.5	1.170	0.51 (0.44)	7.735	7	25.0 (12.6)	9.272 (1.92)
MFFK1	35.68016	-94.45584	67.13	233.0	2.158	2.16 (3.26)	14.593	9	19.2 (20.1)	10.39 (5.56)
OSAG1	36.26593	-94.23777	100.84	337.9	1.220	0.76 (0.30)	8.860	4	1.94 (3.62)	13.56 (3.42)
OSAG2	36.22200	-94.29007	337.40	320.4	1.232	1.32 (0.79)	10.578	3	9.51 (7.94)	28.97 (2.28)
SALI1	36.28154	-95.09321	270.07	192.0	1.266	0.52 (0.42)	9.305	4	0.73 (1.78)	19.72 (4.27)
SPAR1	36.24367	-94.23932	91.66	331.3	1.149	1.12 (0.73)	10.376	4	0.16 (0.37)	15.79 (3.08)
SPAV1	36.38484	-94.48099	173.85	303.7	1.432	0.83 (0.38)	9.288	2	7.02 (9.41)	11.66 (3.52)
SPAV2	36.32323	-94.68543	421.61	255.4	1.500	0.83 (0.56)	8.503	2	0.72 (1.82)	24.83 (14.4)
SPRG1	36.14290	-94.90907	84.03	289.8	1.119	0.31 (0.26)	10.360	4	42.5 (6.65)	11.14 (1.97)
SPRG2	36.09092	-95.01467	194.81	245.9	1.550	0.64 (0.36)	8.620	4	4.29 (6.40)	19.34 (7.86)
SPRG3	36.14833	-95.15475	296.68	203.7	1.165	0.60 (0.38)	8.845	5	0.08 (0.28)	24.05 (5.77)

Table A.2. Continued.

Site	Current velocity (m s ⁻¹)	Substrate embeddedness (%)	Mean site richness	Cumulative site richness	β_t (Richness)	β_t (Shannon)	β_t (MVD)	Total phosphorus (μg L ⁻¹)	Chlorophyll-a (mg m ⁻²)	Invertebrate biomass (g m ⁻²)	Snail biomass (g m ⁻²)
BALL1	0.40 (0.21)	37.77 (8.44)	28.92	78	2.697	2.00	0.326	82.14 (25.52)	282.3 (160.2)	6.62 (5.48)	0.972 (0.91)
BARR1	0.32 (0.14)	40.05 (8.74)	29.83	95	3.184	2.17	0.385	34.03 (11.38)	366.9 (235.0)	4.80 (4.35)	0.002 (0)
BARR2	0.58 (0.17)	42.38 (9.04)	24.92	68	2.729	2.39	0.391	35.20 (7.608)	195.8 (123.4)	5.18 (7.68)	0.538 (1.36)
BARR3	0.61 (0.11)	35.88 (12.2)	25.42	87	3.423	2.65	0.413	36.05 (8.880)	218.7 (113.3)	2.54 (2.74)	0.596 (2.15)
BARR4	0.49 (0.10)	31.75 (10.6)	25.58	82	3.205	2.31	0.378	24.74 (8.035)	192.0 (106.4)	3.16 (4.19)	0.109 (0.34)
BEAT1	0.54 (0.16)	34.66 (7.49)	26.17	67	2.561	2.21	0.381	53.67 (8.808)	265.7 (209.2)	6.18 (5.87)	0.616 (1.11)
CANE1	0.47 (0.15)	40.33 (9.49)	27.40	97	3.540	2.73	0.417	33.44 (8.610)	265.7 (153.0)	7.38 (8.50)	4.170 (8.50)
COVE1	0.31 (0.22)	33.80 (9.58)	21.50	68	3.163	2.44	0.405	8.318 (2.900)	58.12 (35.31)	2.39 (1.49)	0 (na)
EVAN1	0.12 (0.19)	34.32 (9.17)	23.36	81	3.595	2.66	0.427	16.20 (6.80)	174.7 (113.0)	4.06 (2.35)	0.102 (0.08)
FLIN1	0.41 (0.14)	32.80 (9.12)	31.42	71	2.260	2.09	0.349	46.94 (6.20)	207.2 (83.30)	8.36 (7.04)	3.196 (4.52)
FLIN2	0.68 (0.20)	36.86 (12.4)	30.42	76	2.499	1.97	0.340	32.25 (7.71)	258.8 (165.5)	7.05 (4.58)	2.645 (2.02)
FLIN3	0.65 (0.13)	38.47 (7.81)	29.17	73	2.503	2.06	0.319	86.26 (26.63)	207.6 (145.9)	11.8 (7.76)	8.785 (8.06)
GOOS1	0.12 (0.17)	48.69 (8.57)	18.92	52	2.749	1.97	0.362	57.64 (11.33)	438.8 (223.3)	2.34 (1.62)	0 (na)
ILL1	0.29 (0.21)	38.57 (9.82)	20.36	79	3.879	2.82	0.462	9.955 (2.83)	83.74 (54.29)	2.44 (2.28)	0.599 (0.69)
ILL2	0.41 (0.21)	40.52 (9.77)	23.67	71	3.000	2.22	0.395	45.98 (13.88)	333.7 (272.5)	6.93 (7.34)	4.158 (5.89)
ILL3	0.60 (0.15)	40.77 (11.7)	25.92	69	2.662	2.13	0.374	52.46 (16.79)	587.3 (859.9)	5.80 (6.42)	3.314 (5.82)
ILL4	0.62 (0.20)	43.16 (10.3)	28.17	74	2.627	2.21	0.353	47.41 (16.49)	541.9 (575.0)	6.59 (6.63)	5.225 (6.65)
ILL5	0.74 (0.20)	42.38 (11.6)	30.42	89	2.926	2.06	0.348	47.87 (21.19)	638.9 (773.2)	11.0 (10.8)	8.640 (10.2)
ILL6	0.77 (0.20)	44.80 (10.8)	24.92	66	2.649	2.20	0.365	53.68 (15.73)	411.1 (425.6)	2.40 (2.95)	1.327 (2.87)
ILL7	0.48 (0.10)	39.94 (8.50)	26.08	81	3.105	2.29	0.364	43.69 (16.20)	367.5 (402.4)	2.12 (2.61)	0.610 (1.68)
ILL8	0.63 (0.26)	38.73 (8.26)	27.67	78	2.819	2.19	0.333	41.63 (16.24)	352.2 (548.7)	14.0 (11.6)	12.38 (10.4)
LEE1	0.35 (0.23)	33.12 (8.39)	17.92	69	3.851	3.14	0.483	7.253 (1.95)	43.53 (27.28)	1.75 (2.34)	0 (na)
LLEE1	0.40 (0.18)	36.25 (8.70)	31.64	94	2.971	2.34	0.374	8.027 (2.20)	62.14 (38.91)	2.52 (1.20)	0 (na)
LSAL1	0.49 (0.14)	32.97 (5.01)	25.50	65	2.549	2.11	0.358	12.38 (5.02)	119.9 (60.42)	8.79 (6.23)	4.455 (4.41)
MIFK1	0.30 (0.22)	35.97 (7.62)	19.17	66	3.443	2.69	0.435	8.327 (2.51)	57.09 (34.36)	3.36 (2.40)	0 (na)
OSAG1	0.46 (0.20)	37.83 (9.17)	22.67	55	2.426	1.71	0.301	68.51 (23.24)	296.4 (117.9)	17.8 (15.5)	12.86 (12.7)
OSAG2	0.67 (0.19)	41.27 (9.11)	28.67	66	2.302	1.85	0.305	65.97 (17.60)	497.8 (653.1)	13.0 (11.8)	5.462 (6.58)
SALI1	0.45 (0.19)	37.30 (8.89)	26.25	69	2.629	2.20	0.361	11.04 (4.00)	160.8 (151.8)	11.3 (9.11)	8.172 (8.06)
SPAR1	0.62 (0.13)	41.61 (10.0)	25.67	67	2.610	1.77	0.298	107.4 (25.43)	384.3 (324.5)	45.7 (56.9)	41.27 (56.6)
SPAV1	0.61 (0.15)	39.25 (12.3)	30.67	75	2.446	2.25	0.329	27.02 (4.74)	242.1 (123.0)	12.2 (8.74)	5.262 (6.20)
SPAV2	0.52 (0.14)	33.36 (9.20)	31.64	83	2.624	2.11	0.334	55.64 (4.79)	218.3 (136.6)	10.6 (8.88)	6.135 (7.98)
SPRG1	0.42 (0.11)	34.11 (9.57)	27.18	74	2.722	2.34	0.374	32.58 (7.65)	157.3 (85.60)	11.4 (7.73)	7.315 (6.91)
SPRG2	0.40 (0.26)	36.72 (9.91)	27.00	67	2.481	2.20	0.364	15.66 (4.14)	137.3 (84.42)	18.7 (19.6)	12.63 (16.6)
SPRG3	0.58 (0.16)	38.25 (10.3)	25.42	68	2.675	2.15	0.367	10.40 (2.98)	139.3 (114.3)	10.7 (12.4)	6.126 (9.44)

Additional Supporting Information

A list of macroinvertebrate taxa, as well as the sources used to construct length-mass regression for biomass estimates can be found in the online version of this article at <http://onlinelibrary.wiley.com/doi/10.1002/ecy.2069/suppinfo>.

Data Accessibility

Macroinvertebrate data associated with this study are available from the Dryad Digital Repository: <https://doi.org/10.5061/dryad.3r44n>

APPENDIX B

Chapter Three Supplementary Material

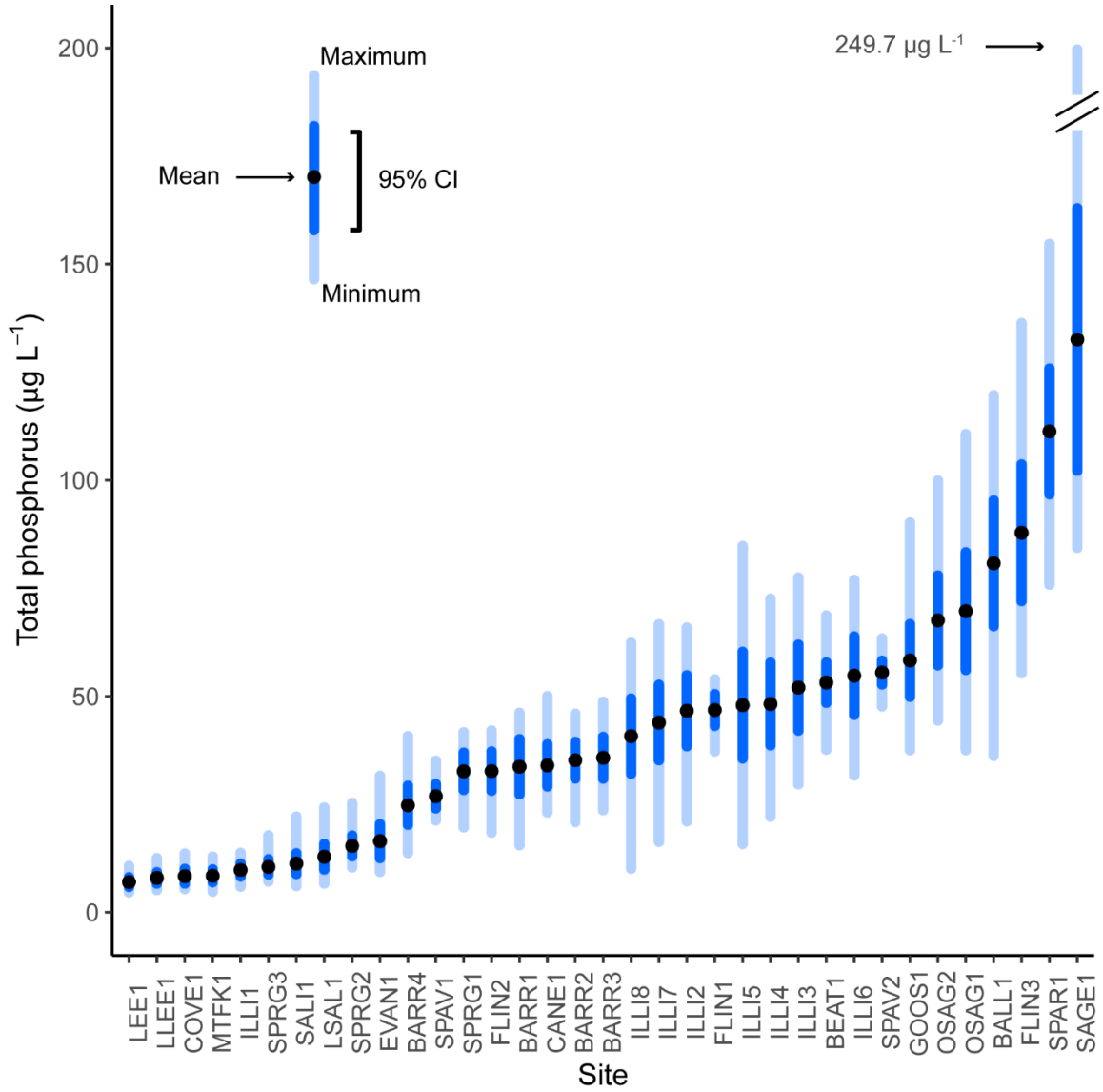


Figure B.1. Total phosphorus (TP, $\mu\text{g L}^{-1}$) concentrations of study sites ranked by increasing mean TP over the 2 year study, which increased roughly log-linearly. Points denote site means, while the darker inner bars and lighter outer bars signify the 95% confidence interval and the range of TP concentrations observed during the study, respectively.

Table B.1. Summary results from environmental vector fitting to NMDS ordinations (NMDS axis 1 and 2) of stream algae using three measures of spatiotemporal dissimilarity.

	NMDS1	NMDS2	r	P	Significance
β_{TOT}					
Temperature	0.24401	-0.96977	0.6670	0.001	***
Discharge	0.43020	0.90273	0.2480	0.001	***
pH	0.87630	0.48176	0.6181	0.001	***
Depth	0.95214	0.30567	0.1334	0.032	*
Canopy cover	0.61899	-0.78540	0.0742	0.365	
TP (log)	0.99994	-0.01073	0.7125	0.001	***
Tissue P (log)	0.86664	0.49894	0.6973	0.001	***
TN (log)	0.98192	0.18928	0.6138	0.001	***
β_{BAL}					
Temperature	0.01583	-0.99987	0.5215	0.001	***
Discharge	0.67196	0.74059	0.2522	0.001	***
pH	0.94876	0.31600	0.4932	0.001	***
Depth	0.95595	0.29353	0.1327	0.034	*
Canopy cover	0.97361	0.22821	0.0693	0.402	
TP (log)	0.99998	-0.00643	0.6982	0.001	***
Tissue P (log)	0.95966	0.28115	0.4571	0.001	***
TN (log)	0.98334	0.18179	0.6248	0.001	***
β_{GRA}					
Temperature	-0.99587	-0.09077	0.4104	0.001	***
Discharge	0.99015	0.14003	0.0656	0.450	
pH	0.99942	0.03408	0.4243	0.001	***
Depth	0.37358	-0.92760	0.0346	0.797	
Canopy cover	-0.35817	0.93365	0.0480	0.632	
TP (log)	0.99997	-0.00795	0.3121	0.001	***
Tissue P (log)	0.83285	0.55349	0.4748	0.001	***
TN (log)	0.99537	0.09616	0.3081	0.001	***

Note:

β_{TOT} - total community dissimilarity, β_{BAL} - balanced variation in abundances, β_{GRA} - dissimilarity resulting from abundance gradients.

TP; total phosphorus, Tissue P; tissue phosphorus, Temperature; water temperature in degrees C, Discharge; stream discharge in cubic feet per second, TN; total nitrogen

***' p < 0.001, '**' p < 0.01, '*' p < 0.05

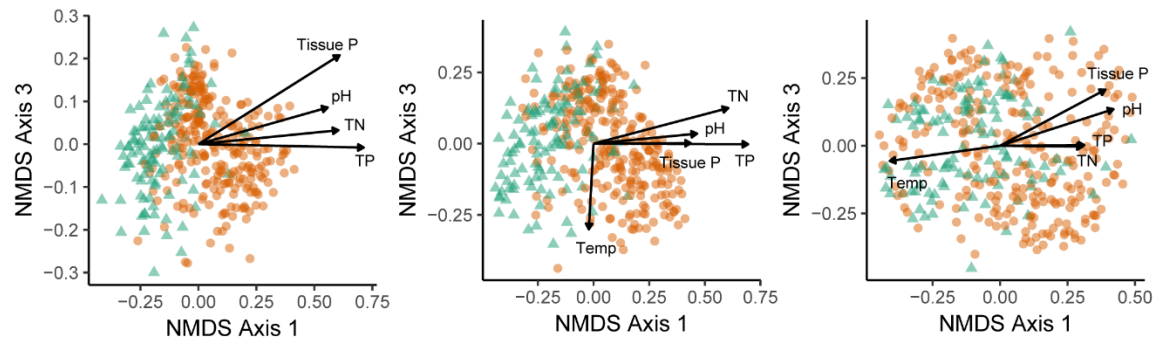


Figure B.2. Third NMDS axis displayed against NMDS axis 1 showing spatiotemporal dissimilarity in community structure across 35 streams and 2 years constructed from pair-wise dissimilarity measures of β_{TOT} (total β -diversity, left column, stress = 0.13), β_{BAL} (measuring compensatory dynamics, center column, stress = 0.18), and β_{GRA} (measuring abundance-gradients, right column, stress = 0.22). Points are colored by low total phosphorus (TP, green triangles) and high TP (orange circles) sites as determined by changepoint analysis. Top panel arrows display significant ($p < 0.001$) environmental vectors predictive of spatiotemporal structure in community composition.

APPENDIX C

Chapter Four Supplementary Materials

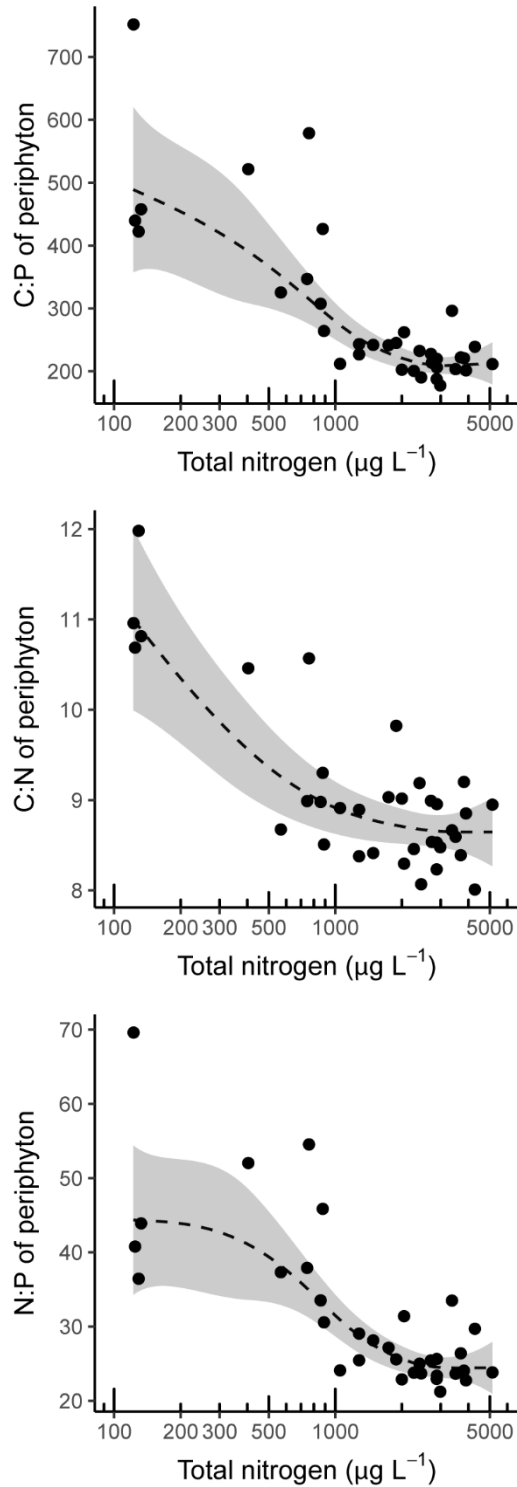


Figure C.1. Periphyton tissue C:P, C:N, and N:P all declined in response to total nitrogen (TN, log-scale) concentrations. GAM smoothers indicated that TN was predictive of C:P ($p < 0.001$, deviance explained = 73.4%) and N:P ($p < 0.001$, dev. exp. = 68.5%) content of periphyton, but explained less deviation in the response of periphyton C:N ($p < 0.001$, deviance explained = 48.0%).

Table C.1. Summary results from environmental vector fitting to NMDS ordinations of periphytic algae and benthic macroinvertebrates using Bray-Curtis dissimilarity as the distance measure.

Variable	NMDS1	NMDS2	r	P	Significance
Algae					
Temperature	0.07137	0.99745	0.3984972	0.068	
C:N (periphyton)	-0.81868	0.57425	0.7569676	0.001	***
Discharge	0.55667	0.83073	0.4320880	0.028	*
pH	0.92338	0.38388	0.7917702	0.001	***
Depth	0.99727	0.07383	0.1915724	0.559	
Canopy cover	0.97431	-0.22521	0.0774597	0.919	
Watershed size	0.50548	0.86284	0.4301163	0.029	*
Velocity	0.84231	-0.53899	0.6212890	0.001	***
TP (log)	1.00000	0.00000	0.9132360	0.001	***
TN (log)	0.98942	-0.14508	0.8777813	0.001	***
C:P (log, periphyton)	-0.99227	-0.12406	0.8966047	0.001	***
N:P (log, periphyton)	-0.95842	-0.28537	0.8906178	0.001	***
Macroinvertebrate					
Temperature	0.23021	-0.97314	0.4337050	0.037	*
C:N (periphyton)	-0.92064	-0.39042	0.6442825	0.001	***
Discharge	0.31133	-0.95030	0.7093659	0.001	***
pH	0.74851	-0.66312	0.7525291	0.001	***
Depth	0.48551	-0.87423	0.4865182	0.012	*
Canopy cover	0.10450	0.99453	0.3155947	0.182	
Watershed size	0.27691	-0.96089	0.7273239	0.001	***
Velocity	0.94684	-0.32170	0.6515366	0.001	***
TP (log)	1.00000	0.00000	0.7506664	0.001	***
TN (log)	0.98597	0.16692	0.7947956	0.001	***
C:P (log, periphyton)	-0.97451	0.22432	0.7152622	0.001	***
N:P (log, periphyton)	-0.94068	0.33931	0.6982120	0.001	***

Note:

TP; total phosphorus, TN; total nitrogen, C; carbon, N; nitrogen, P; phosphorus, Temperature; water temperature in degrees C, Discharge; stream discharge in cubic feet per second ***' p < 0.001, '**' p < 0.01, '*' p < 0.05

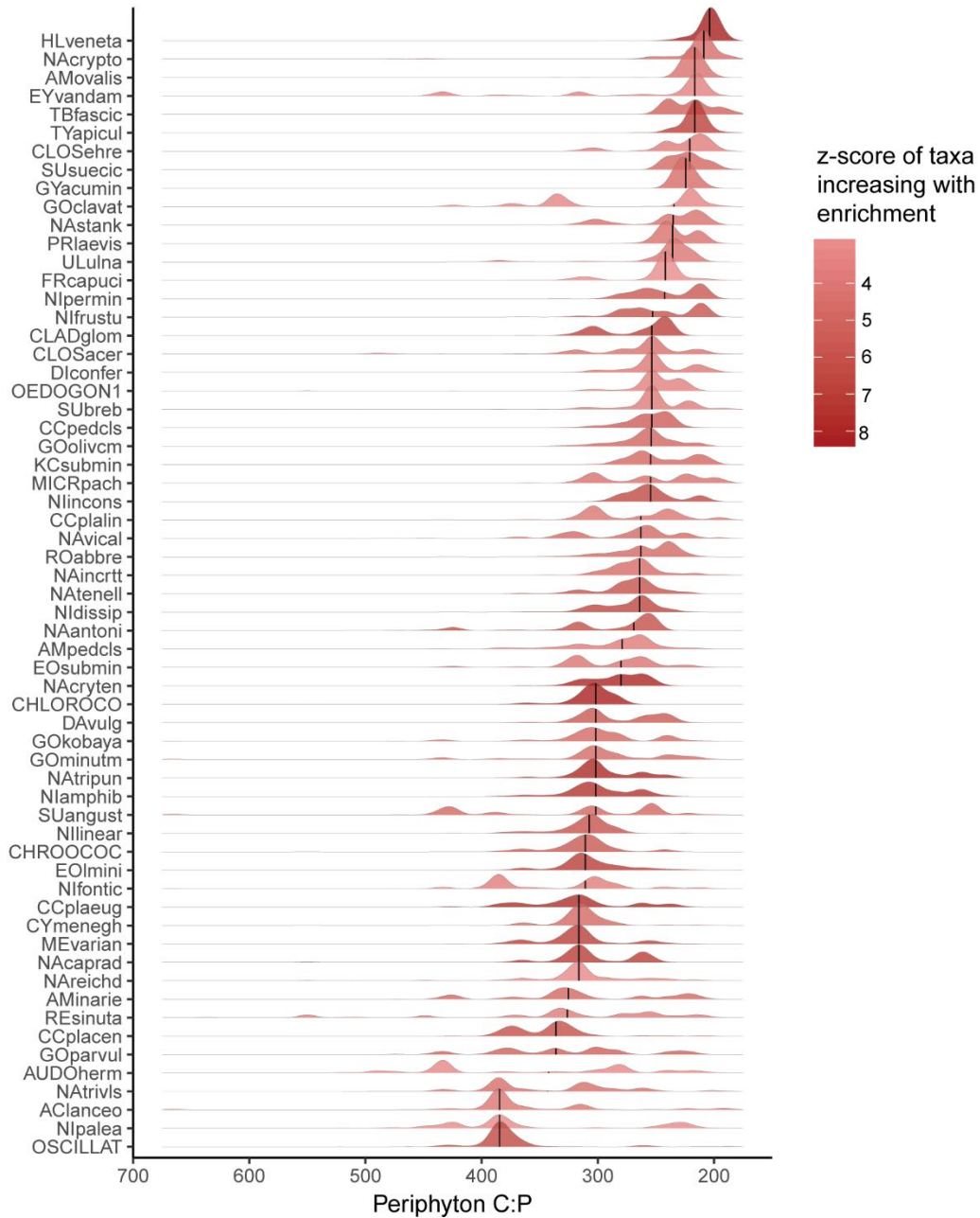
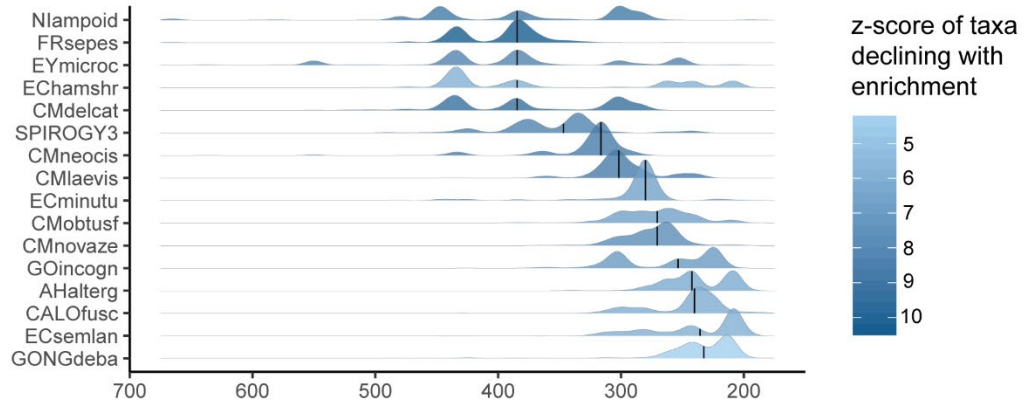


Figure C.2. Significant indicator taxa as identified by Threshold Indicator Taxa ANalysis (TITAN) on 2-year mean algal biovolumes across a gradient periphyton nutrient content as measured by the ratio of tissue carbon to phosphorus (C:P). The distributions of individual taxa decreasing (a, blue) and increasing (b, red) with increasing enrichment represent the location and certainty of taxon changepoints generated from 1000 bootstrap replicates. Vertical black lines within the distribution represent the bootstrap median, with tighter density curves illustrating more certainty about taxon threshold responses to C:P. The color gradients illustrate the magnitude of the response (z-score). Taxon codes are displayed (taxon codes and full species names in Appendix C, Table C.2).

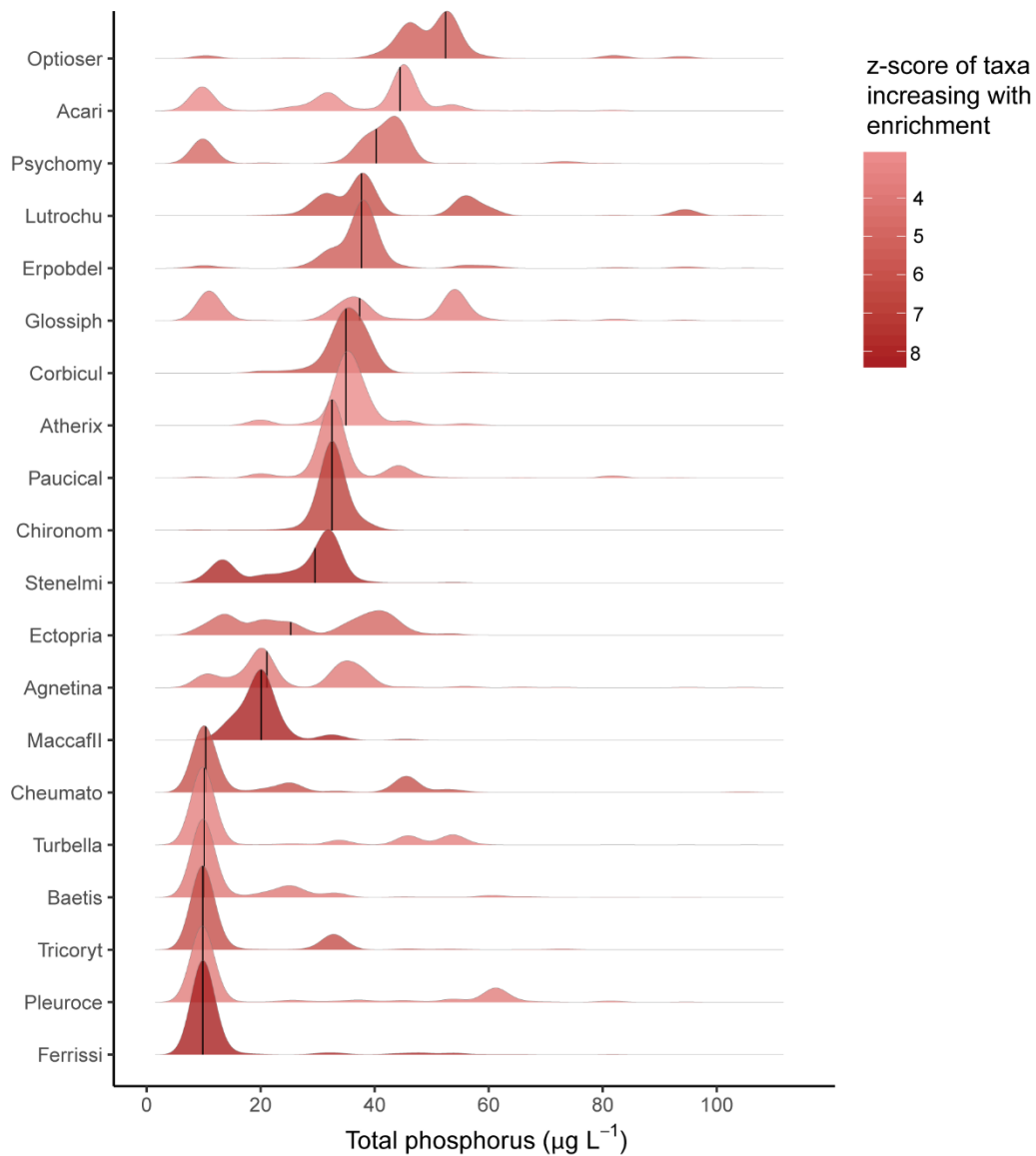
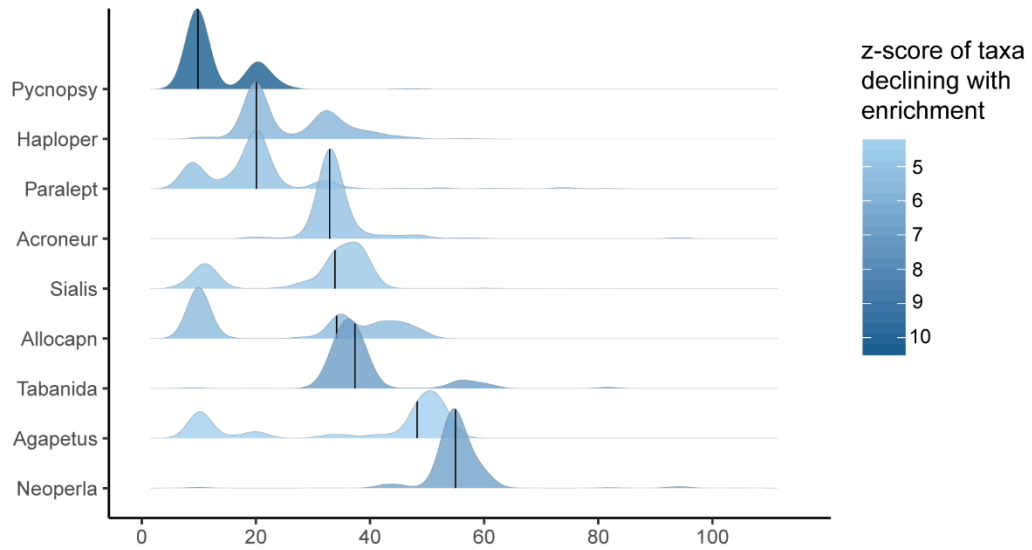


Figure C.3. Significant indicator taxa as identified by Threshold Indicator Taxa ANalysis (TITAN) on 2-year mean macroinvertebrate abundances across a gradient of total phosphorus (TP, $\mu\text{g L}^{-1}$) enrichment. The distributions of individual taxa decreasing (a, blue) and increasing (b, red) with increasing TP represent the location and certainty of taxon changepoints generated from 1000 bootstrap replicates. Vertical black lines within the distribution represent the bootstrap median, with tighter density curves illustrating more certainty about taxon threshold responses to TP. The color gradients illustrate the magnitude of the response (z-score).

Table C.2. Summary of pure and reliable algal taxa as identified by Threshold Indicator Taxa ANalysis (TITAN) responding to total phosphorus enrichment, and comparison of these taxa to analysis by Potapova and Charles (2007).

Code	Taxa	Division	TITAN	Potapova and Charles 2007	Agreement	<i>Cladophora</i> epiphyte
CLOSTERI	Closterium sp.	Charophyta	Decreaser	-	-	
EYmicroc	Encyonopsis microcephala	Bacillariophyta	Decreaser	High NUTs	N	
NIampoid	Nitzschia amphibioides	Bacillariophyta	Decreaser	-	Y/N at genus level	
CMneocis	Cymbella neocistula	Bacillariophyta	Decreaser	-	Y at genus level	
CMobtusf	Cymbella obtusifformis	Bacillariophyta	Decreaser	-	Y at genus level	
FRsepes	Fragilaria sepes	Bacillariophyta	Decreaser	-	Y at genus level	
CMdelcat	Delicata delicatula	Bacillariophyta	Decreaser	-	-	
EUBilun	Eunotia bilunaris	Bacillariophyta	Decreaser	Low NUTs	Y	
CMnovaze	Cymbella novaezeelandiana	Bacillariophyta	Decreaser	-	Y at genus level	
SPIROGY3	Spirogyra sp. 3	Chlorophyta	Decreaser	-	-	
CMlaevis	Cymbella laevis	Bacillariophyta	Decreaser	Low NUTs	Y	
GOincogn	Gomphonema incognitum	Bacillariophyta	Decreaser	-	Y at genus level	
AHalterg	Achnantheidium altergracillima	Bacillariophyta	Decreaser	Low NUTs	Y	
CMsublpt	Cymbella subleptoceros	Bacillariophyta	Decreaser	-	Y at genus level	
GEDecu	Geissleria decussis	Bacillariophyta	Decreaser	High NUTs	N	
CALOfusc	Calothrix fusca	Cyanophyta	Decreaser	-	-	
ECsemlan	Encyonema semilanceolatum	Bacillariophyta	Decreaser	-	Y at genus level	
ACLanceo	Achnantheiopsis lanceolata	Bacillariophyta	Increaser	High NUTs	Y	
AMinarie	Amphora inariensis	Bacillariophyta	Increaser	-	Y at genus level	
AMPedcls	Amphora pediculus	Bacillariophyta	Increaser	High NUTs	Y	
AUDOherm	Audouinella hermannii	Rhodophyta	Increaser	-	-	
CCpedcls	Cocconeis pediculus	Bacillariophyta	Increaser	High NUTs	Y	Y
CCplacen	Cocconeis placentula	Bacillariophyta	Increaser	High NUTs	Y	Y
CCplacug	Cocconeis placentula var. cuglypta	Bacillariophyta	Increaser	High NUTs	Y	Y
CCplalin	Cocconeis placentula var. lineata	Bacillariophyta	Increaser	High NUTs	Y	Y
CHLOROCO	Chlorococcum sp.	Chlorophyta	Increaser	-	-	
CHROOCOC	Chroococcus sp.	Cyanophyta	Increaser	-	-	
CLADglom	Cladophora glomerata	Chlorophyta	Increaser	-	-	
CLOSacer	Closterium acerosum	Charophyta	Increaser	-	-	
CLOSEhre	Closterium ehrenbergii	Charophyta	Increaser	-	-	

Note: Y; yes, N; no. The agreement column indicates that taxa were identified as associated with low and high nutrient sites by both TITAN and analysis by Potapova and Charles (2007). Species that were not present in Potapova and Charles (2007), but were represented by other taxa of the same Genus are identified in this column as well.

Table C.2. (continued)

Code	Taxa	Division	TITAN	Potapova and Charles 2007	Agreement	<i>Cladophora</i> epiphyte
CYmenegh	Cyclotella meneghiniana	Bacillariophyta	Increaser	High NUTs	Y	Y
DAvulg	Diatoma vulgaris	Bacillariophyta	Increaser	High NUTs	Y	Y
DIconfer	Diademesmis confervacca	Bacillariophyta	Increaser	-	Y at genus level	
EOlmini	Eolimna minima	Bacillariophyta	Increaser	High NUTs	Y	
EOsubmin	Eolimna subminuscula	Bacillariophyta	Increaser	-	Y at genus level	Y
GOkobaya	Gomphonema kobayasii	Bacillariophyta	Increaser	High NUTs	Y	Y
GOMinutm	Gomphonema minutum	Bacillariophyta	Increaser	High NUTs	Y	Y
GOolivcm	Gomphonema olivaceum	Bacillariophyta	Increaser	-	Y/N at genus level	Y
GOParvul	Gomphonema parvulum	Bacillariophyta	Increaser	High NUTs	Y	Y
GYacumin	Gyrosigma acuminatum	Bacillariophyta	Increaser	High NUTs	Y	Y
HLveneta	Halamphora veneta	Bacillariophyta	Increaser	-	-	
KCbude	Craticula buderi	Bacillariophyta	Increaser	-	Y at genus level	
KCsubmin	Craticula subminuscula	Bacillariophyta	Increaser	-	Y at genus level	
MEvarian	Melosira varians	Bacillariophyta	Increaser	High NUTs	Y	Y
MICRpach	Microspora pachyderma	Chlorophyta	Increaser	-	-	
NAantoni	Navicula antonii	Bacillariophyta	Increaser	-	Y/N at genus level	
NACaprad	Navicula capitatoradiata	Bacillariophyta	Increaser	High NUTs	Y	
NACryten	Navicula cryptotenella	Bacillariophyta	Increaser	High NUTs	Y	
NAlancel	Navicula lanceolata	Bacillariophyta	Increaser	High NUTs	Y	
NAstank	Navicula stankovici	Bacillariophyta	Increaser	-	Y/N at genus level	
NAtenell	Navicula tenelloides	Bacillariophyta	Increaser	High NUTs	Y	
NATripum	Navicula tripunctata	Bacillariophyta	Increaser	High NUTs	Y	
NATrivls	Navicula trivialis	Bacillariophyta	Increaser	High NUTs	Y	
NAVical	Navicula viridulacalcis	Bacillariophyta	Increaser	High NUTs	Y	
NIamphib	Nitzschia amphibia	Bacillariophyta	Increaser	High NUTs	Y	
NIIdissip	Nitzschia dissipata	Bacillariophyta	Increaser	High NUTs	Y	
NIfontic	Nitzschia fonticola	Bacillariophyta	Increaser	High NUTs	Y	
NIfrustu	Nitzschia frustulum	Bacillariophyta	Increaser	High NUTs	Y	
NIIncons	Nitzschia inconspicua	Bacillariophyta	Increaser	High NUTs	Y	
NIlinear	Nitzschia linearis	Bacillariophyta	Increaser	High NUTs	Y	

Note: Y; yes, N; no. The agreement column indicates that taxa were identified as associated with low and high nutrient sites by both TITAN and analysis by Potapova and Charles (2007). Species that were not present in Potapova and Charles (2007), but were represented by other taxa of the same Genus are identified in this column as well.

Table C.2. (continued)

Code	Taxa	Division	TITAN	Potapova and Charles 2007	Agreement	<i>Cladophora</i> epiphyte
NIpalca	Nitzschia palca	Bacillariophyta	Increaser	High NUTs	Y	
NIpermin	Nitzschia perminuta	Bacillariophyta	Increaser	High NUTs	Y	
NIsolita	Nitzschia solita	Bacillariophyta	Increaser	High NUTs	Y	
OEDOGON1	Oedogonium sp. 1	Chlorophyta	Increaser	-	-	Y
OSCILLAT	Oscillatoria sp.	Cyanophyta	Increaser	-	-	
PRlaevis	Pleurosira laevis	Bacillariophyta	Increaser	High NUTs	Y	
PSEUDULV	Pseudulvella sp.	Chlorophyta	Increaser	-		Y
ROabbre	Rhoicosphenia abbreviata	Bacillariophyta	Increaser	High NUTs	Y	Y
SUangust	Surirella angusta	Bacillariophyta	Increaser	High NUTs	Y	
SUbreb	Surirella brebissonii	Bacillariophyta	Increaser	High NUTs	Y	
SUsuecic	Surirella succica	Bacillariophyta	Increaser	-	Y at genus level	
TBfascic	Tabularia fasciculata	Bacillariophyta	Increaser	High NUTs	Y	
TYapicul	Tryblionella apiculata	Bacillariophyta	Increaser	High NUTs	Y	
ULulna	Ulnaria ulna	Bacillariophyta	Increaser	-	-	

Note: Y; yes, N; no. The agreement column indicates that taxa were identified as associated with low and high nutrient sites by both TITAN and analysis by Potapova and Charles (2007). Species that were not present in Potapova and Charles (2007), but were represented by other taxa of the same Genus are identified in this column as well.

REFERENCES

- Adler, P. B., J. HilleRisLambers, and J. M. Levine. 2007. A niche for neutrality. *Ecology Letters* 10:95–104.
- Allan, J. D. 2004. Landscapes and Riverscapes: The Influence of Land Use on Stream Ecosystems. *Annual Review of Ecology, Evolution, and Systematics* 35:257–284.
- Anderson, D. M., P. M. Glibert, and J. M. Burkholder. 2002. Harmful algal blooms and eutrophication: Nutrient sources, composition, and consequences. *Estuaries* 25:704–726.
- Anderson, M. J., T. O. Crist, J. M. Chase, M. Vellend, B. D. Inouye, A. L. Freestone, N. J. Sanders, H. V. Cornell, L. S. Comita, K. F. Davies, S. P. Harrison, N. J. B. Kraft, J. C. Stegen, and N. G. Swenson. 2011. Navigating the multiple meanings of β diversity: a roadmap for the practicing ecologist. *Ecology Letters* 14:19–28.
- Anderson, M. J., K. E. Ellingsen, and B. H. McCauley. 2006. Multivariate dispersion as a measure of beta diversity. *Ecology Letters* 9:683–693.
- Astorga, A., R. Death, F. Death, R. Paavola, M. Chakraborty, and T. Muotka. 2014. Habitat heterogeneity drives the geographical distribution of beta diversity: the case of New Zealand stream invertebrates. *Ecology and Evolution* 4:2693–2702.
- Back, J. A., and R. S. King. 2013. Sex and size matter: ontogenetic patterns of nutrient content of aquatic insects. *Freshwater Science* 32:837–848.
- Bai, Y., X. Han, J. Wu, Z. Chen, and L. Li. 2004. Ecosystem stability and compensatory effects in the Inner Mongolia grassland. *Nature* 431:181–184.
- Baker, M. E., and R. S. King. 2010. A new method for detecting and interpreting biodiversity and ecological community thresholds. *Methods in Ecology and Evolution* 1:25–37.
- Barbour, M. T., J. Gerritsen, B. D. Snyder, and J. B. Strubling. 1999. Rapid bioassessment protocols for use in streams and wadeable rivers. USEPA, Washington, D.C.
- Baselga, A. 2017. Partitioning abundance-based multiple-site dissimilarity into components: balanced variation in abundance and abundance gradients. *Methods in Ecology and Evolution* 8:799–808.

- Bates, A. E., R. D. Stuart-Smith, N. S. Barrett, and G. J. Edgar. 2017. Biological interactions both facilitate and resist climate-related functional change in temperate reef communities. *Proceedings of the Royal Society B: Biological Sciences* 284.
- Battin, T. J., K. Besemer, M. M. Bengtsson, A. M. Romani, and A. I. Packmann. 2016. The ecology and biogeochemistry of stream biofilms. *Nature Reviews Microbiology* 14:251–263.
- Baumgärtner, D., and K.-O. Rothhaupt. 2003. Predictive Length–Dry Mass Regressions for Freshwater Invertebrates in a Pre-Alpine Lake Littoral. *International Review of Hydrobiology* 88:453–463.
- Bêche, L. A., E. P. McElravy, and V. H. Resh. 2006. Long-term seasonal variation in the biological traits of benthic-macroinvertebrates in two Mediterranean-climate streams in California, U.S.A. *Freshwater Biology* 51:56–75.
- Beck, W. S., D. W. Markman, I. A. Oleksy, M. H. Lafferty, and N. L. Poff. 2018. Seasonal shifts in the importance of bottom-up and top-down factors on stream periphyton community structure. *Oikos*.
- Benke, A. C., A. D. Huryn, L. A. Smock, and J. B. Wallace. 1999. Length-Mass Relationships for Freshwater Macroinvertebrates in North America with Particular Reference to the Southeastern United States. *Journal of the North American Benthological Society* 18:308–343.
- Bernhardt, E. S., B. D. Lutz, R. S. King, J. P. Fay, C. E. Carter, A. M. Helton, D. Campagna, and J. Amos. 2012. How Many Mountains Can We Mine? Assessing the Regional Degradation of Central Appalachian Rivers by Surface Coal Mining. *Environmental Science & Technology* 46:8115–8122.
- Biggs, B. J., C. Kilroy, New Zealand, and Ministry for the Environment. 2000. Stream periphyton monitoring manual. NIWA, Christchurch, N.Z.
- Bini, L. M., V. L. Landeiro, A. A. Padial, T. Siqueira, and J. Heino. 2014. Nutrient enrichment is related to two facets of beta diversity for stream invertebrates across the United States. *Ecology* 95:1569–1578.
- Bolker, B. M. 2008. *Ecological Models and Data in R*. Princeton University Press.
- Bonada, N., N. Prat, V. H. Resh, and B. Statzner. 2006. DEVELOPMENTS IN AQUATIC INSECT BIOMONITORING: A Comparative Analysis of Recent Approaches. *Annual Review of Entomology* 51:495–523.
- Bonada, N., and V. H. Resh. 2013. Mediterranean-climate streams and rivers: geographically separated but ecologically comparable freshwater systems. *Hydrobiologia* 719:1–29.

- Bracken, M. E. S., and J. J. Stachowicz. 2006. Seaweed Diversity Enhances Nitrogen Uptake Via Complementary Use of Nitrate and Ammonium. *Ecology* 87:2397–2403.
- Brooks, B. W., T. M. Riley, and R. D. Taylor. 2006. Water Quality of Effluent-dominated Ecosystems: Ecotoxicological, Hydrological, and Management Considerations. *Hydrobiologia* 556:365–379.
- Brown, B. L. 2003. Spatial heterogeneity reduces temporal variability in stream insect communities. *Ecology Letters* 6:316–325.
- Brown, J. H., J. F. Gillooly, A. P. Allen, V. M. Savage, and G. B. West. 2004. Toward a Metabolic Theory of Ecology. *Ecology* 85:1771–1789.
- Cardinale, B. J. 2011. Biodiversity improves water quality through niche partitioning. *Nature* 472:86–89.
- Cardinale, B. J., J. E. Duffy, A. Gonzalez, D. U. Hooper, C. Perrings, P. Venail, A. Narwani, G. M. Mace, D. Tilman, D. A. Wardle, A. P. Kinzig, G. C. Daily, M. Loreau, J. B. Grace, A. Larigauderie, D. S. Srivastava, and S. Naeem. 2012. Biodiversity loss and its impact on humanity. *Nature* 486:59–67.
- Carpenter, S. R., N. F. Caraco, D. L. Correll, R. W. Howarth, A. N. Sharpley, and V. H. Smith. 1998. Nonpoint pollution of surface waters with phosphorus and nitrogen. *Ecological Applications* 8:559–568.
- Chase, J. M. 2007. Drought mediates the importance of stochastic community assembly. *Proceedings of the National Academy of Sciences* 104:17430–17434.
- Chase, J. M. 2010. Stochastic Community Assembly Causes Higher Biodiversity in More Productive Environments. *Science* 328:1388–1391.
- Cook, S. C., L. Housley, J. A. Back, and R. S. King. 2018. Freshwater eutrophication drives sharp reductions in temporal beta diversity. *Ecology* 99:47–56.
- Cross, W. F., B. R. Johnson, J. B. Wallace, and A. D. Rosemond. 2005. Contrasting response of stream detritivores to long-term nutrient enrichment. *Limnology and Oceanography* 50:1730–1739.
- Cross, W. F., J. B. Wallace, A. D. Rosemond, and S. L. Eggert. 2006. Whole-System Nutrient Enrichment Increases Secondary Production in a Detritus-Based Ecosystem. *Ecology* 87:1556–1565.
- Descamps-Julien, B., and A. Gonzalez. 2005. Stable Coexistence in a Fluctuating Environment: An Experimental Demonstration. *Ecology* 86:2815–2824.
- Dodds, W. K. 1991. Factors associated with dominance of the filamentous green alga *Cladophora glomerata*. *Water Research* 25:1325–1332.

- Dodds, W. K., W. H. Clements, K. Gido, R. H. Hilderbrand, and R. S. King. 2010. Thresholds, breakpoints, and nonlinearity in freshwaters as related to management. *Journal of the North American Benthological Society* 29:988–997.
- Dodds, W. K., and D. A. Gudder. 1992. The Ecology of *Cladophora*. *Journal of Phycology* 28:415–427.
- Dodds, W., and V. Smith. 2016. Nitrogen, phosphorus, and eutrophication in streams. *Inland Waters* 6:155–164.
- Doležal, J., V. Lanta, O. Mudrak, and J. Lepš. 2019. Seasonality promotes grassland diversity: Interactions with mowing, fertilization and removal of dominant species. *Journal of Ecology* 107:203–215.
- Donohue, I., A. L. Jackson, M. T. Pusch, and K. Irvine. 2009. Nutrient enrichment homogenizes lake benthic assemblages at local and regional scales. *Ecology* 90:3470–3477.
- Dorioz, J. M., E. A. Cassell, A. Orand, and K. G. Eisenman. 1998. Phosphorus storage, transport and export dynamics in the Foron River watershed. *HYDROLOGICAL PROCESSES* 12:25.
- Dufrene, M., and P. Legendre. 1997. Species Assemblages and Indicator Species: the Need for a Flexible Asymmetrical Approach. *Ecological Monographs* 67:345–366.
- Edwards, F. K. L., L. Armand, H. M. Vincent, and I. J. Jones. 2009. The relationship between length, mass and preservation time for three species of freshwater leeches (Hirudinea). *Fundamental and Applied Limnology*:321–327.
- Elser, J. J., M. E. S. Bracken, E. E. Cleland, D. S. Gruner, W. S. Harpole, H. Hillebrand, J. T. Ngai, E. W. Seabloom, J. B. Shurin, and J. E. Smith. 2007. Global analysis of nitrogen and phosphorus limitation of primary producers in freshwater, marine and terrestrial ecosystems. *Ecology Letters* 10:1135–1142.
- Elser, J. J., W. F. Fagan, R. F. Denno, D. R. Dobberfuhl, A. Folarin, A. Huberty, S. Interlandi, S. S. Kilham, E. McCauley, K. L. Schulz, E. H. Siemann, and R. W. Sterner. 2000. Nutritional constraints in terrestrial and freshwater food webs. *Nature* 408:578–580.
- Eros, T., P. Saly, P. Takacs, A. Specziar, and P. Biro. 2012. Temporal variability in the spatial and environmental determinants of functional metacommunity organization – stream fish in a human-modified landscape. *Freshwater Biology* 57:1914–1928.

- Evans-White, M. A., W. K. Dodds, D. G. Huggins, and D. S. Baker. 2009. Thresholds in macroinvertebrate biodiversity and stoichiometry across water-quality gradients in Central Plains (USA) streams. *Journal of the North American Benthological Society* 28:855–868.
- Fernandes, I. M., R. Henriques-Silva, J. Penha, J. Zuanon, and P. R. Peres-Neto. 2014. Spatiotemporal dynamics in a seasonal metacommunity structure is predictable: the case of floodplain-fish communities. *Ecography* 37:464–475.
- Fisher, S. G., L. J. Gray, N. B. Grimm, and D. E. Busch. 1982. Temporal Succession in a Desert Stream Ecosystem Following Flash Flooding. *Ecological Monographs* 52:93–110.
- Fox, D. 2007. Back to the No-Analog Future? *Science* 316:823–825.
- Francoeur, S. N., R. A. Smith, and R. L. Lowe. 1999. Nutrient Limitation of Algal Biomass Accrual in Streams: Seasonal Patterns and a Comparison of Methods. *Journal of the North American Benthological Society* 18:242–260.
- Frost, P. C., H. Hillebrand, and M. Kahlert. 2005. Low algal carbon content and its effect on the C : P stoichiometry of periphyton. *Freshwater Biology* 50:1800–1807.
- Frost, P. C., R. S. Stelzer, G. A. Lamberti, and J. J. Elser. 2002. ROSEMARY MACKAY FUND ARTICLE: Ecological stoichiometry of trophic interactions in the benthos: understanding the role of C:N:P ratios in lentic and lotic habitats. *Journal of the North American Benthological Society* 21:515–528.
- Galloway, J. N., A. R. Townsend, J. W. Erisman, M. Bekunda, Z. Cai, J. R. Freney, L. A. Martinelli, S. P. Seitzinger, and M. A. Sutton. 2008. Transformation of the Nitrogen Cycle: Recent Trends, Questions, and Potential Solutions. *Science* 320:889–892.
- Gauch, H. G., and R. H. Whittaker. 1972. Coenocline Simulation. *Ecology* 53:446–451.
- Goldenberg Vilar, A., H. van Dam, E. E. van Loon, J. A. Vonk, H. G. van Der Geest, and W. Admiraal. 2014. Eutrophication decreases distance decay of similarity in diatom communities. *Freshwater Biology* 59:1522–1531.
- Gonzalez, A., and M. Loreau. 2009. The Causes and Consequences of Compensatory Dynamics in Ecological Communities. *Annual Review of Ecology, Evolution, and Systematics* 40:393–414.
- Groffman, P. M., J. S. Baron, T. Blett, A. J. Gold, I. Goodman, L. H. Gunderson, B. M. Levinson, M. A. Palmer, H. W. Paerl, G. D. Peterson, N. L. Poff, D. W. Rejeski, J. F. Reynolds, M. G. Turner, K. C. Weathers, and J. Wiens. 2006. Ecological Thresholds: The Key to Successful Environmental Management or an Important Concept with No Practical Application? *Ecosystems* 9:1–13.

- Gross, K., B. J. Cardinale, J. W. Fox, A. Gonzalez, M. Loreau, H. Wayne Polley, P. B. Reich, and J. van Ruijven. 2014. Species Richness and the Temporal Stability of Biomass Production: A New Analysis of Recent Biodiversity Experiments. *The American Naturalist* 183:1–12.
- Gurevitch, J., and L. V. Hedges. 1999. Statistical Issues in Ecological Meta-Analyses. *Ecology* 80:1142–1149.
- Gutiérrez-Cánovas, C., A. Millán, J. Velasco, I. P. Vaughan, and S. J. Ormerod. 2013. Contrasting effects of natural and anthropogenic stressors on beta diversity in river organisms: Beta diversity along natural and anthropogenic stress gradients. *Global Ecology and Biogeography* 22:796–805.
- Haggard, B. E. 2010. Phosphorus Concentrations, Loads, and Sources within the Illinois River Drainage Area, Northwest Arkansas, 1997–2008. *Journal of Environment Quality* 39:2113.
- Harding, J. S., E. F. Benfield, P. V. Bolstad, G. S. Helfman, and E. B. D. Jones. 1998. Stream biodiversity: The ghost of land use past. *Proceedings of the National Academy of Sciences* 95:14843–14847.
- Hatosy, S. M., J. B. H. Martiny, R. Sachdeva, J. Steele, J. A. Fuhrman, and A. C. Martiny. 2013. Beta diversity of marine bacteria depends on temporal scale. *Ecology* 94:1898–1904.
- Hawkins, C. P., J. N. Hogue, L. M. Decker, and J. W. Feminella. 1997. Channel Morphology, Water Temperature, and Assemblage Structure of Stream Insects. *Journal of the North American Benthological Society* 16:728–749.
- Heino, J., M. Grönroos, J. Ilmonen, T. Karhu, M. Niva, and L. Paasivirta. 2012. Environmental heterogeneity and β diversity of stream macroinvertebrate communities at intermediate spatial scales. *Freshwater Science* 32:142–154.
- Heino, J., A. S. Melo, and L. M. Bini. 2015a. Reconceptualising the beta diversity-environmental heterogeneity relationship in running water systems. *Freshwater Biology* 60:223–235.
- Heino, J., A. S. Melo, L. M. Bini, F. Altermatt, S. A. Al-Shami, D. G. Angeler, N. Bonada, C. Brand, M. Callisto, K. Cottenie, O. Dangles, D. Dudgeon, A. Encalada, E. Göthe, M. Grönroos, N. Hamada, D. Jacobsen, V. L. Landeiro, R. Ligeiro, R. T. Martins, M. L. Miserendino, C. S. Md Rawi, M. E. Rodrigues, F. de O. Roque, L. Sandin, D. Schmera, L. F. Sgarbi, J. P. Simaika, T. Siqueira, R. M. Thompson, and C. R. Townsend. 2015b. A comparative analysis reveals weak relationships between ecological factors and beta diversity of stream insect metacommunities at two spatial levels. *Ecology and Evolution* 5:1235–1248.

- Heino, J., A. S. Melo, T. Siqueira, J. Soininen, S. Valanko, and L. M. Bini. 2015c. Metacommunity organisation, spatial extent and dispersal in aquatic systems: patterns, processes and prospects. *Freshwater Biology* 60:845–869.
- Helms, B. S., J. E. Schoonover, and J. W. Feminella. 2009. Seasonal variability of landuse impacts on macroinvertebrate assemblages in streams of western Georgia, USA. *Journal of the North American Benthological Society* 28:991–1006.
- Hewitt, J. E., S. F. Thrush, and K. E. Ellingsen. 2016. The role of time and species identities in spatial patterns of species richness and conservation: Time, Species Identities, and Richness. *Conservation Biology* 30:1080–1088.
- Hillebrand, H. 2009. Meta-Analysis of Grazer Control of Periphyton Biomass Across Aquatic Ecosystems. *Journal of Phycology* 45:798–806.
- Hillebrand, H., C.-D. Dürselen, D. Kirschtel, U. Pollinger, and T. Zohary. 1999. Biovolume Calculation for Pelagic and Benthic Microalgae. *Journal of Phycology* 35:403–424.
- Hillebrand, H., and U. Sommer. 1999. The nutrient stoichiometry of benthic microalgal growth: Redfield proportions are optimal. *Limnology and Oceanography* 44:440–446.
- Hobbs, R. J., E. Higgs, and J. A. Harris. 2009. Novel ecosystems: implications for conservation and restoration. *Trends in Ecology & Evolution* 24:599–605.
- Houlahan, J. E., D. J. Currie, K. Cottenie, G. S. Cumming, S. K. M. Ernest, C. S. Findlay, S. D. Fuhlendorf, U. Gaedke, P. Legendre, J. J. Magnuson, B. H. McArdle, E. H. Muldavin, D. Noble, R. Russell, R. D. Stevens, T. J. Willis, I. P. Woiod, and S. M. Wondzell. 2007. Compensatory dynamics are rare in natural ecological communities. *Proceedings of the National Academy of Sciences* 104:3273–3277.
- Hubbell, S. P. 2001. *The Unified Neutral Theory of Biodiversity and Biogeography*. Princeton University Press, Princeton, New Jersey.
- Hurn, A. D., and J. B. Wallace. 2000. Life History and Production of Stream Insects. *Annual Review of Entomology* 45:83–110.
- Hynes, H. B. N. 1975. The stream and its valley. *SIL Proceedings, 1922-2010* 19:1–15.
- Ives, A. R., and S. R. Carpenter. 2007. Stability and Diversity of Ecosystems. *Science* 317:58–62.
- Jarvie, H. P., A. N. Sharpley, J. T. Scott, B. E. Haggard, M. J. Bowes, and L. B. Massey. 2012. Within-River Phosphorus Retention: Accounting for a Missing Piece in the Watershed Phosphorus Puzzle. *Environmental Science & Technology* 46:13284–13292.

- Jochimsen, M. C., R. Kümmerlin, and D. Straile. 2013. Compensatory dynamics and the stability of phytoplankton biomass during four decades of eutrophication and oligotrophication. *Ecology Letters* 16:81–89.
- Johnson, R. C., M. M. Carreiro, H.-S. Jin, and J. D. Jack. 2012. Within-year temporal variation and life-cycle seasonality affect stream macroinvertebrate community structure and biotic metrics. *Ecological Indicators* 13:206–214.
- Jost, L. 2007. Partitioning diversity into independent alpha and beta components. *Ecology* 88:2427–2439.
- Justus, B. G., J. C. Petersen, S. R. Femmer, J. V. Davis, and J. E. Wallace. 2010. A comparison of algal, macroinvertebrate, and fish assemblage indices for assessing low-level nutrient enrichment in wadeable Ozark streams. *Ecological Indicators* 10:627–638.
- Jyrkänkallio-Mikkola, J., J. Heino, and J. Soininen. 2016. Beta diversity of stream diatoms at two hierarchical spatial scales: implications for biomonitoring. *Freshwater Biology* 61:239–250.
- King, R. S., and M. E. Baker. 2014. Use, Misuse, and Limitations of Threshold Indicator Taxa Analysis (TITAN) for Natural Resource Management. Pages 231–254 *in* G. R. Guntenspergen, editor. *Application of Threshold Concepts in Natural Resource Decision Making*. Springer New York, New York, NY.
- King, R. S., M. E. Baker, P. F. Kazyak, and D. E. Weller. 2011. How novel is too novel? Stream community thresholds at exceptionally low levels of catchment urbanization. *Ecological Applications* 21:1659–1678.
- King, R. S., and C. J. Richardson. 2002. Evaluating subsampling approaches and macroinvertebrate taxonomic resolution for wetland bioassessment. *Journal of the North American Benthological Society* 21:150–171.
- King, R. S., and C. J. Richardson. 2003. Integrating Bioassessment and Ecological Risk Assessment: An Approach to Developing Numerical Water-Quality Criteria. *Environmental Management* 31:795–809.
- King, R. S., M. Scoggins, and A. Porras. 2016. Stream biodiversity is disproportionately lost to urbanization when flow permanence declines: evidence from southwestern North America. *Freshwater Science* 35:340–352.
- Korhonen, J. J., J. Soininen, and H. Hillebrand. 2010. A quantitative analysis of temporal turnover in aquatic species assemblages across ecosystems. *Ecology* 91:508–517.
- Kovalenko, K. E., V. J. Brady, T. N. Brown, J. J. H. Ciborowski, N. P. Danz, J. P. Gathman, G. E. Host, R. W. Howe, L. B. Johnson, G. J. Niemi, and E. D. Reavie. 2014. Congruence of community thresholds in response to anthropogenic stress in Great Lakes coastal wetlands. *Freshwater Science* 33:958–971.

- Lamberti, G. A., S. V. Gregory, L. R. Ashkenas, R. C. Wildman, and K. M. Moore. 1991. Stream ecosystem recovery following a catastrophic debris flow. *Canadian Journal of Fisheries and Aquatic Sciences* 48:196–208.
- Lamberti, G. A., and V. H. Resh. 1985. Distribution of benthic algae and macroinvertebrates along a thermal stream gradient. *Hydrobiologia* 128:13–21.
- Lange, K., A. Liess, J. J. Piggott, C. R. Townsend, and C. D. Matthaei. 2011. Light, nutrients and grazing interact to determine stream diatom community composition and functional group structure. *Freshwater Biology* 56:264–278.
- Larson, C. A., L. Adumatioge, and S. I. Passy. 2016. The number of limiting resources in the environment controls the temporal diversity patterns in the algal benthos. *Microbial Ecology* 72:64–69.
- Lehman, C. L., D. Tilman, and A. E. S. D. Gaines. 2000. Biodiversity, Stability, and Productivity in Competitive Communities. *The American Naturalist* 156:534–552.
- Levin, S. A. 1992. The Problem of Pattern and Scale in Ecology: The Robert H. MacArthur Award Lecture. *Ecology* 73:1943–1967.
- Lewis, S. L., and M. A. Maslin. 2015. Defining the Anthropocene. *Nature* 519:171–180.
- Loreau, M., and A. Hector. 2001. Partitioning selection and complementarity in biodiversity experiments. *Nature* 412:72–76.
- Loreau, M., and C. de Mazancourt. 2013. Biodiversity and ecosystem stability: a synthesis of underlying mechanisms. *Ecology Letters* 16:106–115.
- Magurran, A., Faye Moyes, Nicholas J. Gotelli, and Brian McGill. 2015. Rapid biotic homogenization of marine fish assemblages. *Nature Communications* 6:8405.
- May, R. M. 1977. Thresholds and breakpoints in ecosystems with a multiplicity of stable states. *Nature* 269:471–477.
- Mazor, R. D., T. B. Reynoldson, D. M. Rosenberg, and V. H. Resh. 2006. Effects of biotic assemblage, classification, and assessment method on bioassessment performance. *Canadian Journal of Fisheries and Aquatic Sciences; Ottawa* 63:394–411.
- McCune, B., J. B. Grace, and D. L. Urban. 2002. *Analysis of Ecological Communities*. MjM Software Design.
- McGoff, E., A. G. Solimini, M. T. Pusch, T. Jurca, and L. Sandin. 2013. Does lake habitat alteration and land-use pressure homogenize European littoral macroinvertebrate communities? *Journal of Applied Ecology* 50:1010–1018.

- Merritt, R. W., K. W. Cummins, and M. B. Berg, editors. 2008. AN INTRODUCTION TO THE AQUATIC INSECTS OF NORTH AMERICA. 4 edition. Kendall Hunt Publishing, Dubuque, Iowa.
- Méthot, G., C. Hudon, P. Gagnon, B. Pinel-Alloul, A. Armellin, and A.-M. T. Poirier. 2012. Macroinvertebrate size–mass relationships: how specific should they be? *Freshwater Science* 31:750–764.
- Midgley, G. F., L. Hannah, D. Millar, M. C. Rutherford, and L. W. Powrie. 2002. Assessing the vulnerability of species richness to anthropogenic climate change in a biodiversity hotspot. *Global Ecology and Biogeography* 11:445–451.
- Morin, X., L. Fahse, C. de Mazancourt, M. Scherer-Lorenzen, and H. Bugmann. 2014. Temporal stability in forest productivity increases with tree diversity due to asynchrony in species dynamics. *Ecology Letters* 17:1526–1535.
- Mulholland, P. J., and A. D. Rosemond. 1992. Periphyton Response to Longitudinal Nutrient Depletion in a Woodland Stream: Evidence of Upstream-Downstream Linkage. *Journal of the North American Benthological Society* 11:405–419.
- Mykrä, H., J. Heino, J. Oksanen, and T. Muotka. 2011. The stability–diversity relationship in stream macroinvertebrates: influences of sampling effects and habitat complexity. *Freshwater Biology* 56:1122–1132.
- Nelson, C. E., D. M. Bennett, and B. J. Cardinale. 2013. Consistency and sensitivity of stream periphyton community structural and functional responses to nutrient enrichment. *Ecological Applications* 23:159–173.
- Newall, P., N. Bate, and L. Metzeling. 2006. A comparison of diatom and macroinvertebrate classification of sites in the Kiewa River system, Australia. *Hydrobiologia* 572:131–149.
- Newbold, J. D., B. W. Sweeney, and R. L. Vannote. 1994. A Model for Seasonal Synchrony in Stream Mayflies. *Journal of the North American Benthological Society* 13:3–18.
- Niu, S. Q., and J. H. Knouft. 2017. Hydrologic characteristics, food resource abundance, and spatial variation in stream assemblages. *Ecohydrology* 10:e1770.
- Omernik, J. M., and G. E. Griffith. 2014. Ecoregions of the Conterminous United States: Evolution of a Hierarchical Spatial Framework. *Environmental Management* 54:1249–1266.
- Pace, M. L., J. J. Cole, S. R. Carpenter, and J. F. Kitchell. 1999. Trophic cascades revealed in diverse ecosystems. *Trends in Ecology & Evolution* 14:483–488.

- Passy, S. I. 2009. The relationship between local and regional diatom richness is mediated by the local and regional environment. *Global Ecology and Biogeography* 18:383–391.
- Passy, S. I., and F. G. Blanchet. 2007. Algal communities in human-impacted stream ecosystems suffer beta-diversity decline. *Diversity and Distributions* 13:670–679.
- Paulsen, S. G., A. Mayo, D. V. Peck, J. L. Stoddard, E. Tarquinio, S. M. Holdsworth, J. V. Sickle, L. L. Yuan, C. P. Hawkins, A. T. Herlihy, P. R. Kaufmann, M. T. Barbour, D. P. Larsen, and A. R. Olsen. 2008. Condition of stream ecosystems in the US: an overview of the first national assessment. *Journal of the North American Benthological Society* 27:812–821.
- Pennekamp, F., M. Pontarp, A. Tabi, F. Altermatt, R. Alther, Y. Choffat, E. A. Fronhofer, P. Ganesanandamoorthy, A. Garnier, J. I. Griffiths, S. Greene, K. Horgan, T. M. Massie, E. Mächler, G. M. Palamara, M. Seymour, and O. L. Petchey. 2018. Biodiversity increases and decreases ecosystem stability. *Nature* 563:109–112.
- Petersen, J. C., B. G. Justus, and B. J. Meredith. 2014. Effects of land use, stream habitat, and water quality on biological communities of wadeable streams in the Illinois River Basin of Arkansas, 2011 and 2012. Scientific Investigations Report, U.S. Geological Survey, Reston, Virginia, USA.
- Peterson, C. G., and N. B. Grimm. 1992. Temporal Variation in Enrichment Effects during Periphyton Succession in a Nitrogen-Limited Desert Stream Ecosystem. *Journal of the North American Benthological Society* 11:20–36.
- Potapova, M., and D. F. Charles. 2007. Diatom metrics for monitoring eutrophication in rivers of the United States. *Ecological Indicators* 7:48–70.
- Power, M. E., A. J. Stewart, and W. J. Matthews. 1988. Grazer Control of Algae in an Ozark Mountain Stream: Effects of Short-Term Exclusion. *Ecology* 69:1894–1898.
- Power, M. E., D. Tilman, J. A. Estes, B. A. Menge, W. J. Bond, L. S. Mills, G. Daily, J. C. Castilla, J. Lubchenco, and R. T. Paine. 1996. Challenges in the Quest for Keystones Identifying keystone species is difficult—but essential to understanding how loss of species will affect ecosystems. *BioScience* 46:609–620.
- Qian, H., and R. E. Ricklefs. 2007. A latitudinal gradient in large-scale beta diversity for vascular plants in North America. *Ecology Letters* 10:737–744.
- Questad, E. J., and B. L. Foster. 2008. Coexistence through spatio-temporal heterogeneity and species sorting in grassland plant communities. *Ecology Letters* 11:717–726.

- Radeloff, V. C., J. W. Williams, B. L. Bateman, K. D. Burke, S. K. Carter, E. S. Childress, K. J. Cromwell, C. Gratton, A. O. Hasley, B. M. Kraemer, A. W. Latzka, E. Marin-Spiotta, C. D. Meine, S. E. Munoz, T. M. Neeson, A. M. Pidgeon, A. R. Rissman, R. J. Rivera, L. M. Szymanski, and J. Usinowicz. 2015. The rise of novelty in ecosystems. *Ecological Applications* 25:2051–2068.
- Resh, V. H. 2008. Which group is best? Attributes of different biological assemblages used in freshwater biomonitoring programs. *Environmental Monitoring and Assessment* 138:131–138.
- Resh, V. H., A. V. Brown, A. P. Covich, M. E. Gurtz, H. W. Li, G. W. Minshall, S. R. Reice, A. L. Sheldon, J. B. Wallace, and R. C. Wissmar. 1988. The Role of Disturbance in Stream Ecology. *Journal of the North American Benthological Society* 7:433–455.
- Rosemond, A. D. 1994. Multiple Factors Limit Seasonal Variation in Periphyton in a Forest Stream. *Journal of the North American Benthological Society* 13:333–344.
- Rosemond, A. D., P. J. Mulholland, and S. H. Brawley. 2000. Seasonally shifting limitation of stream periphyton: response of algal populations and assemblage biomass and productivity to variation in light, nutrients, and herbivores. *Canadian Journal of Fisheries and Aquatic Sciences* 57:66–75.
- Rosemond, A. D., P. J. Mulholland, and J. W. Elwood. 1993. Top-Down and Bottom-Up Control of Stream Periphyton: Effects of Nutrients and Herbivores. *Ecology* 74:1264–1280.
- Roy, A. H., A. D. Rosemond, M. J. Paul, D. S. Leigh, and J. B. Wallace. 2003. Stream macroinvertebrate response to catchment urbanisation (Georgia, U.S.A.). *Freshwater Biology* 48:329–346.
- Sample, B. E., R. J. Cooper, R. D. Greer, and R. C. Whitmore. 1993. Estimation of Insect Biomass by Length and Width. *The American Midland Naturalist* 129:234–240.
- Scheffer, M., and S. R. Carpenter. 2003. Catastrophic regime shifts in ecosystems: linking theory to observation. *Trends in Ecology & Evolution* 18:648–656.
- Schindler, D. E., J. B. Armstrong, and T. E. Reed. 2015. The portfolio concept in ecology and evolution. *Frontiers in Ecology and the Environment* 13:257–263.
- Schwendel, A. C., R. G. Death, I. C. Fuller, and M. K. Joy. 2011. Linking disturbance and stream invertebrate communities: how best to measure bed stability. *Journal of the North American Benthological Society* 30:11–24.
- Scott, J. T., B. E. Haggard, A. N. Sharpley, and J. J. Romeis. 2011. Change Point Analysis of Phosphorus Trends in the Illinois River (Oklahoma) Demonstrates the Effects of Watershed Management. *Journal of Environment Quality* 40:1249.

- Sharpley, A. N., R. W. McDowell, and P. J. A. Kleinman. 2004. Amounts, Forms, and Solubility of Phosphorus in Soils Receiving Manure. *Soil Science Society of America Journal* 68:2048.
- Singer, G. A., and T. J. Battin. 2007. Anthropogenic subsidies alter stream consumer–resource stoichiometry, biodiversity, and food chains. *Ecological Applications* 17:376–389.
- Smith, V. H., S. B. Joye, and R. W. Howarth. 2006. Eutrophication of freshwater and marine ecosystems. *Limnology and Oceanography* 51:351–355.
- Smith, V. H., G. D. Tilman, and J. C. Nekola. 1999. Eutrophication: impacts of excess nutrient inputs on freshwater, marine, and terrestrial ecosystems. *Environmental Pollution* 100:179–196.
- Smucker, N. J., N. E. Detenbeck, and A. C. Morrison. 2013. Diatom responses to watershed development and potential moderating effects of near-stream forest and wetland cover. *Freshwater Science* 32:230–249.
- Snyder, E. B., C. T. Robinson, G. W. Minshall, and S. R. Rushforth. 2002. Regional patterns in periphyton accrual and diatom assemblage structure in a heterogeneous nutrient landscape. *Canadian Journal of Fisheries and Aquatic Sciences; Ottawa* 59:564–577.
- Socolar, J. B., J. J. Gilroy, W. E. Kunin, and D. P. Edwards. 2016. How Should Beta-Diversity Inform Biodiversity Conservation? *Trends in Ecology & Evolution* 31:67–80.
- Stancheva, R., and R. G. Sheath. 2016. Benthic soft-bodied algae as bioindicators of stream water quality. *Knowledge and Management of Aquatic Ecosystems*:15.
- Stanford, J. A., M. S. Lorang, and F. R. Hauer. 2005. The shifting habitat mosaic of river ecosystems. *SIL Proceedings, 1922-2010* 29:123–136.
- Steffen, W., P. J. Crutzen, and J. R. McNeill. 2007. The Anthropocene: Are Humans Now Overwhelming the Great Forces of Nature. *AMBIO: A Journal of the Human Environment* 36:614–621.
- Steffen, W., J. Grinevald, P. Crutzen, and J. McNeill. 2011. The Anthropocene: conceptual and historical perspectives. *Philosophical Transactions of the Royal Society A: Mathematical, Physical and Engineering Sciences* 369:842–867.
- Steiner, C. F. 2014. Stochastic sequential dispersal and nutrient enrichment drive beta diversity in space and time. *Ecology* 95:2603–2612.
- Sterner, R. W., and J. J. Elser. 2002. *Ecological Stoichiometry: The Biology of Elements from Molecules to the Biosphere*. Princeton University Press.

- Stevenson, R. J., B. H. Hill, A. T. Herlihy, L. L. Yuan, and S. B. Norton. 2008. Algae–P relationships, thresholds, and frequency distributions guide nutrient criterion development. *Journal of the North American Benthological Society* 27:783–799.
- Stewart, A. J. 1987. Responses of Stream Algae to Grazing Minnows and Nutrients: A Field Test for Interactions. *Oecologia* 72:1–7.
- Stewart, K. W. 2002. Nymphs of North American Stonefly Genera (Plecoptera), 2nd Edition. 2nd edition. The Caddis Press, Columbus, Ohio.
- Sundermann, A., M. Leps, S. Leisner, and P. Haase. 2015. Taxon-specific physico-chemical change points for stream benthic invertebrates. *Ecological Indicators* 57:314–323.
- Tansley, A. G. 1935. The Use and Abuse of Vegetational Concepts and Terms. *Ecology* 16:284–307.
- Taylor, J. M., R. S. King, A. A. Pease, and K. O. Winemiller. 2014. Nonlinear response of stream ecosystem structure to low-level phosphorus enrichment. *Freshwater Biology* 59:969–984.
- Thompson, R., and C. Townsend. 2006. A truce with neutral theory: local deterministic factors, species traits and dispersal limitation together determine patterns of diversity in stream invertebrates. *Journal of Animal Ecology* 75:476–484.
- Tilman, D. 1977. Resource Competition between Plankton Algae: An Experimental and Theoretical Approach. *Ecology* 58:338–348.
- Tilman, D. 1985. The Resource-Ratio Hypothesis of Plant Succession. *The American Naturalist* 125:827–852.
- Tilman, D. 1996. Biodiversity: Population Versus Ecosystem Stability. *Ecology* 77:350–363.
- Tilman, D., C. L. Lehman, and K. T. Thomson. 1997. Plant diversity and ecosystem productivity: Theoretical considerations. *Proceedings of the National Academy of Sciences* 94:1857–1861.
- Tilman, D., and S. W. Pacala. 1993. The maintenance of species richness in plant communities. *Species diversity in ecological communities*:13–25.
- Tilman, D., P. B. Reich, and J. M. H. Knops. 2006. Biodiversity and ecosystem stability in a decade-long grassland experiment. *Nature* 441:629–632.
- Tonkin, J. D., M. T. Bogan, N. Bonada, B. Rios-Touma, and D. A. Lytle. 2017. Seasonality and predictability shape temporal species diversity. *Ecology* 98:1201–1216.

- Tonkin, J. D., and R. G. Death. 2012. Consistent effects of productivity and disturbance on diversity between landscapes. *Ecosphere* 3:1–19.
- Tucker, C. M., L. G. Shoemaker, K. F. Davies, D. R. Nemergut, and B. A. Melbourne. 2016. Differentiating between niche and neutral assembly in metacommunities using null models of β -diversity. *Oikos* 125:778–789.
- Tuomisto, H. 2010. A diversity of beta diversities: straightening up a concept gone awry. Part 1. Defining beta diversity as a function of alpha and gamma diversity. *Ecography* 33:2–22.
- Turner, B. L., and L. M. Condon. 2013. Pedogenesis, nutrient dynamics, and ecosystem development: the legacy of T.W. Walker and J.K. Syers. *Plant and Soil* 367:1–10.
- Vannote, R. L., G. W. Minshall, K. W. Cummins, J. R. Sedell, and C. E. Cushing. 1980. The River Continuum Concept. *Canadian Journal of Fisheries and Aquatic Sciences* 37:130–137.
- Vannote, R. L., and B. W. Sweeney. 1980. Geographic Analysis of Thermal Equilibria: A Conceptual Model for Evaluating the Effect of Natural and Modified Thermal Regimes on Aquatic Insect Communities. *The American Naturalist* 115:667–695.
- Vasseur, D. A., U. Gaedke, and K. S. McCann. 2005. A seasonal alternation of coherent and compensatory dynamics occurs in phytoplankton. *Oikos* 110:507–514.
- Wagenhoff, A., J. E. Clapcott, K. E. M. Lau, G. D. Lewis, and R. G. Young. 2016. Identifying congruence in stream assemblage thresholds in response to nutrient and sediment gradients for limit setting. *Ecological Applications*:n/a-n/a.
- Wagenhoff, A., A. Liess, A. Pastor, J. E. Clapcott, E. O. Goodwin, and R. G. Young. 2017. Thresholds in ecosystem structural and functional responses to agricultural stressors can inform limit setting in streams. *Freshwater Science* 36:178–194.
- Wallace, A. M., and R. G. Biastoch. 2016. Detecting changes in the benthic invertebrate community in response to increasing chloride in streams in Toronto, Canada. *Freshwater Science* 35:353–363.
- Wehr, J. D., R. G. Sheath, and J. P. Kociolek, editors. 2015. *Freshwater algae of North America: ecology and classification*. Second edition. Elsevier/AP, Academic Press is an imprint of Elsevier, Amsterdam ; Boston.
- Whittaker, R. H. 1960. Vegetation of the Siskiyou Mountains, Oregon and California. *Ecological Monographs* 30:279–338.
- Whittaker, R. H. 1972. Evolution and Measurement of Species Diversity. *Taxon* 21:213–251.

- Wolda, H. 1988. Insect Seasonality: Why? *Annual Review of Ecology and Systematics* 19:1–18.
- Wood, P. J., J. Gunn, H. Smith, and A. Abas-Kutty. 2005. Flow permanence and macroinvertebrate community diversity within groundwater dominated headwater streams and springs. *Hydrobiologia* 545:55–64.
- Wood, S. N. 2017. *Generalized Additive Models: An Introduction with R*, Second Edition. 2 edition. Chapman and Hall/CRC, Boca Raton.
- Zalasiewicz, J., M. Williams, A. Haywood, and M. Ellis. 2011. The Anthropocene: a new epoch of geological time? *Philosophical Transactions of the Royal Society of London A: Mathematical, Physical and Engineering Sciences* 369:835–841.
- Zhang, Q.-G., and D.-Y. Zhang. 2006. Resource Availability and Biodiversity Effects on the Productivity, Temporal Variability and Resistance of Experimental Algal Communities. *Oikos* 114:385–396.
- Zhang, Y., L. Cheng, K. E. Tolonen, H. Yin, J. Gao, Z. Zhang, K. Li, and Y. Cai. 2018. Substrate degradation and nutrient enrichment structuring macroinvertebrate assemblages in agriculturally dominated Lake Chaohu Basins, China. *Science of The Total Environment* 627:57–66.
- Zulkifly, S. B., J. M. Graham, E. B. Young, R. J. Mayer, M. J. Piotrowski, I. Smith, and L. E. Graham. 2013. The Genus *Cladophora* Kützing (Ulvophyceae) as a Globally Distributed Ecological Engineer. *Journal of Phycology* 49:1–17.
- Zuppinger-Dingley, D., B. Schmid, J. S. Petermann, V. Yadav, G. B. De Deyn, and D. F. B. Flynn. 2014. Selection for niche differentiation in plant communities increases biodiversity effects. *Nature* 515:108–111.
- Zuur, A. F., editor. 2009. *Mixed effects models and extensions in ecology with R*. Springer, New York, NY.